

Wageningen University & Research

Enlarging the alcohol dehydrogenase applications in organic synthesis with nicotinamide cofactor biomimetics

15/02/2019

MSc thesis ORC

ORC-80436

Sophie de Smet: sophie.desmet@wur.nl
930611773130

Supervision ORC

Alice Guarneri: alice.guarneri@wur.nl
Caroline E. Paul: C.E.Paul@tudelft.nl

Abstract

The classical synthetic methods in the chemical industry are shifting towards the use of greener methods [1]. Whereas classical chemical redox reactions use heavy metal based reagents, white biotechnology uses the enzymes produced by microorganisms for the catalysis of redox reactions. The enzymes found in nature provide advantages over the classical synthetic methods, as they show a high selectivity and specificity towards their substrates [2]. Alcohol dehydrogenases (ADHs) are considered to be valuable catalysts in organic synthesis. They catalyse the reversible conversion of primary and secondary alcohols into aldehydes and ketones. This project focuses on a zinc dependent ADH from the thermophilic *Thermus* sp. ATN1 that has potential as a biocatalyst because of its broad substrate spectrum, and high conversion rates with primary alcohols and aldehydes. The isolation of TADH from this thermophilic bacterium, gives this enzyme the advantage that it can catalyse redox reactions at high temperatures, and the purification steps are easier [3]. There are still some hurdles to overcome to enable the use of ADHs on an industrial scale. One of them is the dependency on nicotinamide adenine dinucleotide (NAD) cofactor, as these hydrogenases use the NAD^+/NADH or $\text{NADP}^+/\text{NADPH}$ as a coenzyme. The challenge of using NAD as a cofactor is its sensitivity and it is too expensive for its stoichiometric use in industrial procedures [4].

In this study a library of synthetic analogues of NAD(H), which are called nicotinamide cofactors biomimetics (NCBs) were created. Their design should allow the mimics to replace the natural cofactor NAD(H). TADH should therefore be able to perform catalytic reactions in the presence of the NCB, and in addition lead to an economically feasible alternative for industrial purposes. In this study transformation of an *E. coli* BL21 (DE3) strain with a plasmid containing the TADH gene has led to successful expression by the host organism. The TADH enzyme was purified using anion exchange and gel permeation chromatography leading to a final yield of 2.9 mg of relatively pure TADH. The viability of two reduced NCBs, namely 1-Carbamoylmethyl-1,4-dihydronicotinamide (AmNAH) and 1-benzyl-1,4-dihydronicotinamide (BNAH) as a cofactor for TADH in bio-catalytic reactions was studied.

It has been shown that using the excited states of common cofactors, new reactivity from existing enzymes could be created. This was done by using photo-induced bio-catalytic techniques to create excited states of NAD(P)H and non-natural substrates [2]. Therefore, the conversion of cyclohexanone to cyclohexanol by TADH in the different light conditions (wavelengths from 400-700 nm and 300-700 nm) and in presence of the natural cofactor NADH or the analogues AmNAH and BNAH were measured by gas chromatography. Cyclohexanone was reduced to cyclohexanol by TADH for all reactions in which the natural cofactor NADH was provided. Among those, no significant differences in conversion could be detected for the different light conditions. The reaction in the presence of AmNAH and BNAH was also not improved by light excitation, since no conversion of cyclohexanone to cyclohexanol was detected, both in dark and light conditions. Therefore we postulate that the current mimics AmNAH and BNAH are not accepted as a cofactor by the TADH enzyme.

Abbreviations

ADH	: alcohol dehydrogenase
AmNAH	: 1-Carbamoylmethyl-1,4-dihydronicotinamide
BCA	: bicinchoninic acid bovine serum albumin
BNAH	: 1-benzyl-1,4-dihydronicotinamide
BSA	: bovine serum albumin
COSY	: correlation spectroscopy
HSQC	: heteronuclear single quantum coherence
GC	: gas chromatography
GPC	: gel permeation chromatography
HP	: heat purification
LB medium	: lysogeny broth medium
NMR	: nuclear magnetic resonance
pTADH	: plasmid TADH
SDS-page	: sodium dodecyl sulphate polyacrylamide gel electrophoresis
SE(C)	: size- exclusion (chromatography)
AEX	: anion- exchange chromatography
TADH	: thermostable alcohol dehydrogenase from <i>Thermus</i> sp. ATN1
NCB	: nicotinamide cofactor biomimetic
NAD(P)(H)	: nicotinamide adenine dinucleotide (phosphate) :
TAE buffer	: tris-acetate-EDTA
TB medium	: terrific broth medium

Table of content

Abstract.....	0
Abbreviations.....	2
1 Introduction	5
1.1 Scientific relevance	5
1.2 NADP ⁺ /NADH as a cofactor	5
1.3 Alcohol dehydrogenase (ADHs)	6
1.4 ADH from <i>Thermus</i> sp. ATN1 (TADH).....	7
1.5 Nicotinamide cofactor biomimetics (NCBs).....	8
1.6 Photo-induction	9
1.7 Objectives.....	10
2 Materials and methods.....	11
2.1 Synthesis of the NCBs	11
2.2 TADH expression with pTADH, obtained from Aarhus University	13
2.2.1 Transformation of <i>E. coli</i> BL21 DE3 with pTADH	13
2.2.2 TADH expression: restriction analysis.....	14
2.2.3 TADH expression: SDS-page analysis	14
2.2.4 TADH large scale expression	14
2.2.5 Cell lysis.....	14
2.2.6 Anion-exchange chromatography (AEX).....	15
2.3 TADH expression from pTADH obtained from TU Delft.....	15
2.3.1 Large scale expression	15
2.3.2 Cell lysis.....	15
2.3.3 Heat purification	16
2.3.4 Size-exclusion chromatography (SEC).....	16
2.3.5 Out of the 15 mL, 5 were submitted to a second heat purification step. Enzyme activity	16
2.3.6 Determination of total protein with BCA assay	17
2.3.7 Protein analysis SDS-page	17
2.4 TADH biocatalysed conversion of cyclohexanone in the presence of NADH, AmNAH BNAH in different light conditions	17
3 Results.....	19
3.1 Synthesis of the NCBs	19
3.2 TADH expression	19
3.3 TADH purification.....	22
3.3.1 Anion exchange chromatography (AEX)	22
3.3.2 Size-exclusion (SE) with gel permeation chromatography (GPC)	24
3.3.3 Determination of total protein	26

3.4	TADH bio-catalysed conversion of cyclohexanone in the presence of NADH, AmNAH and BNAH in different light conditions	27
4	Discussion.....	29
5	Conclusion.....	32

1 Introduction

1.1 Scientific relevance

The pharmaceutical industry is in a large part dependent on the use of synthetic organic chemistry. This industry uses redox reactions for the production of active pharmaceutical ingredients or their precursors. In oxidation and reduction reactions, oxidizing and reducing agents are needed to enable the reaction to occur. Traditional chemical oxidation uses metal based reagents, like chromium, osmium and other compounds. The chemical industry is nowadays shifting towards the use of greener methods [5]. White biotechnology makes use of enzymes produced by microorganisms as catalysts for many chemical reactions, such as redox reactions. The use of bio-catalysis has shown to be a potential tool to make chemical processes greener [1].

1.2 $\text{NADP}^+/\text{NADH}$ as a cofactor

For the enzyme-catalysed redox reaction to occur, there is often need for a cofactor. In nature several important coenzymes have been reported, which are mostly derived from vitamins. Many oxidoreductases are nicotinamide adenine dinucleotide (NAD) dependent enzymes, which use the $\text{NAD(P)}^+/\text{NAD(P)H}$ as coenzymes. Electron transfer can directly take place between the coenzymes and the substrates, although there are many cases in which there is need for intermediary redox cofactors [6]. NAD(P)^+ has the ability to obtain a hydride (H^-), donated by a substrate in an oxidoreductase catalysed reaction. After transfer of the hydride the cofactor will be in its reduced form NAD(P)H . The nicotinamide ring of the coenzyme is directly involved in the transfer of electrons in oxidoreductase catalysed reactions. The C4 carbon in the nicotinamide ring functions as the actual proton donor/acceptor. $\text{NADP}^+/\text{NADPH}$ are the phosphorylated forms of NAD^+/NADH , in which a phosphate group is attached to adenosine monophosphate in the molecule [7]. The addition of a phosphate group does not interfere with the capability of electron transfer because of the large distance towards the electron transfer region. However, it does interfere with the structure of the coenzymes. The differences in specificities towards the phosphorylated and non-phosphorylated coenzymes by oxidoreductases can be explained by this structural difference. The ability to bind NAD^+ can be deduced from the 3D structure of dehydrogenases, which share highly conserved recognition domains such as the Rossmann fold. In addition, NAD^+ shows nearly the same conformation when bound within different dehydrogenases [4]. The NADH molecule as found in nature is capable of fluorescent emission at 430-445 nm when it is excited at 340 nm [8].

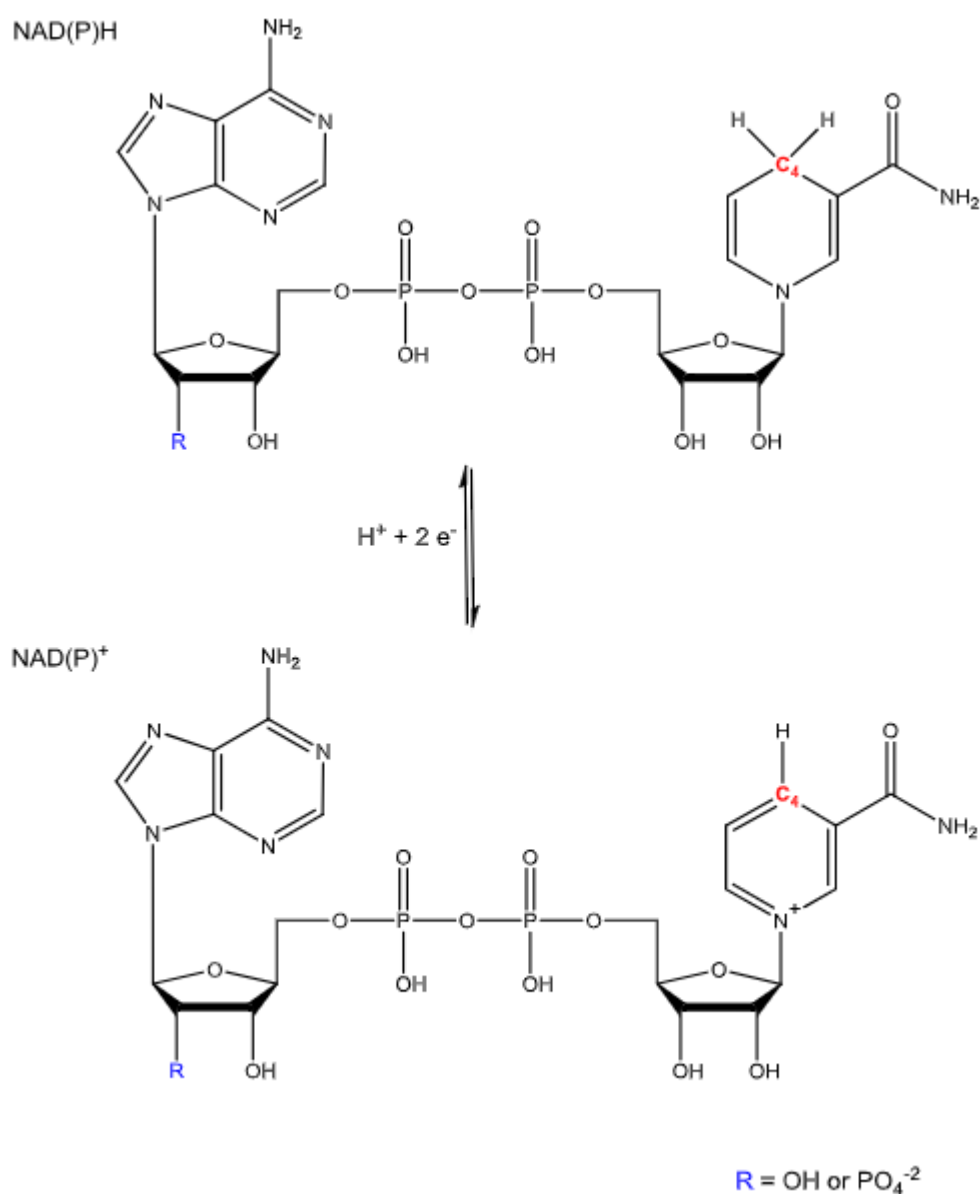


Figure 1: Natural nicotinamide cofactor NAD(P)H and NAD(P)⁺ in their reduced (top) and oxidized form (bottom). The reactions, consisting in giving or receiving a hydride at the carbon C-4 of the pyridine ring and thereby moving two electrons, is shown. The phosphorylated forms contain a phosphate group at the position C2 of the adenosine moiety, indicated with 'R'. Figure taken from [7].

1.3 Alcohol dehydrogenase (ADHs)

Alcohol dehydrogenases (ADHs) belong to the group of oxidoreductases (EC 1). ADHs are enzymes that catalyse the reduction of the carbonyl group of aldehydes or ketones to form primary and secondary alcohols, respectively (Figure 2) [7]. The cofactors NAD(P)H are the direct electron donors/acceptors that catalyse the interconversion of alcohols to aldehydes/ketones [6]. This reaction is a reversible process, which the enzymes can potentially catalyse in both directions. In practice the direction is largely dependent on thermodynamics, concentration of substrates, products and the availability of cofactors [7]. The reductive reactions are used for the generation of stereocenters, whereas the reversed oxidative reaction, is used for the deconstruction of a chiral centre. Applications are found in the production of commercially available drugs, for example statin [9]. The medium-chain alcohol dehydrogenases (MDRs) are a family of ADHs, that need zinc as a cofactor which is involved in

substrate activation. The Zn^{2+} ion plays a role in the catalytic mechanism. By ligation of the substrate to this ion, the activation energy of the reaction is lowered, causing an effect on the reactivity of the substrate [10]. The zinc ion is meant to reduce the electron density at the carbonyl carbon, by coordinating with the carbonyl oxygen of the substrate [11] [7]. In MDRs, the Zn^{2+} coordination in absence of substrate takes place by the binding to a water molecule and three residues to construct a tetrahedral geometry. In oxidation reactions, the water molecule is displaced from the Zn^{2+} when the alcohol substrate binds to the enzyme. Next, a proton is transferred from the alcohol substrate to the solvent, by which an alkoxide intermediate is formed. This intermediate is stabilised by the catalytic Zn^{2+} ion, a hydride is then transferred to the oxidised cofactor by the alkoxide, which consequently forms a ketone/aldehyde [7].

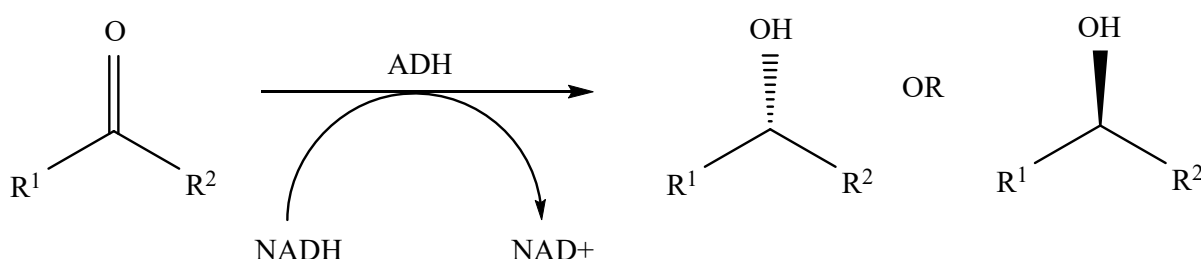


Figure 2: Redox reaction catalysed by a NAD^+/NADH dependant ADH, the carbonyl group of the substrate is reduced to form an alcohol group.

Alcohol dehydrogenases have been isolated from several organisms, showing differences in the accepted substrates, which gives a spectrum that can be narrow or broad, and selective for certain functional groups (i.e. aldehyde or ketones).

1.4 ADH from *Thermus* sp. ATN1 (TADH)

In this project a metal containing ADH from *Thermus* sp. ATN1 (TADH) was expressed and purified. The isolation of TADH from this thermophilic bacterium, gives the advantage that it can catalyse redox reactions at high temperatures, and the enzyme purification steps are easier since heat purification is possible without activity loss [3]. In addition to this advantages, TADH has a broad substrate spectrum, it can accept primary, secondary and cyclic alcohols and shows highest conversion rates with primary aliphatic alcohols (for oxidation reactions) and short aliphatic aldehydes (for reduction reactions) [12]. In this project cyclohexanone was used as a substrate, which has already been proven to be a good substrate in the reductive direction. In this reaction, the TADH catalyses the reduction of cyclohexanone to form cyclohexanol, which can be measured by the consumption of NADH. For the reduction of cyclohexanol, a specific activity of 15.14 U/mg was shown by Höllrigl et al (measured at 60 °C, pH 6) . Another interesting characteristic of TADH that makes it valuable as an biocatalyst is its selectivity in yielding high enantiomeric excess (S-enantiomer), which is essential in organic synthesis [3].

A crystal structure of TADH is available thanks to Henry Man et al. (PDB ID 4CPD) [13]. The TADH enzyme consists of four subunits A, B, C and D, that form a homotetramer. This structure is composed of two dimers as the monomers A-B and the monomers C-D are closely associated. The subunits consist of 347 residues and have a mass of 37.2 kDa each [3]. The monomers have two characteristic domains, the catalytic (metal binding) domain and the nucleotide-binding domain (Rossman fold) [13]. In Figure 3 the homotetrameric structure of TADH is illustrated including the binding of NAD and the

Zn^{2+} ions. A difference is made between catalytic zinc and structural zinc, the first is bound by a tetrahedral structure of three specific residues (Cys38, His 59 and Asp152) and an additional water molecule. The structural zinc is described to be bound by four cysteines (89, 92, 95 and 103) [12].

NADH binds to TADH in a crevice between the catalytic domain and the nucleotide-binding domain where the substrate can access. The nicotinamide ring of the NADH is placed at the bottom of the crevice, when cofactor binding takes place the two domains move slightly towards each other. Ser40, an amino acid located in the active site, seems to be the possible proton donor in the reductive catalysis. An interaction between the amide carbonyl of the nicotinamide ring with residue Ala239 in the TADH secures the binding. The active site of TADH is largely hydrophobic [13].

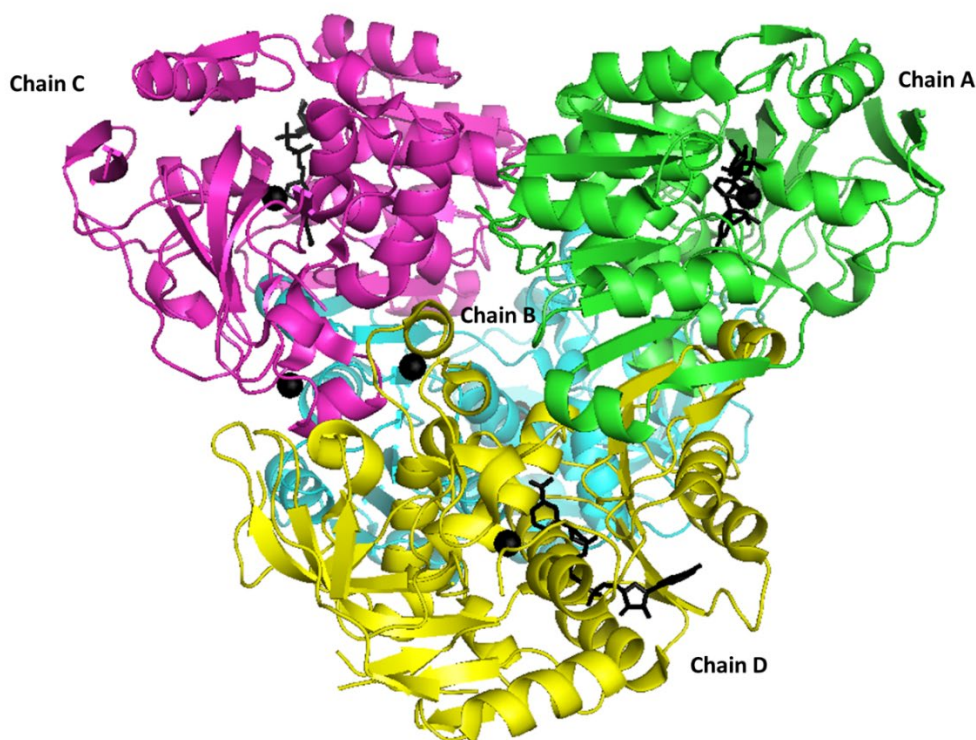


Figure 3: Homotetrameric structure of TADH, consisting of four monomers (ribbons) A,B C and D in green, blue purple and yellow respectively. In this crystal structure NADH is bound only to the subunits A C and D, shown as black sticks. The zinc is depicted as black spheres. The structure of TADH was obtained from [13]

1.5 Nicotinamide cofactor biomimetics (NCBs)

The challenge of using NAD as a cofactor is its sensitivity, it is easily broken down by undesired

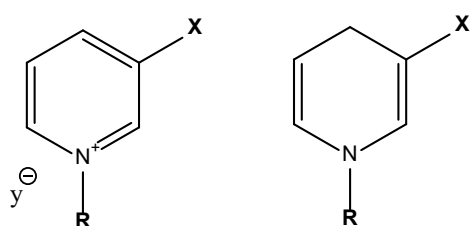


Figure 4: Oxidised an reduced forms of NCBs, the X and R groups can be varied.

reactions and it is too expensive for its stoichiometric use in industrial procedures. A possible solution is the creation of synthetic analogues of NAD, which are called nicotinamide cofactors biomimetics (NCBs). The mimics should be able to replace the natural cofactor, and therefore allow the redox enzyme (in this project TADH) to catalyse redox reactions. The reactive part, the nicotinamide ring, which is a pyridine derivative from the vitamin niacin, will therefore be present [4].

The structures of oxidised and reduced forms of the NCBs can be seen in figure Figure 4, the X and R substituents are varied in the design of NCBs. The X substituent is described to be essential for the coordination and redox potential, whereas the R substituent is essential for the enzyme binding [6]. Thus their simpler structure could allow a more economically feasible and stable alternative to NAD(H) for use in bio-catalysis. The NCBs are divided into two categories; the semi-synthetic and truncated (synthetic) NCBs. The production of synthetic NCBs starts from commercially available pyridine derivatives, which are chemically converted to the desired final NCBs. The production of semisynthetic NCBs starts from the natural cofactor to produce the final NCBs, these cofactors resemble the more natural counterparts since the sugar or adenine moieties are still present [4]. The creation of NCBs in this project will follow the methods for synthetic production, as this is a more economically feasible strategy.

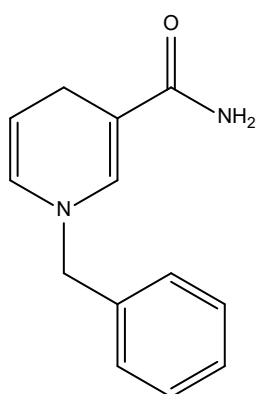


Figure 5: structure of BNAH

Flavin-dependant oxidoreductases are enzymes that are more indirectly dependant on NAD(P)H than ADHs, which show acceptance to a wide variety of synthetic cofactors. 1-benzyl-1,4-dihydronicotinamide (BNAH, Figure 5), a NCB already proposed by Mauzerall et al in 1955, had shown the ability to replace NADH as a natural cofactor by flavin-dependant oxidoreductases as well as reactions catalysed by ADHs [14] [15]. The acceptance of BNAH by ADHs was questioned by Paul et al. they state the apparent enzyme activity could be due to the presence of a regeneration system that uses BNAH to recycle NAD(H). The presence of NAD(H) was caused by the use of ADHs which were not purified from their natural cofactor [15].

In 2014, Paul et al. suggested that the poor acceptance of simple synthetic NCBs by ADHs is caused by the catalytic mechanism of the enzymes. The cofactor directly accepts or donates an hydride from or to the substrate. Likely, for the cofactor to bind the ADH, a phosphate group is necessary. Another suggested reason for the poor acceptance is the positioning of the NCBs in the ADH. Overall, semisynthetic NCBs are well accepted by ADHs, contradictory to synthetic NCBs, which were not accepted by ADHs as cofactors [4]. However, the acceptance could be increased by optimising the design of the NCBs or the option of photo-induction could be considered.

1.6 Photo-induction

NADH has unique photo physical properties, in its ground state it is only known for its hydride transfer. When the NADH is photo-excited it gains the capability to transfer single electrons and therefore reduce several functional groups [2]. Emmanuel et al. describe the potential of using light to excite the biological cofactor NAD(P)H, bound in the active site of a ketoreductase (KRED) enzyme. When the excited states of the bound NAD(P)H were created, new reactivity from the enzyme was accessed. Ketoreductase is a NAD dependant dehydrogenase that normally reduces carbonyl groups, by photoexcitation it gained new reactivity and was changed into an initiator of radical species and a chiral source of hydrogen atoms [2] [16]. Gargiulo et al. have shown that photo-excited flavin catalyst could be created by irradiation with visible light. The rate of flavin-mediated NAD(P)H oxidation could be accelerated by two-fold [17]. Also non-enzymatic photo-induction has been shown possible. BNAH under irradiation $\lambda > 300$ nm has shown that it could function as a catalyst for the hydrogenation of

various di-aromatic α,β -epoxy ketones to β -hydroxy ketones. If the design of the NCBs allows for photo-induction, the NCB may be activated within the enzyme to catalyse redox reactions [6].

1.7 Objectives

In this study a library of NCBs was created. Expression and purification of TADH from *E. coli* BL21 (DE3) was established. The NCBs AmNAH and BNAH were tested on their viability as a cofactor for TADH in the bio-catalytic conversion of cyclohexanone to cyclohexanol. The effect of photo-induction at wavelengths from 400-700 nm and 300-700 nm on the bio-catalytic reactions was studied.

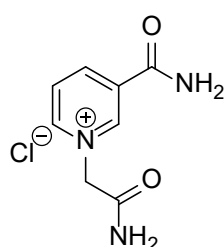
2 Materials and methods

Materials

All the materials were obtained from the Organic Chemistry department and Biochemistry laboratories department of Wageningen University & Research. All chemicals were purchased from Sigma-Aldrich (Merck) or Alfa Aesar and were used without further purification unless otherwise specified. The natural nicotinamide adenine dinucleotide cofactors, both oxidized and reduced, were purchased from Prozomix.

2.1 Synthesis of the NCBs

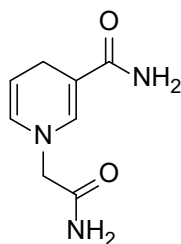
1-Carbamoylmethylnicotinamide chloride (AmNA^+Cl^-)



AmNA^+Cl^-

AmNA^+Cl^- was already available.

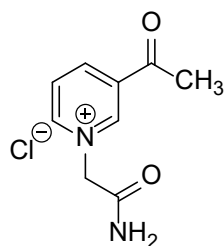
1-Carbamoylmethyl-1,4-dihydronicotinamide (AmNAH)



AmNAH

The reduction of AmNAH was performed by the addition of AmNA^+Cl^- (10 mmol, 1.8 g), Na_2CO_3 (20 mmol, 10.6 g) and $\text{Na}_2\text{S}_2\text{O}_4$ (22.5 mmol, 19.6 g) to 75 mL of milli-Q. The reaction was stirred under nitrogen flow for 20 minutes at room temperature after which it was placed on ice for five minutes (continued stirring), and filtered over vacuum. The obtained product was recrystallized from cold milli-Q (yield 1.2 g, 14.2%)

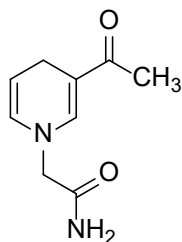
1-Carbamoylmethyl-3-acetyl chloride (AmAP^+Cl^-)



AmAP^+Cl^-

3-acetylpyridine (120 mmol, 13.19 ml) was added to 2-chloroacetamine (120 mmol, 11.22 g) in 60 mL acetonitrile while stirring at 60°C. After dissolving, the reaction was continued for 22 hours. The mixture was cooled to room temperature and placed on ice for 45 minutes after reaching room temperature. The precipitate was washed multiple times with cold diethyl ether and filtered over vacuum. The resulting powder was dried for four hours in vacuum at 60°C (yield 25.8 g, 47%). 2 grams of this compound were used for recrystallization from 1:1 methanol/acetone in a total volume of 40 mL. The mixture was placed in the fridge for two days. Brown crystals formed, which were washed with cold diethyl ether and filtered over vacuum (yield 0.86 g, 43%).

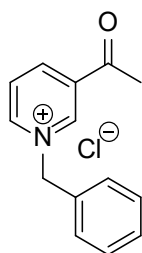
1-Carbamoylmethyl-3-acetyl-1,4-dihydropyridine (AmAPH)



AmAPH

Several methods have been performed for the reduction of AmAP^+Cl^- , however none of the attempts have led to the formation of the desired compound. The reduction reactions were, as for the other NCBs, performed by the addition of Na_2CO_3 and $\text{Na}_2\text{S}_2\text{O}_4$ to the oxidised NCB AmAP^+Cl^- . As a solvent milli-Q or a 2:1 mixture of milli-Q and DCM have been attempted, which have both led to the formation of an impure compound. Recrystallization from ethyl acetate, DCM or MQ have not led to the extraction of the product.

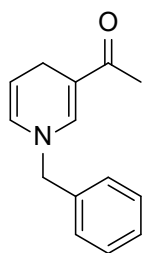
1-benzyl-3-acetylpyridinium chloride (BAP^+Cl^-)



BAP^+Cl^-

3-acetylpyridine (60 mmol, 6.6 ml) was added to benzyl chloride (62 mmol, 7.13 ml) in 103 mL acetonitrile while stirring and at 60°C . After dissolving, the reaction was continued for 24 hours. The precipitate was washed multiple times with cold diethyl ether and filtered over vacuum. The resulting powder (yield 4.84 g, 33%) was dried overnight under vacuum over phosphorus pentoxide.

1-benzyl-3-acetylpyridinium chloride (BAPH)

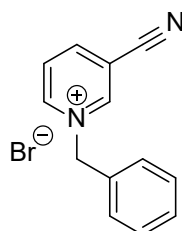


BAPH

17%).

The reduction reaction was performed by adding BAP^+Cl^- (30 mmol, 7.48 g) to Na_2CO_3 (127 mmol, 13.46 g) and $\text{Na}_2\text{S}_2\text{O}_4$ (120 mmol, 20.94 g) in 180 mL milli-Q. After dissolving, the reaction was stirred under nitrogen in the dark on ice for 7 hours and incubated in the fridge overnight. Next day, the product was washed with cold milli-Q over vacuum and dried over phosphorus pentoxide over the weekend (yield 2.5 g, 38%). 1 gram of the product was recrystallized from 100 ml MQ, by the slow addition of a ethanol (10 mL), the mixture was filtered and placed in the fridge for four days. Yellow crystals formed, which were washed with cold milli-Q and filtered over vacuum (yield 0.17 g,

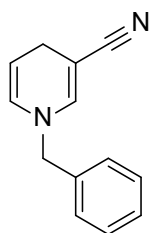
1-benzyl-3-cyanopyridine bromide (CNNA^+Br^-)



CNNA^+Br^-

3-pyridinecarbonitrile (40 mmol, 4.16 g) was dissolved in 40 mL acetonitrile and benzyl bromide (40 mmol 4.8 mL) was added. The reaction was performed under stirring at reflux conditions, for 15 hours. The reaction mixture was cooled to room temperature and the precipitate was washed multiple times with cold diethyl ether and filtered over vacuum. The resulting powder was dried overnight under vacuum over phosphorus pentoxide (yield 15.2 g, 85%)

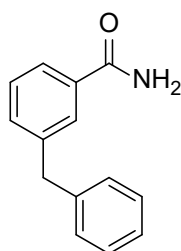
1-benzyl-3-cyano-1,4-dihydropyridine (CNNAH)



CNNAH

The reduction of CNNA^+Cl^- was performed by adding CNNA^+Cl^- (10.9 mmol, 3 g) to NaHCO_3 (36.4 mmol, 3.06 g) and $\text{Na}_2\text{S}_2\text{O}_4$ (43.6 mmol, 7.59 g) in 60 mL milli-Q. After dissolving, the reaction was stirred under nitrogen in the dark at room temperature for 3 hours. The product was washed with cold milli-Q over vacuum and dried over phosphorus pentoxide under vacuum overnight. A product was obtained with a higher yield than 100% and was therefore excluded.

1-benzyl-1,4-dihydronicotinamide (BNAH)



BNAH

BNAH was already available.

Of the synthesised NCBs ^1H -NMR, ^{13}C -NMR, COSY and HSQC spectra were recorded on a Bruker Avance III 400 NMR spectrometer at 400 MHz. The internal reference to residual proton signals were set corresponding to the solvent, either $\text{C}_2\text{D}_6\text{OS}$ or D_2O . Chemical shifts (δ in ppm) and their multiplicity (s = singlet, d = doublet, t = triplet, m = multiplet), the coupling constant (J values in Hz), integration and assignment are given in the Appendix.

2.2 TADH expression with pTADH, obtained from Aarhus University

2.2.1 Transformation of *E. coli* BL21 DE3 with pTADH

First, *E. coli* BL21 DE3 cells were grown in 6 mL of LB medium overnight at 37 °C. Next day, a small volume was transferred to fresh LB medium and incubated at 37 °C for 3 hours. To make competent cells, 200 μL 0.1 M CaCl_2 was added to 1.2 mL of the cell culture and placed on ice for another 3 hours. The competent cells were transformed with plasmid TADH (pTADH). 200 ng (1 μL) of the plasmid was added to the cells and placed at 42 °C for 2 minutes, after which they were grown for one hour at 37°C in LB medium. 30 μL this medium was spread on LB agar with 100 $\mu\text{g}/\text{mL}$ ampicillin. The remaining medium was centrifuged to collect all cells present and spread on a second LB agar plate with 100 $\mu\text{g}/\text{mL}$ ampicillin. The plates were incubated overnight at 37 °C. The next day, only one single colony was obtained from the plate inoculated with the highest culture concentration. The colony was used to prepare a streak-plate on LB agar with 100 $\mu\text{g}/\text{mL}$ ampicillin which was incubated overnight at 37 °C. The streak-plate was used to confirm the presence and structure of the plasmid and for the expression of TADH.

2.2.2 TADH expression: restriction analysis

One colony of the streak-plate was transferred to 6 mL LB medium 100 µg/mL ampicillin overnight at 37 °C to subject it to plasmid analysis. 2 mL of this culture was used for plasmid DNA isolation using the ThermoFisher plasmid DNA miniprep kit & protocol. Restriction analysis was performed on the isolated plasmid DNA as well as the plasmid DNA used in the transformation (starting material) using restriction enzymes BamHI, PstI and EcoRV. A mixture of 7 µL plasmid DNA, 1 µL of the restriction enzyme(s), 2 µL 10x reaction buffer 3 (Invitrogen) and 10 µL (9 µL for restriction with two enzymes) Milli-Q were placed at 37 °C for 1 hour. The reaction was stopped by placing the samples at 65 °C for 15 min. Restriction enzymes were chosen based on structure of the TADH vector as described by Hollman et al [18], depicted in Figure 7. and Figure 18. A 1% agarose gel was prepared, 4 µL of 6x loading buffer was added to the samples, 1 kb DNA marker was applied on the gel for size-comparison. The gel was applied at 80 V in 0.5 TAE buffer and run for 1.5 hours.

2.2.3 TADH expression: SDS-page analysis

Several colonies from this streak-plate (section 2.1.1) were used to inoculate 200 ml overnight express instant TB medium (EMP Millipore Corp), in order to check TADH activity. The medium was incubated at 37° C, 130 rpm overnight. The 200 ml medium was centrifuged at 10.000 rpm at 4° C for 15 minutes, and the cell pellet was dissolved in 20 mM TrisHCl buffer pH 7.5. This mixture was incubated at 80°C for 20 minutes, to lyse the cells and increase the solubility of the TADH. The insoluble fraction and precipitated proteins were separated by centrifugation at 22.000 rpm at 4°C, expected is that the TADH will be in the supernatant. However not only the supernatant was analysed with SDS-page, also the pellet fraction was analysed to check for the presence of TADH (SDS-page analysis performed as described in section 17). The pellet fraction was therefore dissolved in 20 mM TrisHCl buffer pH 7.5.

2.2.4 TADH large scale expression

After the conformation of TADH expression by the *E. coli* BL21 DE3 the expression of TADH was performed on a larger scale. First a pre-culture was prepared by inoculating 8 mL TB medium with 100 µg/mL ampicillin with a single colony from the streak-plate (section 13) and incubated at 37 °C, 180 rpm. Next day, the pre-culture was incubated on ice to prevent the cells from lysis. 1800 mL of overnight express instant TB medium (EMP Millipore Corp) was autoclaved for 15 minutes at 121°C. The fermentation was performed in four Erlenmeyers, each containing a volume of 450 mL medium with a final concentration of 100 µg/mL ampicillin and 1% glycerol. The flasks were inoculated with 0.5 mL of the pre-culture and incubated for 24 hours at 37 °C at 130 rpm. Next day the cultures were harvested by transfer to flasks following centrifugation at 8000 rpm (rotor JA10) for 15 minutes. The cell pellets (around 2 grams of cell pellet was obtained for every 450 mL culture) were washed in 5 mL 50 mM Tris HCl pH 7 by centrifugation at 5000 x g for 15 minutes. The cells pellets were combined and dissolved in a total volume of +/- 32 mL of 20 mM Tris HCl pH 7.5 to which MgCl₂ was added to a final concentration of 25 mM, 2 spoontips of DNaseI inhibitor and a 2 tablets of protease inhibitor were added to prepare the cell pellets for cell lysis using French press.

2.2.5 Cell lysis

The solution of the cell pellets obtained as described were applied three times to 1000 PSI using a French press and placed at heat block of 80 °C for 20 minutes following centrifugation for 45 min, 22000 rpm (rotor 25.50 JA) at 6°C. Since the pellet fraction after centrifugation was also expected to

contain TADH, this fraction was again dissolved in 20 mM Tris HCl pH 7.5. Both fractions with a total volume of +/- 64 mL were subjected to anion-exchange chromatography.

2.2.6 Anion-exchange chromatography (AEX)

AKTA system anion exchange with a 15Q column was used to purify TADH from the pellet and supernatant fraction. To remove all solid parts before applying, the samples were centrifuged at 4°C rotor 25.50 JA 18000 rpm for 20 minutes. 1-butanol was added to a final concentration of 10 mM to facilitate the purification. A buffer solution of 20 mM Tris HCl pH 7 was used. For the elution the same buffer but with the addition of 1 M NaCl, was used. A 180 mL gradient with a flow of 0.7 mL/min was applied while collecting 45 fractions of 4 mL. Enzyme activity was determined (see section 16) for all fractions that showed a peak in the absorbance at 280 nm, and the samples were subjected to SDS-page analysis (section 17). The fractions that contained TADH were combined and concentrated over an Amicon filter with a 10 kDa molecular weight cut-off, by centrifugation at 4000 x g until a final volume of around 3 mL was obtained. To remove the remaining NaCl salt, the sample was subjected to dialysis in a membrane cartridge placed in 2L 20 mM Tris HCl pH 7 at 3°C for 24 hours.

2.3 TADH expression from pTADH obtained from TU Delft

2.3.1 Large scale expression

Because TADH expression and purification did not lead to a high yield of TADH, cell pellets were obtained by expression of TADH in *E. coli* BL21 DE3 pTADH as performed by Caroline E. Paul: a preculture was prepared in a 4 x 5 mL LB medium with 100 µg/mL by adding small dot of cells from a glycerol stock. The tubes were placed in a platform shaker, at 37 °C, 180 rpm, overnight. Next day, two 2L erlenmeyers with 500 mL Novagen overnight express instant TB with 100 µg/mL were incubated with 5 mL of pre-culture in a platform shaker at 37 °C and 180 rpm for 6 hours, the temperature was decreased to 30 °C for 25 hours. The solution was centrifuged at 10 000 rpm for 20 min (at 4 °C). The supernatant was discarded and the cell pellets were re-suspended with minimal amounts of buffer 10 mM Tris-HCl pH 7.5, combined, and centrifuged at 10 000 rpm for 20 min (at 4 °C). The supernatant was discarded. The cell pellet obtained was re-suspended, transferred to a 50 mL falcon tube, and centrifuged at 4 000 rpm for 30 min (at 4 °C). The supernatant was discarded. The cell pellet weighed about 11 g and was frozen at -80 °C, and sent to Wageningen.

2.3.2 Cell lysis

From this material the obtained cell pellets could be immediately subjected to TADH purification, starting with cell lysis. The obtained 11 mL of cell pellet was thawed and diluted 3.5 times by the addition of 38.5 mL 20 mM kPi buffer pH 7.5. To prepare the sample for cell lysis the following mixtures were added; 1.6 mL of 0.5 M MgCl₂, a protease tablet (first dissolved in 500 µL buffer) and a spoon tip of DNaseI. Three times around 8000 PSI was applied to the cell mixture using a French press following centrifugation at 6°C for 45 min at 22,000 rpm (rotor JA 25.50) leaving a pellet supernatant fraction. The fractions were collected separately, the cell pellet was re-dissolved in a small volume of buffer.

2.3.3 Heat purification

Both the pellet and the supernatant fraction were incubated on a heat block of 80 °C for 20 minutes following centrifugation for 45 min, 22000 rpm at 6°C. Centrifugation of both samples (supernatant and pellet fraction) again lead to the formation of a supernatant and a pellet fraction. These two samples were collected. The two supernatant fractions after heat purification and centrifugation were combined to give a total volume of +/- 72 mL to which the sample containing 3 mL of TADH solution as obtained by AEX was added. This solution was applied to Amicon filter tubes with a cut-off of 10 kDa to concentrate the enzyme solution to a total volume of 2 mL, the amount that is needed to perform size exclusion by gel-filtration chromatography. The Amicon tubes were centrifuged at 5000 x g until the samples reached a total volume of around 2 mL. During concentrating a mistake was made, leading to the use of sample from only one of the two tubes, while the others underwent a second heat purification step. The concentrated sample was centrifuged 7000 rpm for 2 min at 4 °C to leave a clear solution that should be used for SEC.

2.3.4 Size-exclusion chromatography (SEC)

AKTA system was used to perform gel chromatography with a Superdex 75 26/60 column, which was equilibrated with 50mM kPi buffer with 150 mM KCl, pH 7, following elution with 300 mL (2 mL/min) of the same buffer, collecting 10 mL fractions. The enzyme activity was measured and analysed with SDS-page as described in section 14 the TADH containing fractions (3*10 mL) were combined. The combined TADH sample was concentrated by centrifugation at 4°C, 3000 xg with an Amicon filter with a 10 kDa cut-off to a total volume of 15 mL. Dialysis was performed on the concentrated sample to remove KCl from the concentrated sample. This was done by applying it to a Thermofisher snakeskin membrane with a 10.000 MWCO and placing the membrane in 1L kPi 50 mM pH 7. After 4 hours at 4°C the membrane was transferred to fresh 1L kPi 50 mM pH 7 buffer. 5 mL from the 15 mL sample was subjected to a second heat purification step (80 °C for 20 minutes).

2.3.5 TADH activity

The enzyme activity measurements were performed in 10 mM 1-butanol, 1 mM NAD⁺ in 50 mM Tris HCl buffer at pH 9 and the addition of 10 µL enzyme solution. The reactions were performed at 60 °C in a 1 cm cuvette with a total volume of 1 mL sample, measuring at a wavelength of 340 nm (conversion of NAD⁺ to NADH). Kinetic measurements were performed with Carry 300 Bio UV-Vis spec at 60 °C. From the kinetic measurements the TADH concentration was calculated, using the parameters as follows:

Lambert-Beer law= $A = \epsilon lc$,

A= absorbance

ϵ (the extinction coefficient of NADH at 340 nm)= 6220 M/cm

l= cuvette length (1 cm)

c = concentration in M

U=1*10⁻⁶ mol/min

To estimate the concentration of TADH present in the samples the calculated U/mL were compared with the TADH activity of 29.5 U/mg that is described by Höllrigl et al., for the conversion of 1-butanol at pH 9, at 60°C [3].

2.3.6 Determination of total protein with BCA assay

For the total protein determination on the TADH sample as obtained by SEC and AEX, the Thermo Scientific Pierce BCA Protein Assay Kit was used. A bovine serum albumin (BSA) dilution series with concentrations of 2000 µg/mL, 1500 µg/mL, 1000 µg/mL, 750 µg/mL, 500 µg/mL, 500 µg/mL, 250 µg/mL, 125 µg/mL, 25 µg/mL and 0 µg/mL were used. The TADH sample was used undiluted and diluted 2x, 5x 10x and 100x in 50 mM kPi buffer with a pH 7. 200 µL of a 50:1 dilution of BCA reagent A:B was added to 25 µL of the samples, in a 96-well plate and incubated at 37°C for 30 minutes. The absorption of the samples was measured at 562 nm.

2.3.7 Protein analysis SDS-page

Samples that were subjected to sodium dodecyl sulfate (SDS) polyacryl amide gel electrophoresis (page) were diluted 1:1 with SDS-page loading buffer with 5% β-mercaptoethanol and incubated for 10 minutes at 100°C. Analysis was performed using 12% polyacryl amide gels, prepared as instructed by the manufacturer's protocol (BIO-RAD). As protein standard Precision Plus Protein™ Dual Color Standards (BIO-RAD) was used. The proteins were separated by applying the gel to 100 V (30-40 mA) for 1.5 hours. Gels were stained with Coomassie.

2.4 TADH biocatalysed conversion of cyclohexanone in the presence of NADH, AmNAH BNAH in different light conditions

To study the TADH catalysed reaction with 1-Carbamoylmethyl-1,4-dihydronicotinamide (AmNAH), the solution of TADH in 50 mM kPi buffer pH 7 was added to contain 100 µg/mL of TADH in 1 mL final volume. The reaction was performed in a GC vial with 5 mM cyclohexanone as substrate and either 10 mM AmNAH (0.0018g), 10 mM NADH (0.0072 g) or 10 mM BNAH (0.0021 g). Control reactions were performed. The substrates and cofactors were first dissolved in 50 mM kPi buffer pH 7. The reactions were performed for 4 hours at 60 °C while stirring. The reactions were performed in three different light conditions to study the influence of light on the conversion of cyclohexanone to cyclohexanol by TADH. After the reaction the GC samples were prepared by extraction with 500 µL of ethyl acetate. After the addition, the sample was vortexed and centrifuged at 13.000 rpm for 1 minute. The ethyl acetate layer was transferred to a fresh tube and Na₂SO₄ was added to remove the remaining water and separated again by centrifugation at 13.000 rpm for 1 minute. 200 µL of the dried ethyl acetate was transferred to a GC vial to subject it to GC analysis.

Gas chromatography (GC) analyses were carried out on a Shimadzu GC-2010 gas chromatograph equipped with a flame ionization detector (FID). The column CP-Wax 52 CB (25 m × 0.25 mm × 1.20 µm), using the following instrument parameters: injection temperature at 250 °C, column flow 1.51 mL/min, linear velocity 37.8 cm/s, split ratio 30. Column oven program: 60 °C for 4 min, ramp 20 °C/min to 160, hold 2.5 min, ramp 30 °C/min to 190 °C, hold 0.5 min, ramp 30 °C/min to 250, hold 1 min. Total program time: 16 min.

Table 1: Bio-catalytic reactions that were performed (three different light conditions) to study the influence of light on the conversion of cyclohexanone to cyclohexanol by TADH.

Light conditions	TADH added	Cofactor	Comments
Dark	Yes	NADH	Positive control
		AmNAH	
		x	No cofactor, negative control
LEDs (400-700 nm) ^A	Yes	NADH	
		AmNAH	
		BNAH	
		x	No cofactor, negative control
	No	NADH	No TADH, negative control
		AmNAH	
		BNAH	
UV-Vis light (300-700 nm) ^B	Yes	NADH	
		AmNAH	
		BNAH	
		X*	No cofactor, negative control*
	No	NADH	No TADH, negative control
		AmNAH	
		BNAH	

A: ISY Led stripe 5m RGB ILG5000-1 (400nm to 700 nm emission)

B: Lightningcure[®] LC8 light source type L9566-03 without UV-filter (300 nm to 700 nm emission)

*: the reaction was spilled during the experiments and could not be measured.

3 Results

3.1 Synthesis of the NCBs

An overview the oxidised mimics and their reduced forms is given in Figure 6 A and B, respectively. The ^1H -NMR, ^{13}C -NMR, COSY and HSQC spectra are given in the Appendix. The spectrum of AmNA^+Cl^- is not shown, as this mimic was already available and was not synthesised within this project. Spectrums for the mimic AmAP and are also not shown, as the reduction of AmAP^+Cl^- to give AmAPH was unsuccessful and did not lead to product. For all other NCBs, assignments of the peaks are given in the spectra.

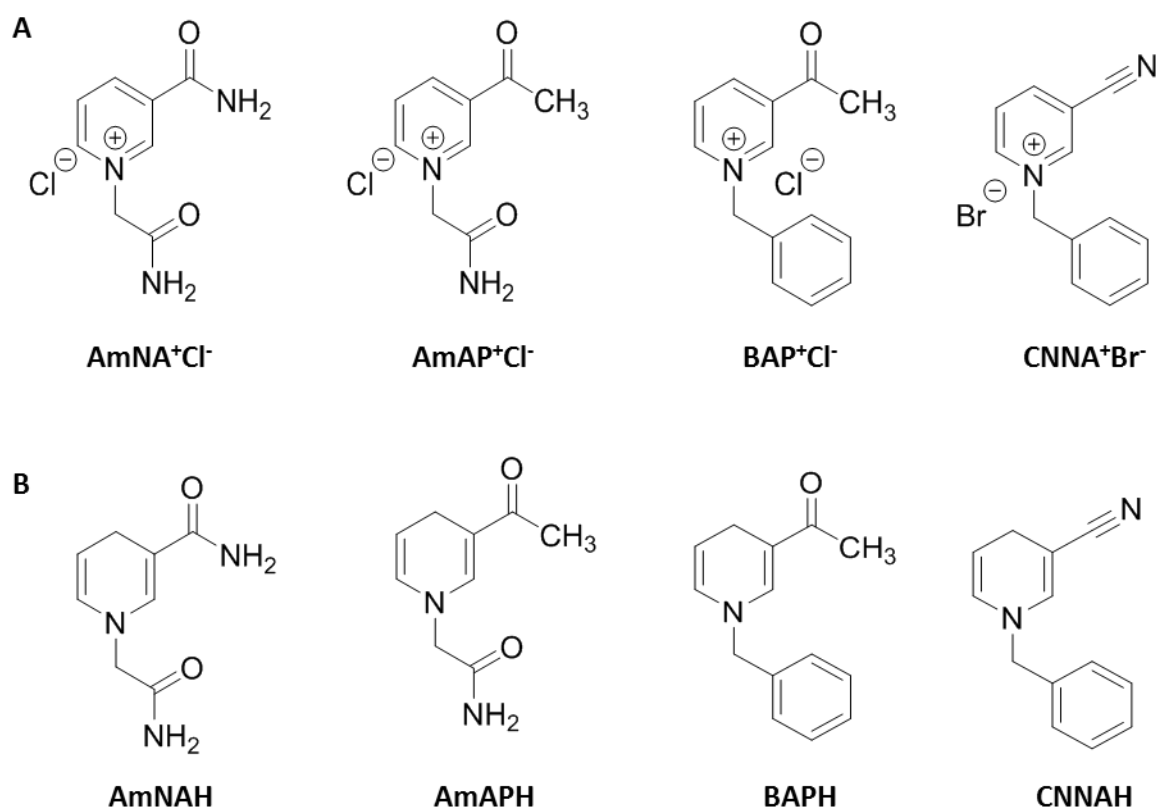


Figure 6: Chemical structures of the synthesised oxidised (A) and reduced (B) NCBs

3.2 TADH expression

A pET11a backbone vector (Figure 7) containing the *TADH* gene (an ADH originally isolated from *Thermus* sp. ATN1) was obtained from Aarhus University, Denmark. The plasmid was used for transformation of the expression host *E. coli* BL21 (DE3). The structure of the plasmid as obtained and the plasmid isolated from *E. coli* BL21 (DE3) transformants were analysed. The structure and sequence of the *TADH* plasmid were not available in literature, although the creation is described by Hollman et al. First an *EcoRI* restriction site was introduced, between the *NdeI* restriction site and the ribosome binding site (RBS). The *TADH* gene was inserted between the *BamHI* and the introduced *EcoRI* site [18]. The pET11A backbone vector consist of 5677 bp and the *TADH* gene is 1044 bp in length (Appendix, Figure 18), resulting in the pTADH plasmid with a size of around 6700 bp. Restriction analyses with *BamHI* or *PstI*, both having one restriction site in the plasmid, indeed give one fragment

of around 7000 bp (Figure 8, lane 2 and 3 respectively). This result is consistent with the plasmid structure as described by Hollman et al.

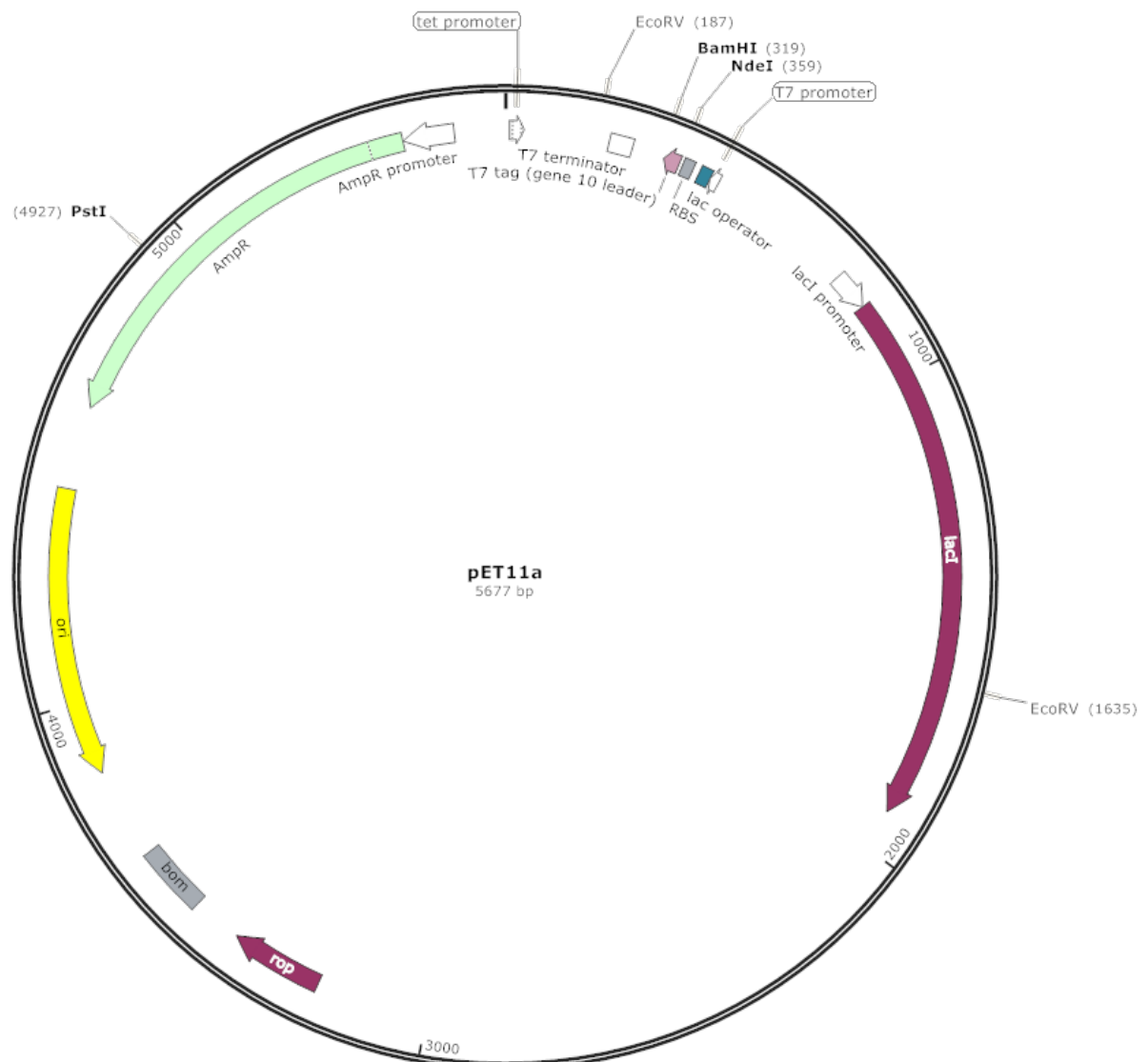


Figure 7: Structure and size of the pET11a vector (obtained from addgene vector-database 2625)

Restriction with both enzymes, PstI and BamHI, does not give two the fragments, as expected. Both restriction enzymes have one recognition site in pTADH, but only one fragment is shown Figure 8, lane 4. It is highly likely that one of two enzymes was accidentally not added, as the enzymes show restriction at one site when added separately (Figure 8 lane 2 and 3). Most importantly, the restriction

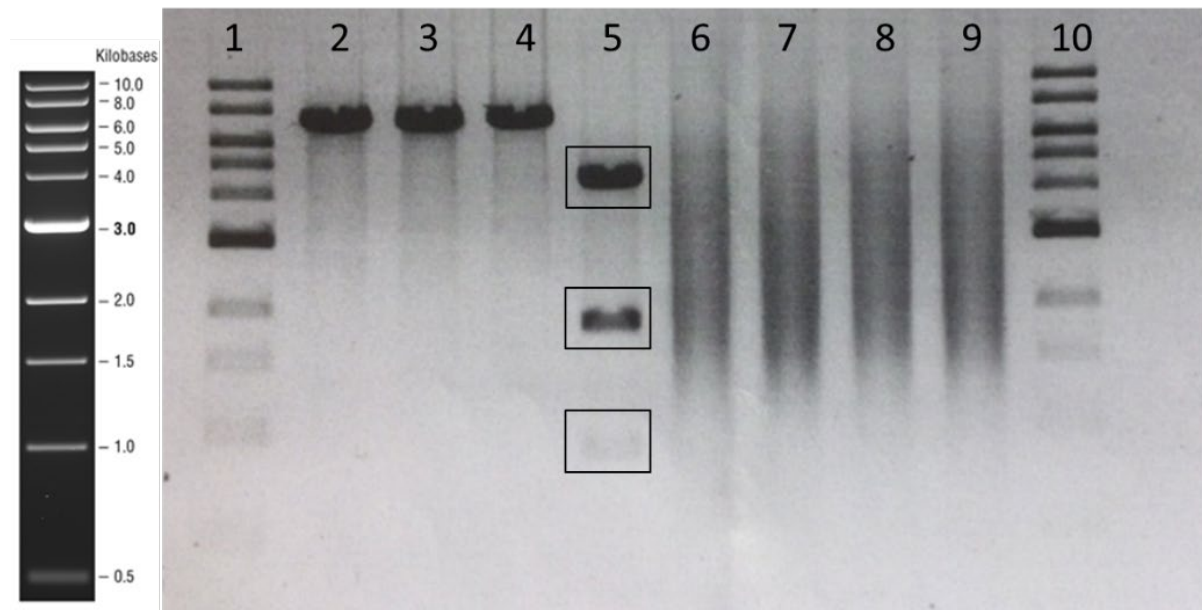


Figure 8: 1% agarose gel of restriction analysis on plasmid TADH isolated from streak-plate colonies after transformation of *E. coli* BL21 (DE3) (lane 2-5) and the plasmid as used for transformation) (lane 6-9). Lane 1,10 : 1kb DNA ladder lane, sizes of the ladder fragments are given in kb on the left. 2,6: Restriction with BamHI. Lane 3,7: restriction with Pst. Lane 4,8: restriction with PstI & BamHI. Lane 5,9: restriction with EcoRV.

with EcoRV shows three fragment of around 4500, 1800 and 100 bp. This restriction enzyme has two recognition sites within the pET11A vector and one within the TADH gene, which strongly indicates the presence of pTADH. Since only one colony was obtained after transformation of the plasmid to the *E. coli* host strain, restriction analysis on the starting material was performed. The plasmid used for the transformation of *E. coli* BL21 (DE3) indeed shows highly damaged DNA (Figure 8, lane 6 to 9), which could explain the appearance of only one colony after the transformation.

After establishing that the *E. coli* BL21 (DE3) strain contained the TADH plasmid, several colonies were used to study if the TADH was actually expressed in a small scale fermentation. If expression of TADH by the host strain takes place, it could be visualised using SDS-page analysis. A fragment is expected of around 40 kDa, as the subunit of TADH is 37.2 kDa in size [3]. The expected fragment of around 40 kDa is present in the supernatant fraction of the *E. coli* BL21 (DE3) pTADH which indicates the presence of the TADH (lane 2 and 3). Furthermore, the TADH is expected to be mainly present as a soluble product. Here it is also shown to be present in the pellet fraction (Figure 9, lane 4 and 5). The expression host *E. coli* BL21 (DE3) without expression of the pTADH, shows a pattern for proteins which are normally expressed in this strain (Figure 9, lane 6 and 7). The decrease in the presence of fragments of the *E. coli* BL21 (DE3) host shows that, with heat purification, the presence of host proteins can be reduced and lead to (partial) TADH purification.

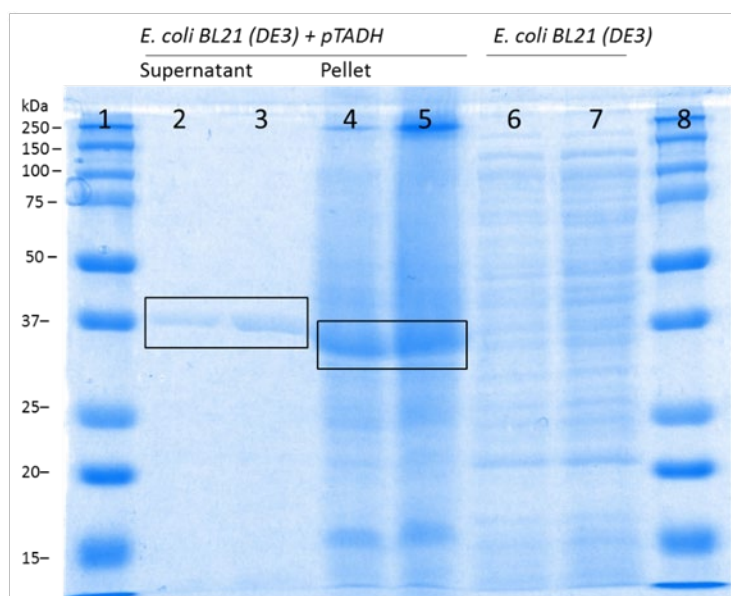


Figure 9: 12% SDS-page gel with in lane 1,8: Biorad protein marker 2,3: 10µl and 20µl, respectively, of supernatant *E. coli* BL21 (DE3) + pTADH, both showing the TADH fragment (37.2 kDa) around 40 kDa. 4,5: 10µl and 20µl, respectively, of pellet fraction *E. coli* BL21 (DE3) + pTADH 6,7: 10µl and 20µl, respectively, of *E. coli* BL21 (DE3) host strain shows multiple fragments of proteins as expressed by the host strain.

After the confirmation of TADH expression by the *E. coli* host, a larger scale fermentation was performed. A total cell pellet of around 8 grams was obtained. After cell lysis and heat purification the kinetic activity of TADH was measured. 1-butanol was added as a substrate, while measuring the formation of NADH from NAD⁺. Here the formation of NADH was measured at a wavelength of 340 nm for both the supernatant fraction and the pellet fraction (data not shown), indicating the presence of TADH in both fractions. This result in consistent with the SDS-page analysis of the small scale fermentation shown in Figure 9. Based on these results, it was decided to not only subject the supernatant to anion exchange chromatography (AEX). Indeed, by dissolving the pellet fraction in buffer and centrifuging it, a clear solution was obtained and combined with the above mentioned supernatant and subjected to AEX.

3.3 TADH purification

3.3.1 Anion exchange chromatography (AEX)

The absorbance spectrum as obtained by anion exchange chromatography indicates the presence of multiple proteins in the sample, as an increase in the absorbance at a wavelength of 280 nm is found at several elution volumes. The fractions that showed an increase in absorbance at this wavelength were screened on kinetic activity of TADH, again using the formation of NADH from NAD⁺ and 1-butanol as a substrate. The fractions with a peak in the absorbance at 280 nm are indicated with an arrow in Figure 10 (fractions 6, 7, 12, 18, 22, 24 and 29). Only low activity (units were not determined) was found in the samples corresponding to the fractions 7 and 12. No activity was measured in all the other fractions (data not shown). The presence of TADH is supported by the SDS-page analysis that was performed on the fractions 7-13 (Figure 11A): a gradient can be deduced from this figure, which shows highest TADH concentration in fraction 9 (Figure 11, lane 4). From the AEX chromatograph and the SDS-page analysis, it can be concluded that TADH elutes after a volume of around 140 mL.

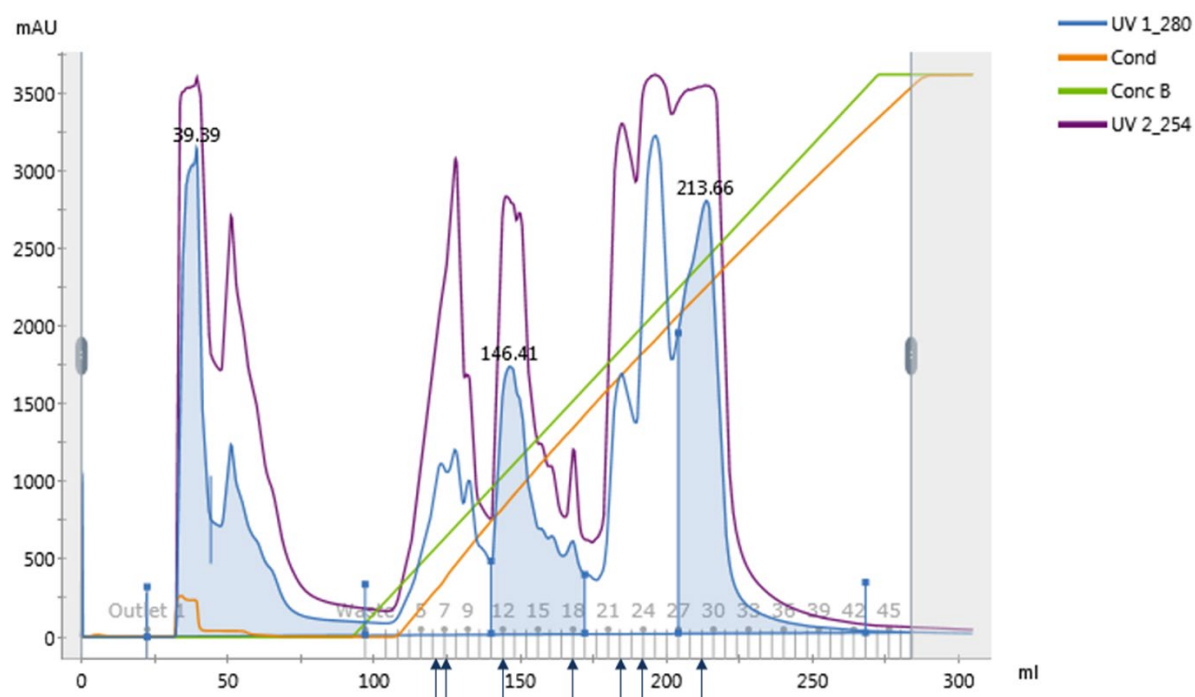


Figure 10: TADH purification with anion exchange chromatography using a Source 15Q column. Buffer A, 20 mM Tris HCl pH 7 was exchanged with an increasing concentration of buffer B (green line), 20 mM Tris HCl pH 7+1M NaCl. The conductivity was measured to check for the increasing salt concentration (green line). A 180 mL gradient (elution volume in mL, on the x-axis) with a flow of 0.7 mL/min was applied while collecting 45 fractions of 4 mL. 1-butanol was added to a final concentration of 10 mM to facilitate the purification. Several collected fractions (6, 7, 12, 18, 22, 24 and 29) showed a peak in the absorbance (in mAU, y-axis) at an wavelength of 280 nm, indicated with blue arrows.

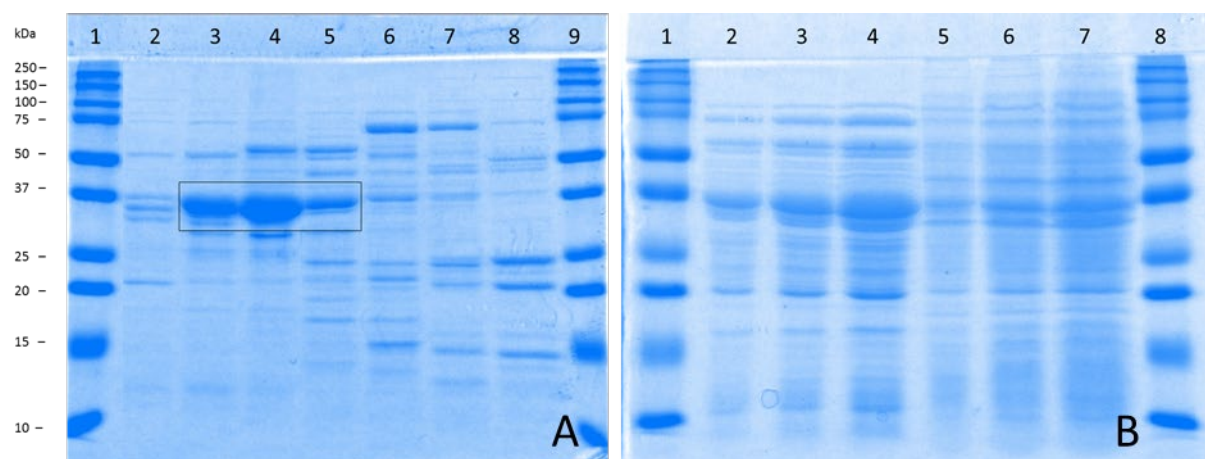


Figure 11 A: 12% SDS-page gel for analysis of TADH purification with AEX. In lane 1,9: Biorad protein marker with fragment sizes in kDa given on the left. Lane 2-8: AEX fractions 7,8,9,10,11,12 and 13, respectively. In all samples the presence of the TADH (37.2 kDa) fragment around 40 kDa is found. The highest concentrations of TADH is found in the fractions 8, 9 and 10. **B:** 12% SDS-page gel with in lane 1,8: Biorad protein marker. The TADH containing fractions were combined (Figure 8A lane 2-8), concentrated, dialysed and centrifuged to give in Lane 2-4: 5, 10 and 20 μ L supernatant and in Lane 5-7: 5, 10 and 20 μ L of pellet.

The TADH containing fractions were combined (Figure 11A lane 2-8), concentrated and dialysed to remove the high salt concentration and again analysed with SDS-page. Again aggregates were present in the sample so that a supernatant (Figure 11B, lane 2-4) and pellet fraction (Figure 11B, lane 5-7)

was formed which where both subjected to analysis. The TADH is more abundant in the supernatant fraction, compared to the pellet fraction. The formation of aggregates that contain TADH will lead to a loss of total purified TADH. The kinetic activity of TADH was determined (the formation of NADH from NAD⁺ and 1-butanol as a substrate) with the results as shown in the Appendix, Figure 19. Based on the reaction speed during the first 0.2 minutes, an estimation of the TADH concentration was made. A total volume of 3 mL was recovered as a result of anion-exchange chromatography, with a final concentration of 167 µg/mL. It has to be mentioned that this value is a rough estimation, the assumptions that were made to perform the calculations are explained in more detail in the Discussion section. A concentration of 100 µg/ml will be used to study the acceptance of the NCBs by TADH, therefore another fermentation was performed to express the TADH in *E. coli* BL21 (DE3) cells. The cell pellet was kindly provided by Caroline E. Paul (TU Delft) which performed the expression of *TADH* in *E. coli* BL21 (DE3) pTADH. This second cell culture had led to a cell pellet of around 11 grams, which were again subjected to purification. It was decided to separate the TADH from other proteins using size-exclusion (SE) by gel permeation chromatography (GPC).

3.3.2 Size-exclusion (SE) with gel permeation chromatography (GPC)

The obtained cells were lysed and centrifuged leaving a cell pellet, (Figure 12 lane 6) and supernatant fraction (Figure 12, lane 7). Again it has to be noticed that the 37.2 kDa TADH fragment is seen in both fractions, indicating the presence of TADH not only as a soluble product, but also in a large amount as insoluble product in the pellet fraction, as shown before. Heat purification following centrifugation on both fractions reduced the presence of *E. coli* BL21 (DE3) proteins in the obtained supernatant from

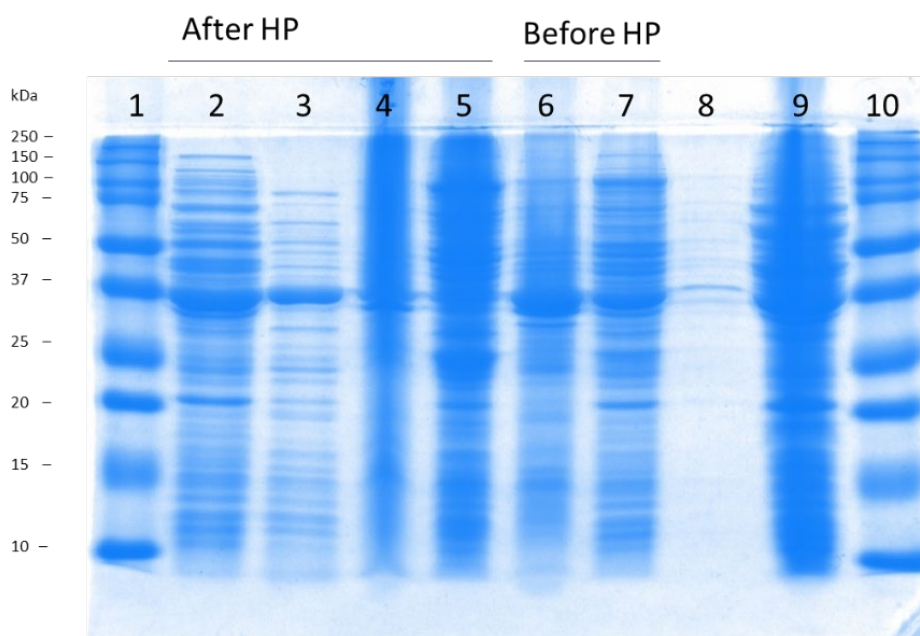


Figure 12: 12% SDS-page gel for analysis of lysed *E. coli* BL21 (DE3) + pTADH cells with in lane 1,10: Biorad protein marker with fragment sizes in kDa given on the left. Lane 2: supernatant after HP and centrifugation of the sample in lane 7. Lane 3: supernatant after HP and centrifugation obtained by centrifugation of sample in lane 6. Lane 4: Pellet after HP and centrifugation of the sample in lane 6. Lane 5: Pellet after HP and centrifugation of the sample in lane 7. Lane 6: Pellet fraction before HP. Lane 7: Supernatant fraction before HP. Lane 8: flow through of concentration. Lane 9: Combined and concentrated sample of supernatant fraction in lane 2 and 3.

both the supernatant and the pellet fraction (Figure 12 lane 2 and 3 respectively), leaving many other proteins as insoluble product in their corresponding pellets (Figure 12 lane 5 and lane 4, respectively).

The supernatant of both the supernatant and pellet fraction (Figure 12, lane 2 and 3) were combined. Here, also the 3 mL sample of as recovered with AEX (Figure 11, lane 2-4) was combined and concentrated to give the sample depicted in Figure 12, lane 9. This final sample was subjected to GPC to separate the TADH. GPC and the simultaneous UV measurement at a wavelength of 280 nm show the largest absorption around an elution volume of 200 mL (Figure 13), indicating the presence of TADH in the corresponding fractions. SDS-page analysis confirms the presence of TADH in the corresponding three fractions (Figure 14A lane 5,6,7). The gradient as seen for the SDS-page analysis is also supported by the kinetic activity on the three TADH containing fractions (Appendix Figure 20, 21 and 22). This activity test was again performed with 1-butanol as a substrate, with the measurement based on the consumption of NAD⁺, with concomitant formation of NADH. The TADH containing fractions were combined, concentrated and dialysed giving the final TADH enzyme solution (Figure 15, lane 1) that was used as enzyme stock for the bio-catalytic reactions reported in this thesis. The final concentration as determined by kinetic measurements was 195 $\mu\text{L/mL}$ (Appendix Figure 23) recovering a total amount of 2.9 mg of TADH.

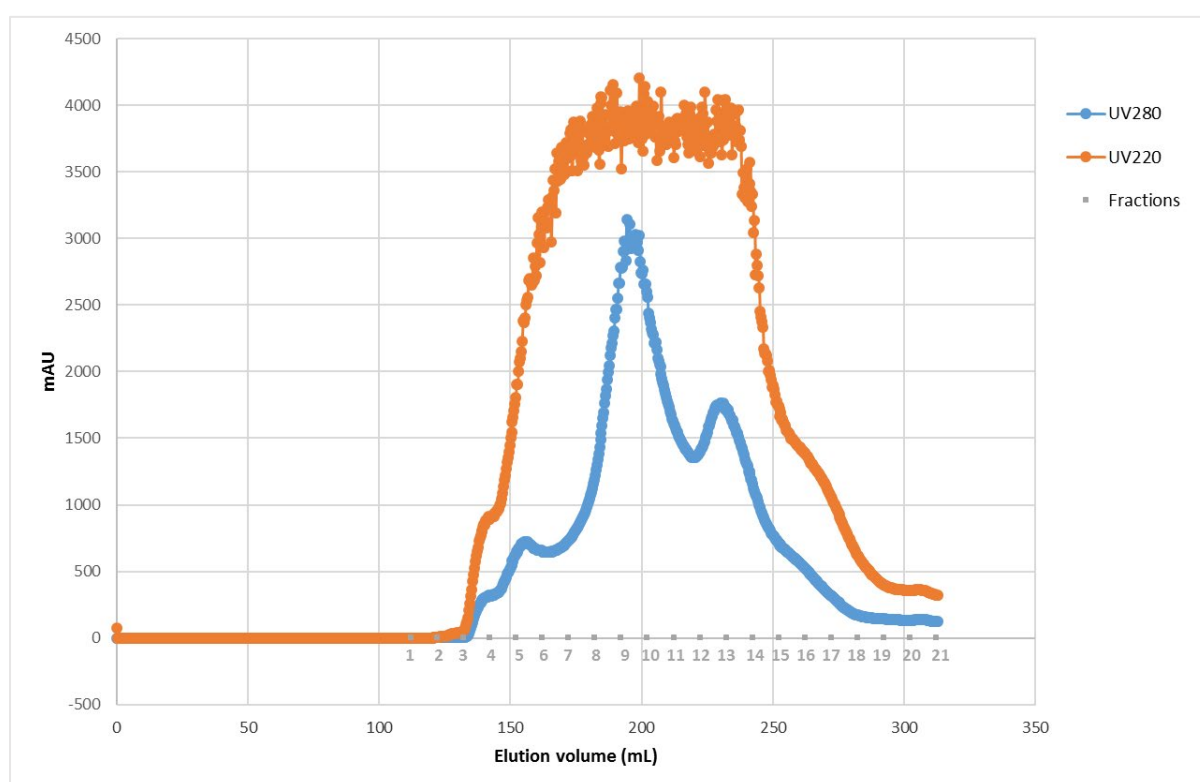


Figure 13: TADH purification with gel permeation chromatography using a Superdex 75 26/60 column, elution with 300 mL (2 mL/min) of 50 mM KPi buffer with 150 mM KCl pH 7. 10 mL fractions were collected given as numbered grey spheres on the x-axis. UV measurements were performed at wavelengths of 280 nm (blue line) and 220 nm (orange line), absorption given in mAU on the y-axis. Largest absorption at 280 nm is present around an elution volume of 200 mL, corresponding to fraction 9.

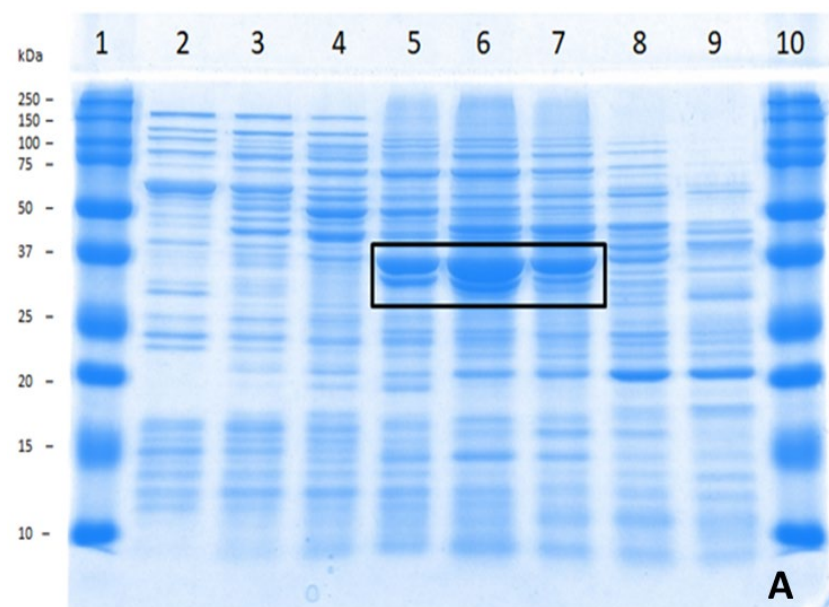


Figure 14: 12% SDS-page gel for analysis of A: fractions 5-12 from TADH purification with GPC. In lane 1,10: Biorad protein marker with fragment sizes in kDa given on the left. Lane 2-9: GPC fraction 5-12 respectively. 20 μ L SDS-page sample was applied for all samples.

A small volume of the combined, concentrated and dialysed TADH enzyme solution that underwent SEC purification (Figure 15, lane 1) was subjected to a second heat purification. It can be deduced from Figure 15 lane 4, that heat purification at this stage leads to effective purification of the enzyme.

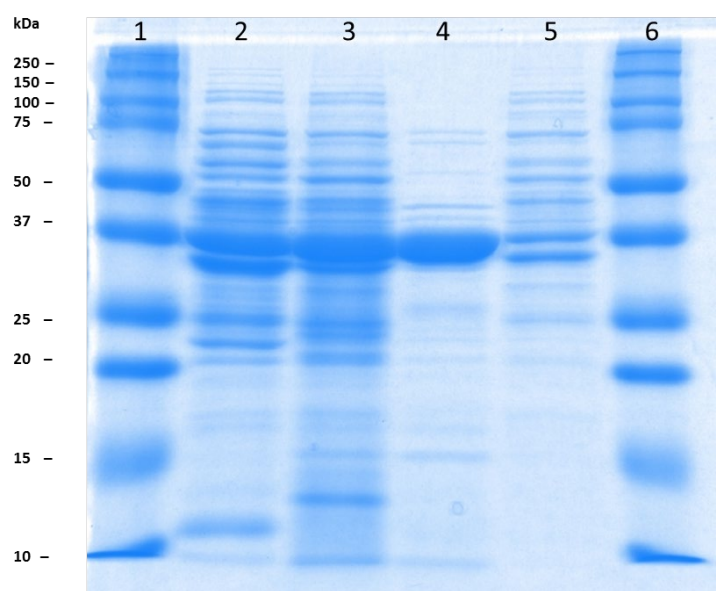


Figure 15: 12% SDS-page gel for analysis of the combined, concentrated and dialysed TADH containing GPC fractions, before and after HP. In lane 1,6: Biorad protein marker with fragment sizes in kDa given on the left. Lane 2: before HP. Lane 3: Total sample after HP. Lane 4: supernatant after HP. Lane 5: pellet fraction after HP. 20 μ L SDS-page sample was applied for all samples.

3.3.3 Determination of total protein

The amount of TADH used in the GC measurements were determined by calculations from kinetic measurements. However, since concerns rose about the accuracy of this method for enzyme

concentration determination, the TADH concentration was determined with the well-known bicinchoninic acid (BCA) method, using a dilution series of bovine serum albumin (BSA) as a reference. The total protein concentration in the sample based on this method indeed showed a difference with the concentration as determined with kinetic measurements. With the BCA method a total protein concentration was determined to be 1926 µg/mL as shown in the appendix Figure 24 and Table 3. Here it has to be taken into account that TADH was not the only protein that was present in the final sample, as shown with SDS-page analysis.

3.4 TADH bio-catalysed conversion of cyclohexanone in the presence of NADH, AmNAH and BNAH in different light conditions

After the purification of TADH had led to a sufficient concentration, the viability of the reduced NCBs 1-carbamoylmethyl-1,4-dihydronicotinamide (AmNAH) and BNAH (Figure 6B and Figure 5, respectively) as a cofactor for the TADH-catalyzed redox reactions were studied. This was done using a solution of 100 µg/mL TADH with 5 mM cyclohexanone as substrate and either 10 mM AmNAH, 10 mM BNAH or 10 mM of NADH. The bio-catalytic reactions were performed for four hours at 60°C in 1 mL total volume. The TADH-catalysed reduction of cyclohexanone to cyclohexanol is only expected when the cofactor allows the TADH for catalytic conversion of the substrate. The possibility of photo-induction using LEDs (400-700 nm) or using UV-Vis light (300-700 nm) of the bio-catalytic reactions with TADH was studied. To determine the presence of cyclohexanone and cyclohexanol, their corresponding retention times on the used GC column were determined. Cyclohexanone showed a retention time of 9.85 minutes, cyclohexanol a retention time of 10.84 minutes. The obtained GC chromatograms are depicted in the Appendix. A summary of the measured retention times for the different reaction conditions can be seen in Table 2. The formation of cyclohexanol from cyclohexanone results in a peak with a retention time of 10.84 minutes, indicating that cyclohexanol is formed in all reactions in which NADH was present. This result is as expected, cyclohexanone is reduced to cyclohexanol by TADH when the natural cofactor is available. No full conversion of cyclohexanone is established by NADH, between the different light conditions no significant differences in the conversion can be deduced from the integration of the peaks.

The GC measurements show a retention time of 5.74 minutes in three of the reactions, however a very small peak around this retention time is visible for all chromatograms, also in the negative control. It is likely caused by contamination in either the column or the solvent and is not expected to have an influence on the obtained results.

For all light conditions (dark, LEDs and UV-Vis light) the reactions with the NCBs AmNAH and BNAH do not show a peak with a retention time of 10.84. This results shows the absence of conversion of cyclohexanone to cyclohexanol, which indicates that both BNAH and AmNAH are unable to replace the natural cofactor NADH.

Table 2: Summary of the bio-catalytic reaction with the different reaction conditions indicated. Measured retention times for the different reaction conditions are given.

Light conditions	TADH added	Cofactor	Retention time(s) in minutes
Dark	Yes	NADH	9.852 & 10.843
		AmNAH	9.854
		x	9.853
LEDs (400-700 nm)	Yes	NADH	9.852 & 10.843
		AmNAH	5.744 & 9.854
		BNAH	9.853
		x	9.853
	No	NADH	9.854
		AmNAH	9.854
		BNAH	9.853
UV-Vis light (300-700 nm)	Yes	NADH	5.744, 9.852 & 10.842
		AmNAH	9.854
		BNAH	9.853
		x	Not measured
	No	NADH	9.854
		AmNAH	9.853
		BNAH	9.853

4 Discussion

To optimise the expression of *TADH* from *E. coli* BL21 (DE3) several steps should be adjusted. To have highly efficient transformations of *E. coli* BL21 (DE3) with pTADH it is obviously desired to have undamaged plasmid DNA. In this thesis, the transformation of the host strain was performed with severely damaged DNA, Figure 8. Although the starting material (plasmid obtained from the Aarhus University) was damaged, it has led to the transformation of *E. coli* BL21 (DE3). The transformant contained the pTADH as desired (Figure 8) and was able of successful TADH expression (Figure 8). The pTADH plasmid was subjected to restriction analysis although there was no sequence of the complete plasmid available. The likely structure of the plasmid was obtained from a the description of the origin and creation of the plasmid [18], however the exact sequence remains unknown. It is highly advisable to perform sequencing on the pTADH as obtained: gaining access to its complete structure would provide information about the expression and purification of TADH. For example, the presence of a HIS-tag could enhance and ease the enzyme purification. As seen in Figure 7, the forward and reverse primers could be designed on the common T7 promoter for sequencing of the plasmid. It was also shown that expression with *E. coli* BL21 (DE3) pTADH that TADH is not only present in the soluble fraction, but also as insoluble product in the cell pellet. This could be an indication of troublesome expression of the pTADH by the host strain. By optimising the construct, for example using another promoter sequence, the expression could lead to a higher expression of TADH.

For the determination of the TADH concentration in the purification steps, kinetic measurements were performed. The measurements were based on the formation of NADH from NAD⁺ using 1-butanol as a substrate. It was decided during this project to have the kinetic measurements in the oxidative direction as production of NADH, it could be considered to use kinetic measurements in the reductive reaction as a decrease in NADH concentration. Indeed, the amount of units is a good indicator for the amount of TADH, however, the units were converted into mg amounts. This was done using the U/mg reported in literature (1-butanol substrate, pH 9 and 60°C) [3]. With this method, a concentration of 195 μ L/mL was determined for the purified TADH enzyme solution. The amount of TADH enzyme solution used in the bio-catalytic reactions was dependent on this determination. The determination may give an indication of the mg amount, but might be inaccurate. It was therefore decided to measure the total protein concentration with the well-established BCA assay (1926 μ g/mL). As this method is not selective for TADH, the purity of the enzyme solution should be taken into account. This is visualised with SDS-page (Figure 15, lane 1), TADH represents roughly half of the total protein concentration (37.2 kDa). Still this would not be enough to explain the large concentration differences between the different determination methods. Furthermore, comparison of the purification methods AEX and SEC (SDS-page analyses Figure 11 Figure 14) would suggest better separation is established when AEX (source 15Q column, elution with 20 mM Tris HCl pH 7 with a linear gradient from 0 to 1 M NaCl) is used. In this thesis fractions within one purification method and also between different purification methods were combined. This was done in order to obtain a higher yield of TADH,, but has led to a loss in purity. Heat treatment purification has shown nice potential (Figure 15) and could be further explored as purification method for TADH, by varying the temperature and time of the treatment. To gain more knowledge about TADH purification in general, more parameters should be taken into account. After all purification steps total protein(mg)/activity (U), specific activity(U/mg) and yield(%) should be determined.

The design of the oxidised and reduced NCBs was already established [6, 11, 19]. The X substituent on the pyridine ring is essential for the coordination and redox potential. Especially for use on industrial scale, it is important to take into account that 1,4-dihydropyridines that contain more electron withdrawing groups become very acid-labile and the pyridinium ions become very base-labile when they contain more electron-withdrawing groups [19]. In this thesis, the cofactor analogues were successfully synthesised with a yield ranging from 33% to 85% for the oxidised cofactors and from 14% to 17% for the reduced cofactors. The general reaction scheme of the syntheses are shown in Figure 16. The reduction reaction of AmAP⁺Cl⁻ led to a product with impurity of 2-chloroacetamide. Therefore recrystallization was necessary to obtain AmAPH. The recrystallization however, has only led to failed attempts. The formation of yellow needles, as described by Norris et al was not accomplished [19].

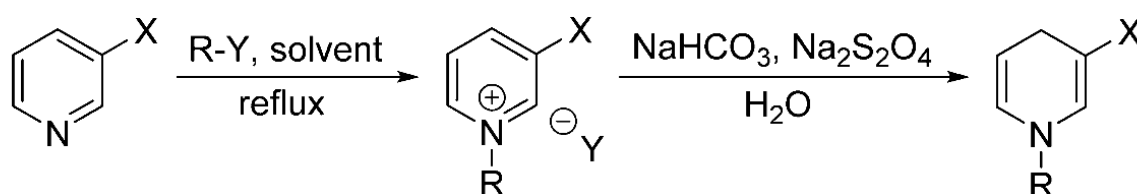


Figure 16: General reaction scheme for the synthesis of NCBs, adapted from [4].

The natural cofactor NADH can be excited at a wavelength of 340 nm. This potential has been used by Emmanuel et al. to excite the biological cofactor NAD(P)H, bound in the active site of a ketoreductase (KRED) enzyme [8]. In another study, the synthetic cofactor BNAH has shown capability of catalysing hydrogenation of various di-aromatic α,β -epoxy ketones to β -hydroxy ketones under irradiation larger than 300 nm. It is reasoned that, if the design of the NCBs allows for photo-induction, the NCB may be activated within the TADH enzyme to catalyse redox reactions [6].

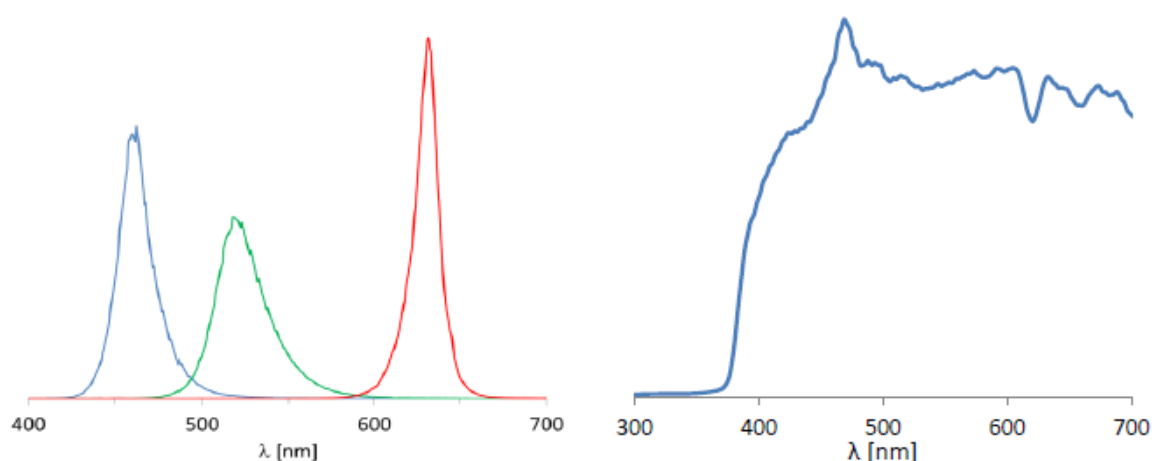


Figure 17: Relative emissionspectrum of the LED lights (on the left) and Lightningcure® LC8 light source type L9566-03 induction with visible light from +/- 300 nm to 700 nm was performed using the set-up without filter. Spectra are obtained from SI of [20].

The ability of photo-induction using LEDs (400-700 nm) or UV-Vis light (300-700 nm) on bio-catalytic reactions with TADH and the cofactors AmNAH, BNAH and NADH was studied. The emission spectra of the two set-ups are shown in Figure 17). The reduction of cyclohexanone to cyclohexanol was only

expected when the cofactor allows the TADH for catalytic conversion of the substrate. The reactive part of the cofactor (nicotinamide ring) is present in the NCBs. The absence of the adenine dinucleotide however, interferes with the ability of binding to the nucleotide-binding domain (Rossmann fold) of the TADH. The design of the NCBs allow for photo-induction, it is reasoned that by excitation of the NCBs within the active site of the TADH hydride transfer can be completed [6].

The reactions with NADH show conversion of cyclohexanone to cyclohexanol in dark conditions, when induced with LEDs (400-700 nm) and UV-Vis light (300-700 nm). As natural cofactor of TADH, this was as expected. It is a good indication that the settings of the reactions and measurements have been performed so that, if the NCBs allow for the bio-catalytic conversion, the result would be visible in the GC measurements. The GC measurements did however show a small peak with a retention time of 5.743 minutes for multiple reactions. A very small peak around this retention time is visible for all chromatograms, also the negative control in which only ethyl acetate is injected. Therefore it is concluded to be caused by contamination in either the column or the ethyl acetate and is not likely to interfere with the results. No full conversion of the cyclohexanone is achieved for reactions with NADH. A possible explanation for this observation is the instability of NADH. Wu et al. have shown that the factors temperature and pH have the greatest impact on the rate of degradation of NAD(P)H. The half-life time of NAD(P)H decreased drastically with temperature, for example, it would take more than 8 hours for NADPH to degrade at 19°C and only 1 hour at 41°C [21]. From the obtained data no conclusion can be made on the differences between the dark and the photo-induced conditions of the bio-catalytic reaction with NADH. To gain more insight on the photo-induction of NADH when bound to TADH, kinetic activity measurements during the bio-catalytic reactions could be performed.

The reduced NCBs AmNAH and BNAH did not lead to substrate conversion by TADH. The reduction of cyclohexanone to cyclohexanol was only expected when the cofactor allows the TADH for catalytic conversion of the substrate. No formation of cyclohexanol was detected, therefore it is concluded that the NCBs AmNAH and BNAH are not able to replace the natural cofactor in the described bio-catalytic reactions. BNAH has in a previous study shown the ability of replacing the natural cofactor NAD(P) for a range of enoate reductases (ERs, EC 1.3.1.31) which are flavoproteins that selectively reduce C=C double bonds. A possible explanation for the difference in the acceptance of cofactors can be explained by their catalytic mechanism. ERs includes a flavin mononucleotide (FMN) that functions as a mediator between the cofactor and the substrate. In contrary to ADHs, the ERs seem to be less specific for NADH or NADPH [4]. BNAH was reported capable of replacing NADH as a natural cofactor by reactions catalysed by ADHs [14] [15]. The acceptance of BNAH by ADHs was questioned by Paul et al, they state the apparent enzyme activity was causative of a regeneration system that uses BNAH to recycle NAD(H). The presence of NAD(H) was caused by the use of ADHs which were not purified from their natural cofactor [15]. The presence of NAD(H) and the presence of the described regeneration system would have led to bio-catalytic conversion in the reaction with BNAH, which was not detected in this project, also when control reactions were carried out. Ideally the complete library here synthesized would have been subjected to the reactions and measurements with GC, as this was done for only AmNAH, BNAH and NADH.

5 Conclusion

A plasmid containing ADH from thermophilic *Thermus* sp. ATN1 was successfully expressed in *E. coli* BL21 (DE3) and purified using heat purification, anion exchange chromatography and size-exclusion chromatography. A library of NCBs was successfully created. The cofactors AmNAH and BNAH have shown to be incapable to function as a cofactor for TADH in bio-catalytic conversions with cyclohexanone as a substrate. The viability to function as a cofactor could not be photo-induced using LEDs (400-700 nm) or UV-Vis (300-700 nm).

References

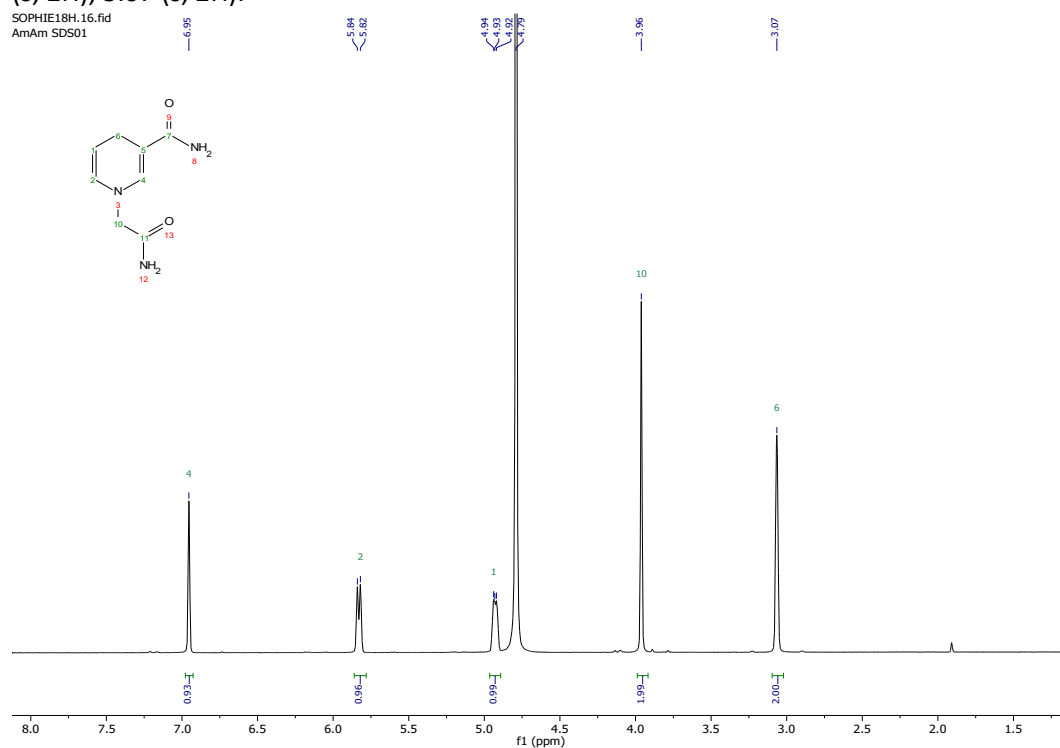
1. Ni, Y., D. Holtmann, and F. Hollmann, How Green is Biocatalysis? To Calculate is To Know. *ChemCatChem*, 2014. 6(4): p. 930-943.
2. Emmanuel, M.A., et al., Accessing non-natural reactivity by irradiating nicotinamide-dependent enzymes with light. *Nature*, 2016. 540: p. 414.
3. Höllrigl, V., et al., TADH, the thermostable alcohol dehydrogenase from *Thermus* sp. ATN1: a versatile new biocatalyst for organic synthesis. *Applied Microbiology and Biotechnology*, 2008. 81(2): p. 263-273.
4. Paul, C.E., I.W.C.E. Arends, and F. Hollmann, Is Simpler Better? Synthetic Nicotinamide Cofactor Analogues for Redox Chemistry. *ACS Catalysis*, 2014. 4(3): p. 788-797.
5. Alfonsi, K., et al., Green chemistry tools to influence a medicinal chemistry and research chemistry based organisation. *Green Chemistry*, 2008. 10(1): p. 31-36.
6. Guarneri, A., Synthetic nicotinamide coenzyme biomimetics in photobiocatalysis, in *Laboratory of Organic Chemistry, Laboratory of Biochemistry*,. 2017, WUR.
7. Sellés Vidal, L., et al., Review of NAD(P)H-dependent oxidoreductases: Properties, engineering and application. *Biochimica et Biophysica Acta (BBA) - Proteins and Proteomics*, 2018. 1866(2): p. 327-347.
8. Bai, C.-B., et al., A Petal-type Chiral NADH Model: Design, Synthesis and its Asymmetric Reduction. *Scientific reports*, 2015. 5: p. 17458-17458.
9. Ma, S.K., et al., A green-by-design biocatalytic process for atorvastatin intermediate. *Green Chemistry*, 2010. 12(1): p. 81-86.
10. Franssen, M.C.R., van Berkel W.J.H, *Enzymology, Biocatalysis*. 2017: WUR, Laboratory of ORC and BIC.
11. Ohnishi, Y., M. Kagami, and A. Ohno, Reduction by a model of NAD(P)H. Effect of metal ion and stereochemistry on the reduction of .alpha.-keto esters by 1,4-dihydronicotinamide derivatives. *Journal of the American Chemical Society*, 1975. 97(16): p. 4766-4768.
12. Nethercott, A.M., in *Department of Chemical and Environmental Engineering*. 2017, University of Nottingham.
13. Man, H., et al., Structure of the NADH-dependent thermostable alcohol dehydrogenase TADH from *Thermus* sp. ATN1 provides a platform for engineering specificity and improved compatibility with inorganic cofactor-regeneration catalysts. *Journal of Molecular Catalysis B: Enzymatic*, 2014. 105.
14. Mauzerall, D. and F.H. Westheimer, 1-Benzyl dihydronicotinamide—A Model for Reduced DPN. *Journal of the American Chemical Society*, 1955. 77(8): p. 2261-2264.
15. Paul, C.E. and F. Hollmann, A survey of synthetic nicotinamide cofactors in enzymatic processes. *Applied microbiology and biotechnology*, 2016. 100(11): p. 4773-4778.
16. Bornscheuer, U.T., A radical change in enzyme catalysis. *Nature*, 2016. 540: p. 345.
17. Gargiulo, S., I.W.C.E. Arends, and F. Hollmann, A Photoenzymatic System for Alcohol Oxidation. *ChemCatChem*, 2011. 3(2): p. 338-342.
18. Hollmann, F., et al., Coupled chemoenzymatic transfer hydrogenation catalysis for enantioselective reduction and oxidation reactions. 2005. 3512-3519.
19. Norris, D.J. and R. Stewart, The pyridinium–dihydropyridine system. I. Synthesis of a series of substituted pyridinium ions and their 1,4-dihydro reduction products and a determination of their stabilities in aqueous buffers. *Canadian Journal of Chemistry*, 1977. 55(10): p. 1687-1695.
20. Willot, S.J.P., et al., Expanding the Spectrum of Light-Driven Peroxygenase Reactions. *ACS Catalysis*, 2019. 9(2): p. 890-894.
21. Wu, J.T., L.H. Wu, and J.A. Knight, Stability of NADPH: effect of various factors on the kinetics of degradation. *Clinical Chemistry*, 1986. 32(2): p. 314.

Appendix

Synthesis of the NCBs

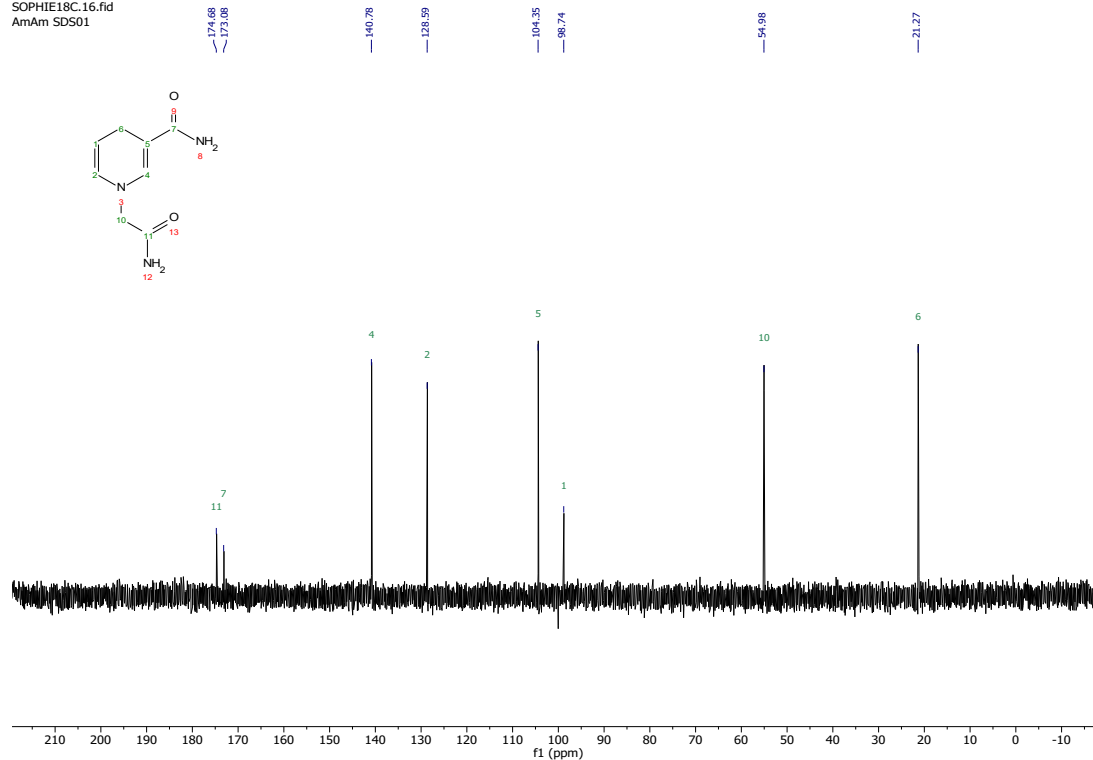
NMR spectra

^1H NMR (400 MHz, Deuterium Oxide) δ 6.95 (s, 1H), 5.83 (d, J = 8.0 Hz, 1H), 4.96 – 4.90 (m, 1H), 3.96 (s, 2H), 3.07 (s, 2H).

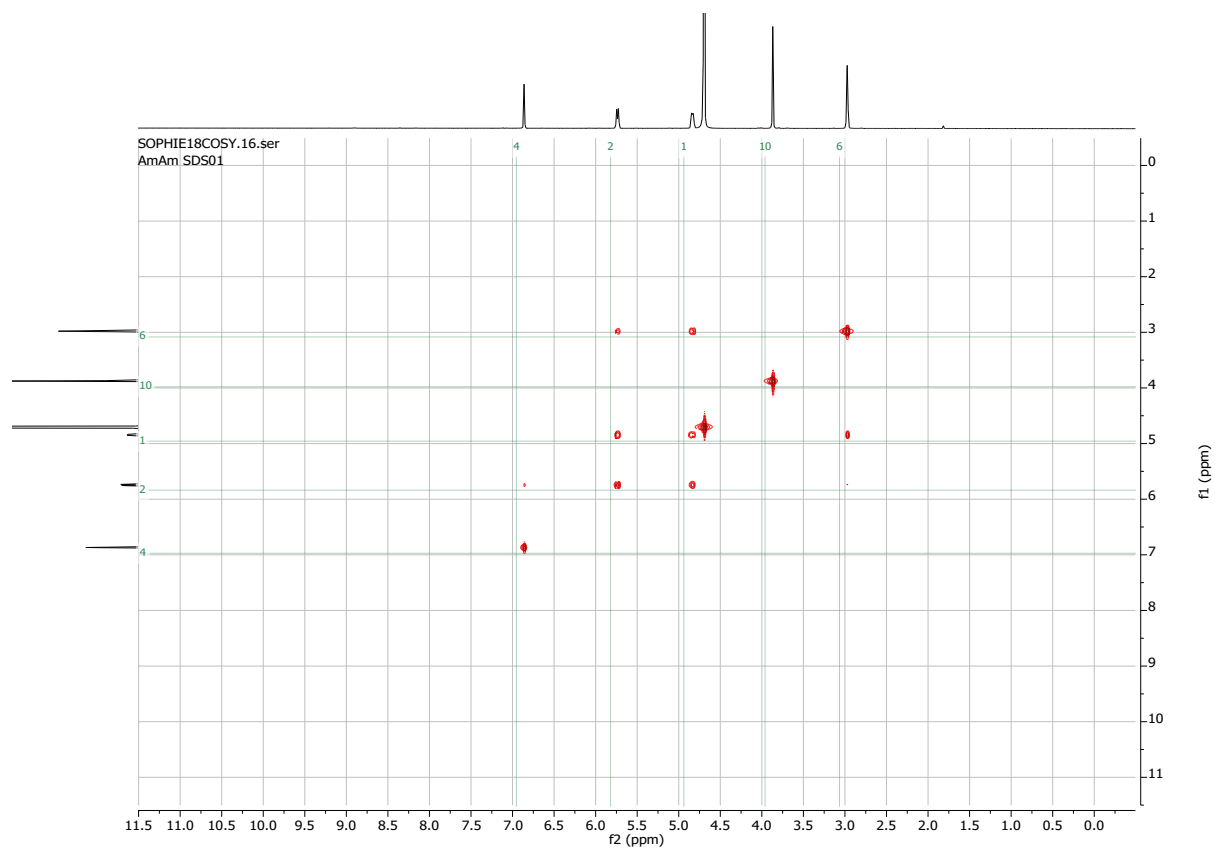


^{13}C NMR (400 MHz, Deuterium Oxide)

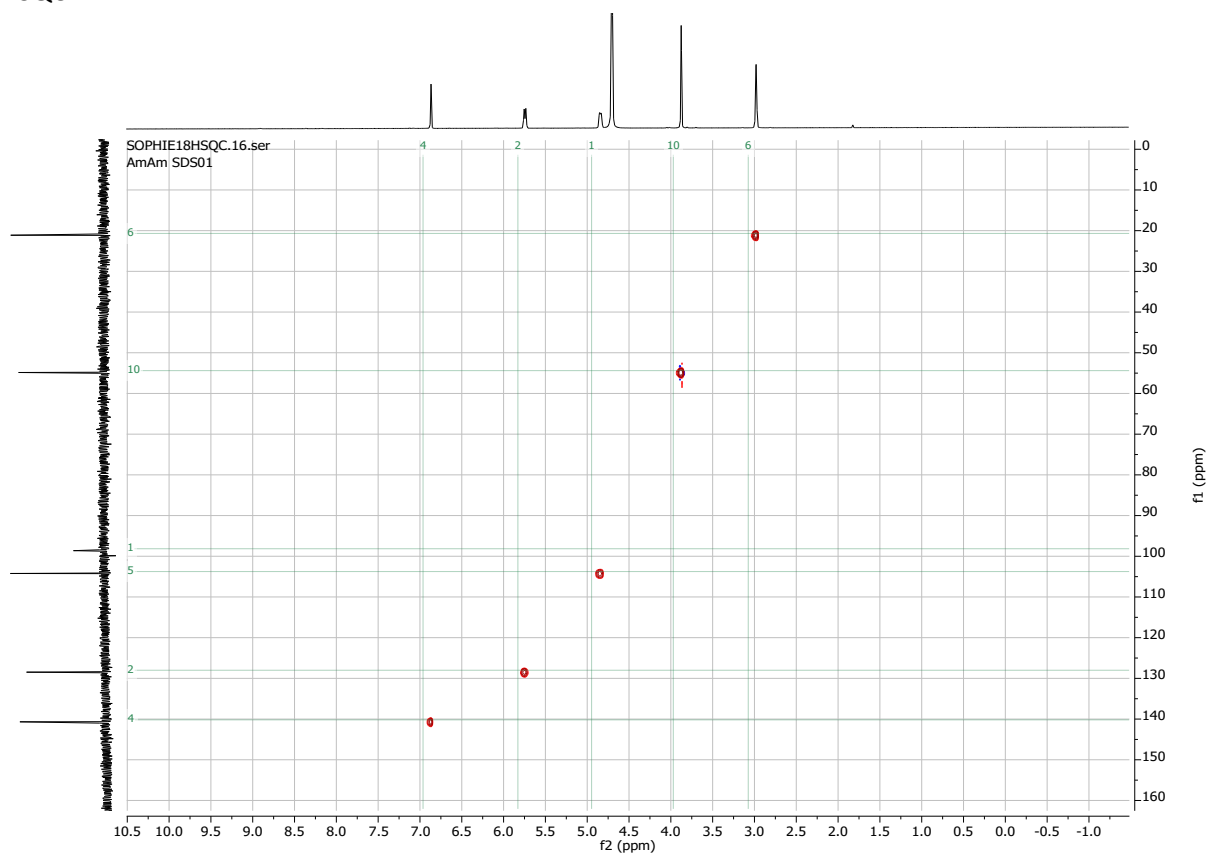
SOPHIE18C.16.fid
AmAm SDS01



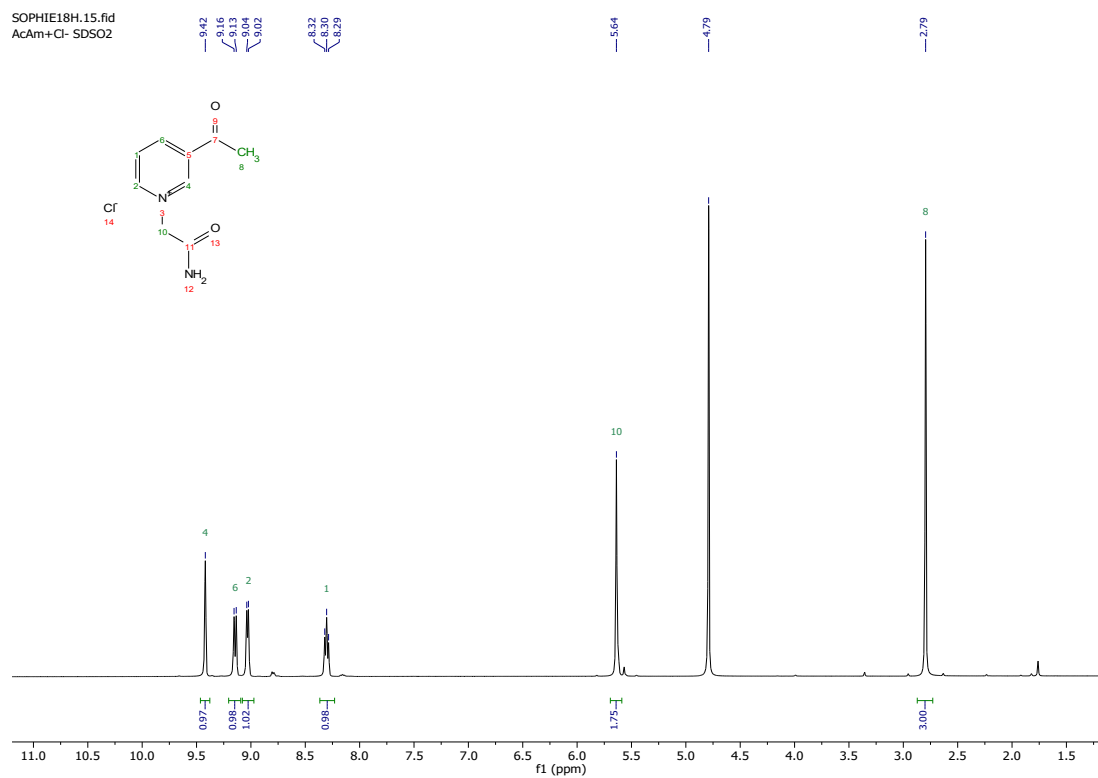
COSY



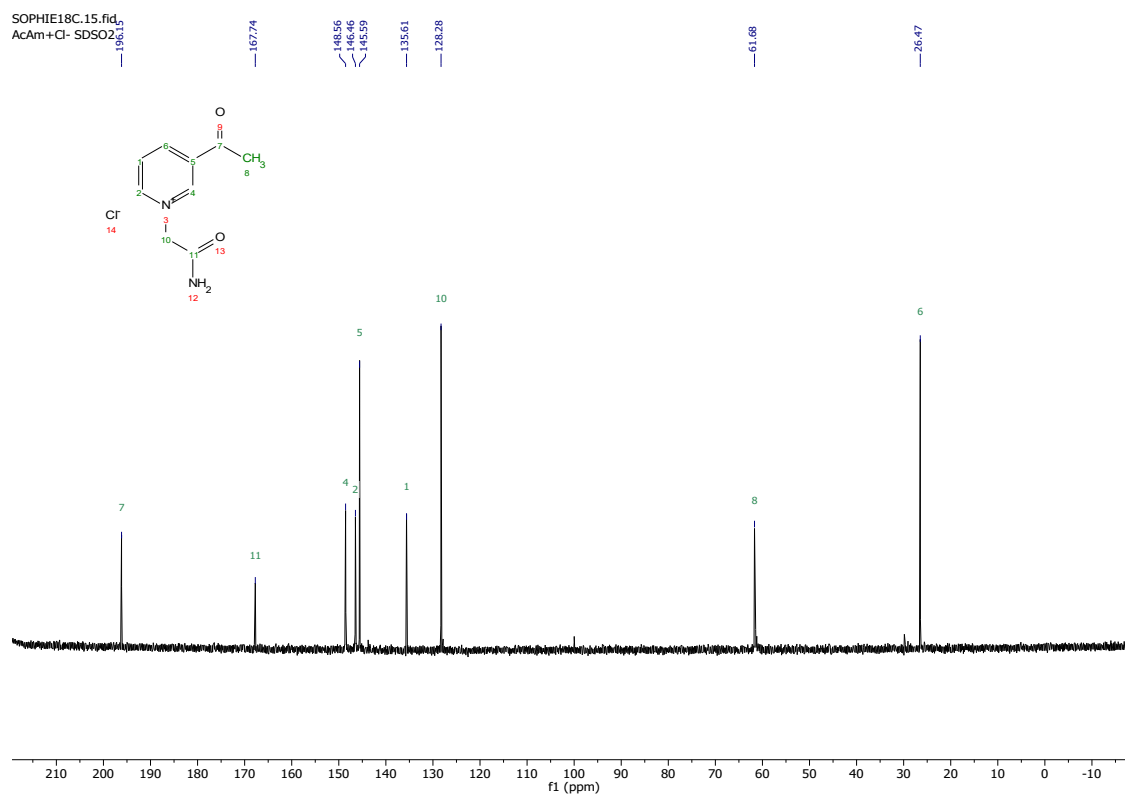
HSQC



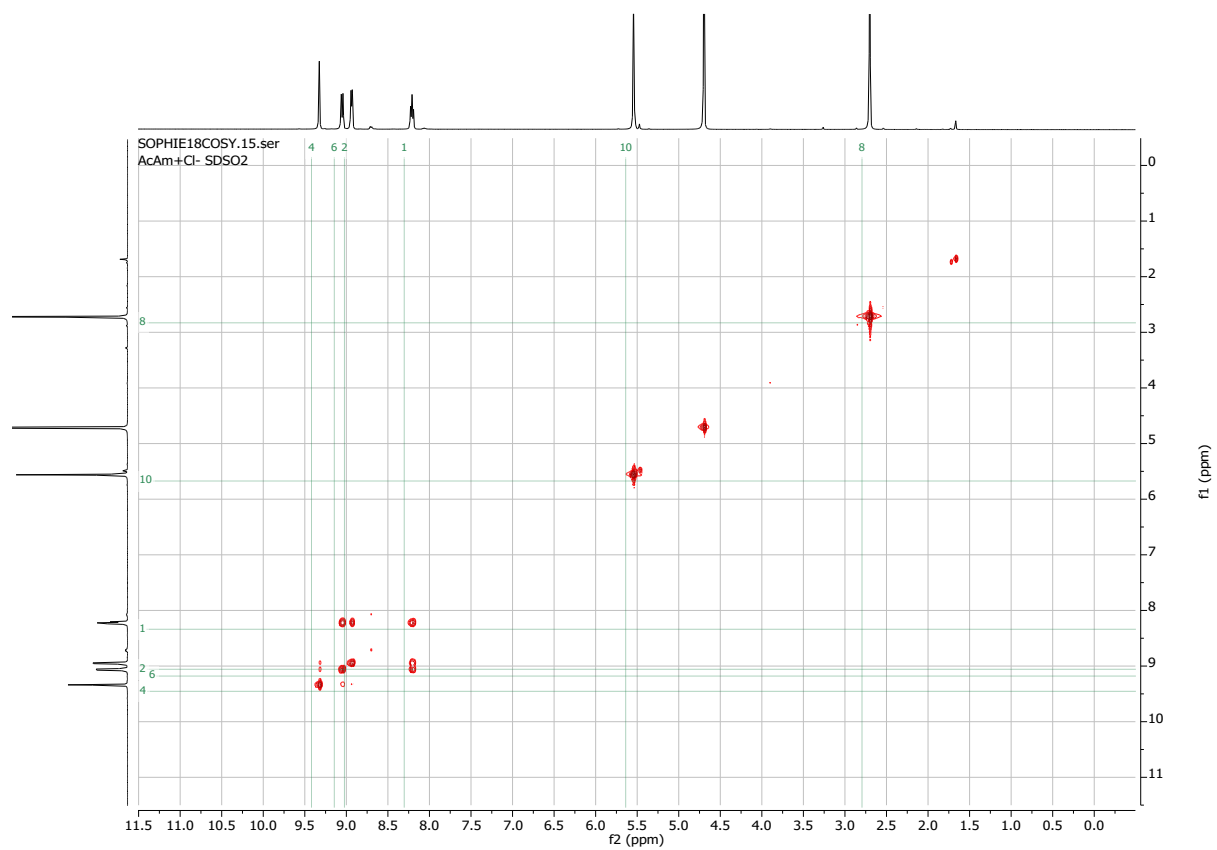
^1H NMR (400 MHz, Deuterium Oxide) δ 9.42 (s, 1H), 9.14 (d, J = 8.1 Hz, 1H), 9.03 (d, J = 6.0 Hz, 1H), 8.30 (t, J = 7.1 Hz, 1H), 5.64 (s, 1H), 2.79 (s, 2H).



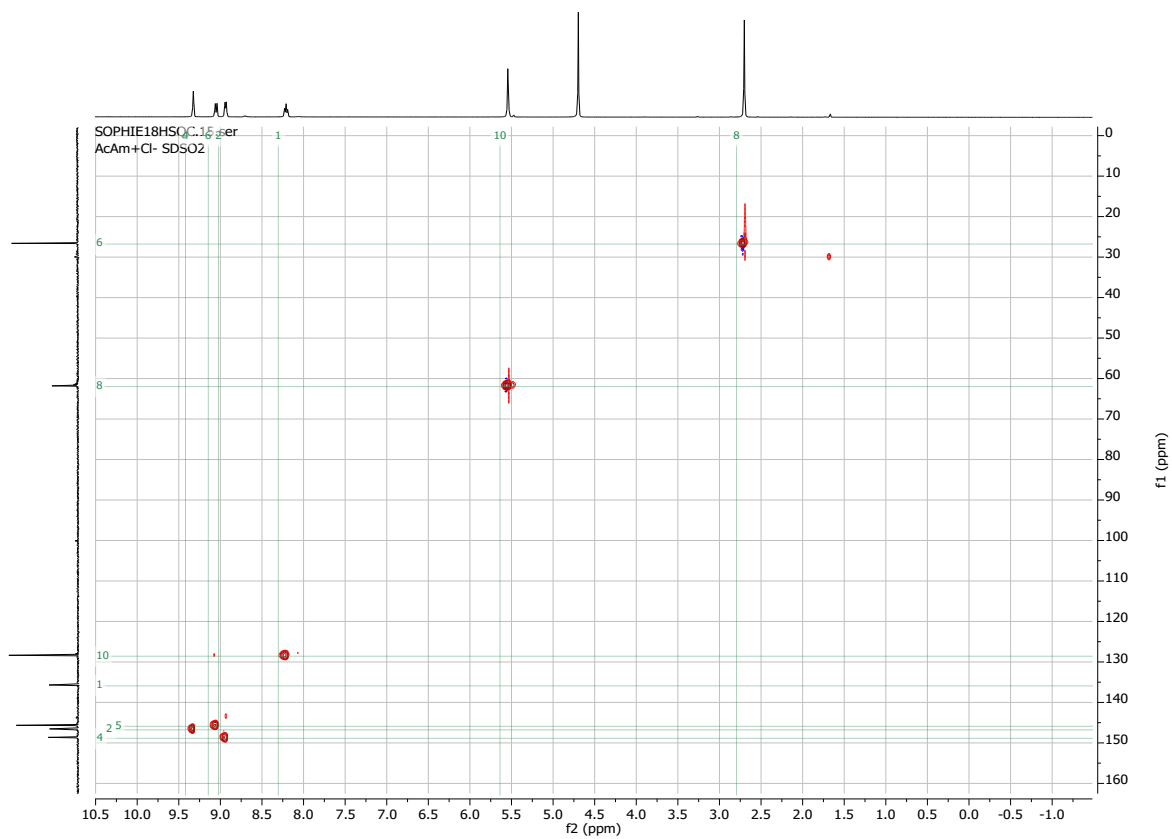
^{13}C NMR (400 MHz, Deuterium Oxide)



COSY



HSQC



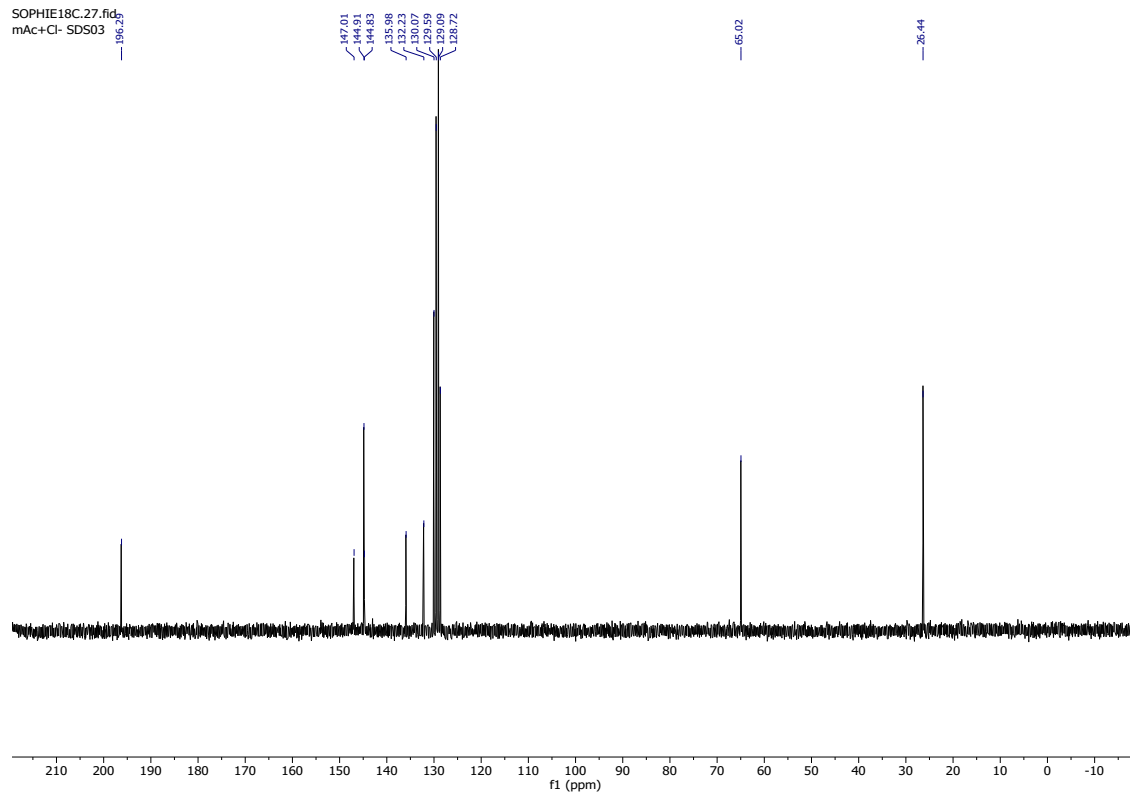
^1H NMR (400 MHz, Deuterium Oxide) δ 9.46 (s, 1H), 9.08 (d, J = 6.0 Hz, 1H), 9.04 (d, J = 8.1 Hz, 1H), 8.22 (t, J = 7.1 Hz, 1H), 7.51 (s, 5H), 5.92 (s, 2H), 2.76 (s, 3H).

SOPHIE18H.27.fid
mAc+Cl- SDS03

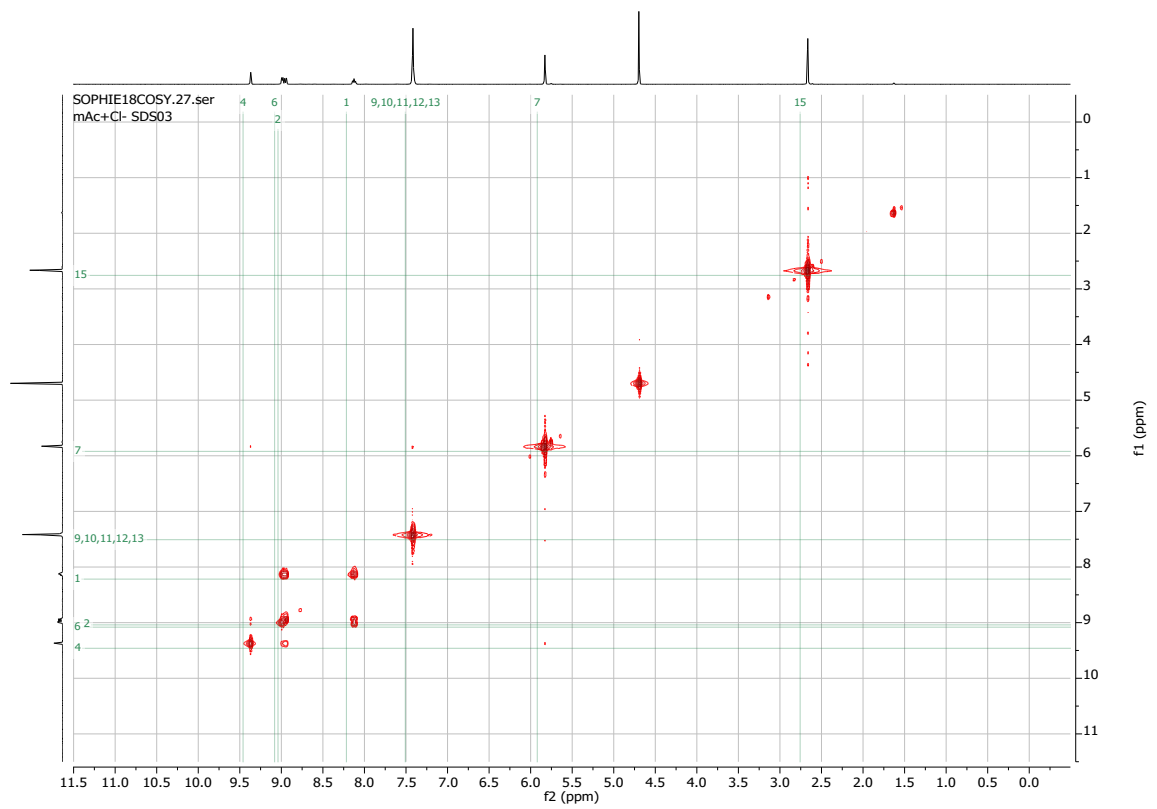


^{13}C NMR (400 MHz, Deuterium Oxide)

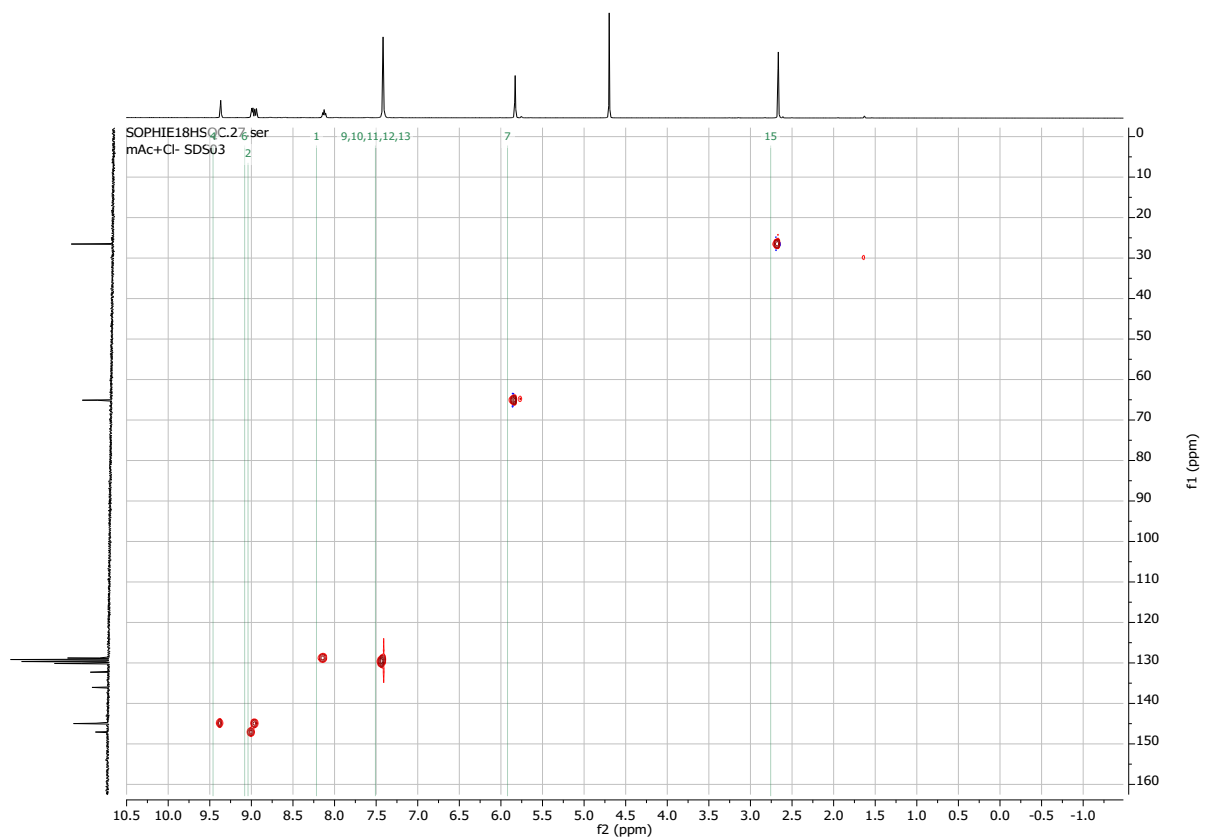
SOPHIE18C.27.fid
mAc+Cl- SDS03



COSY

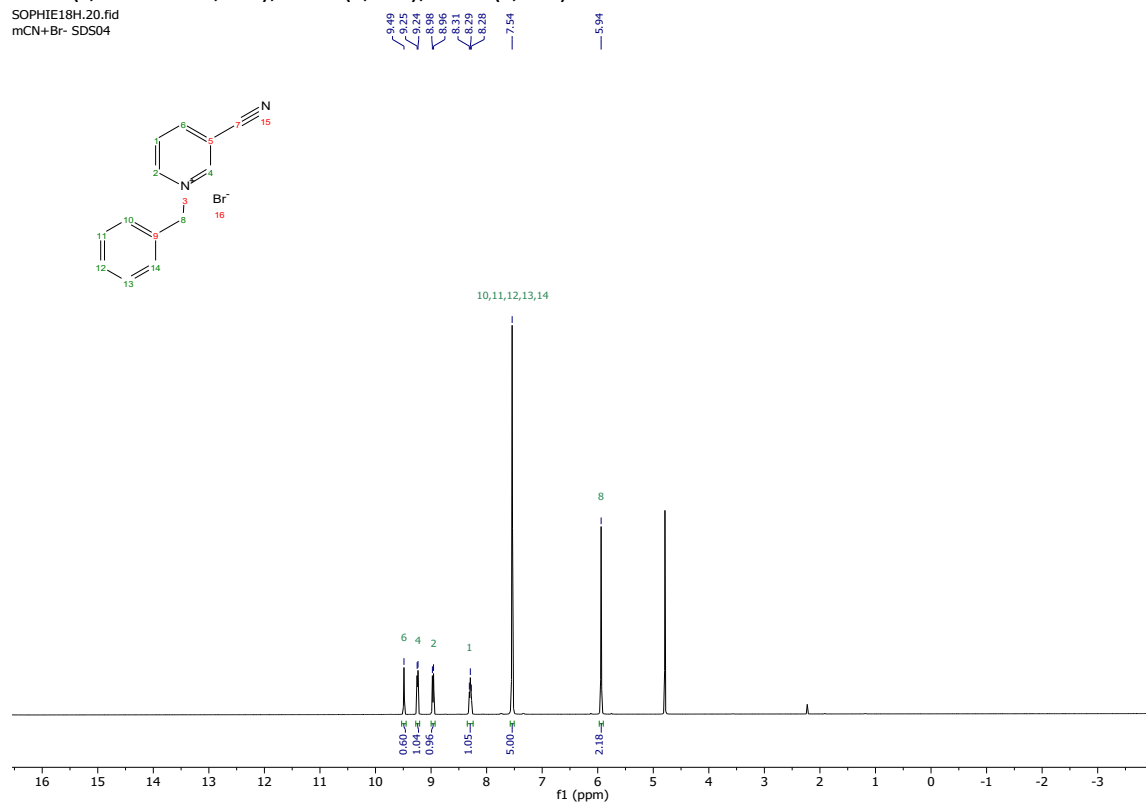


HSQC



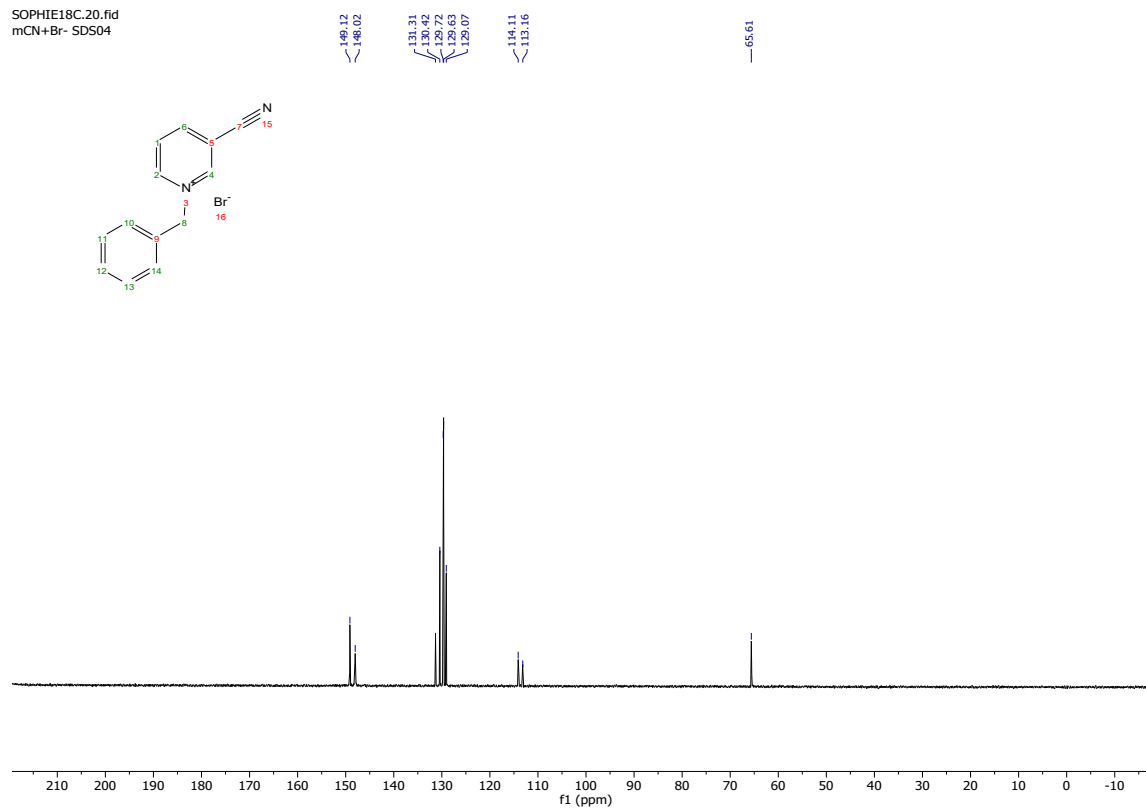
^1H NMR (400 MHz, Deuterium Oxide) δ 9.49 (s, 1H), 9.24 (d, J = 6.1 Hz, 1H), 8.97 (d, J = 8.1 Hz, 1H), 8.29 (t, J = 7.0 Hz, 1H), 7.54 (s, 5H), 5.94 (s, 2H).

SOPHIE18H.20.fid
mCN+Br- SDS04

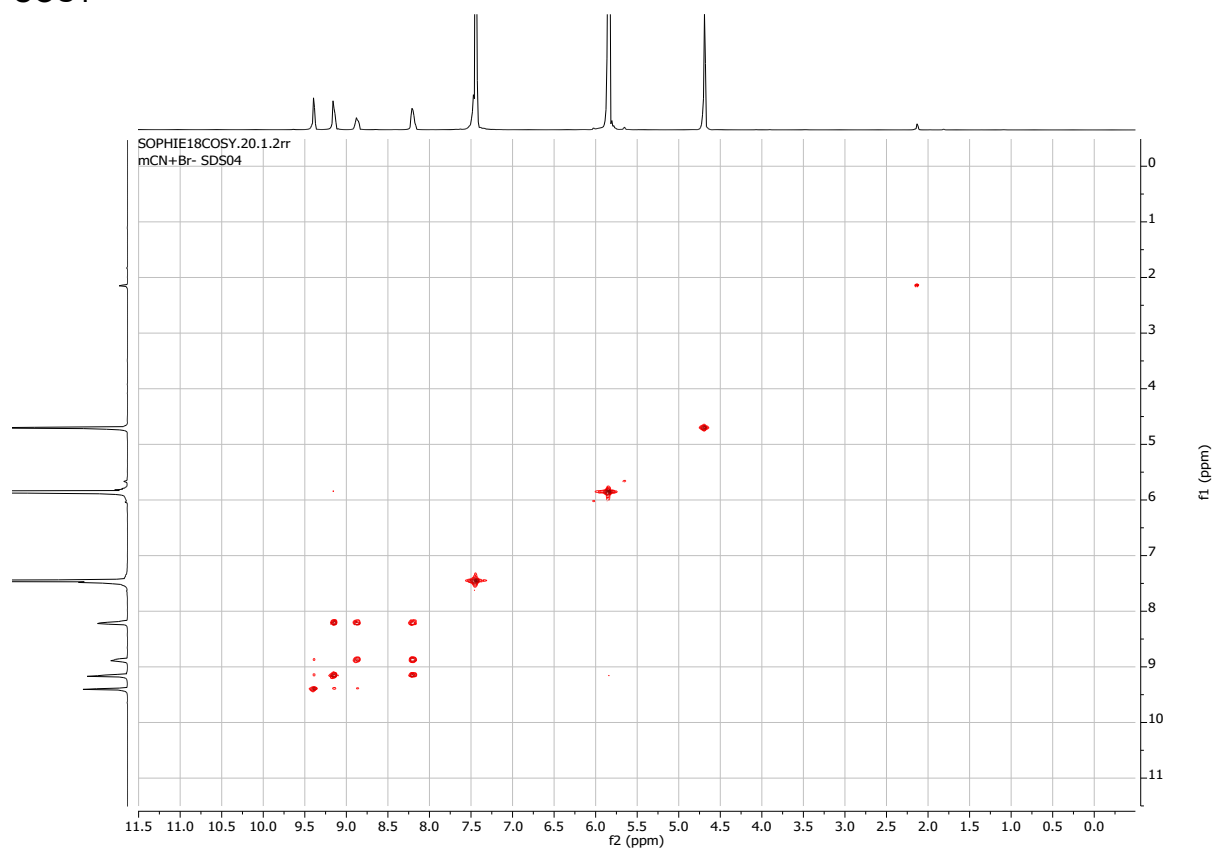


^{13}C NMR (400 MHz, Deuterium Oxide)

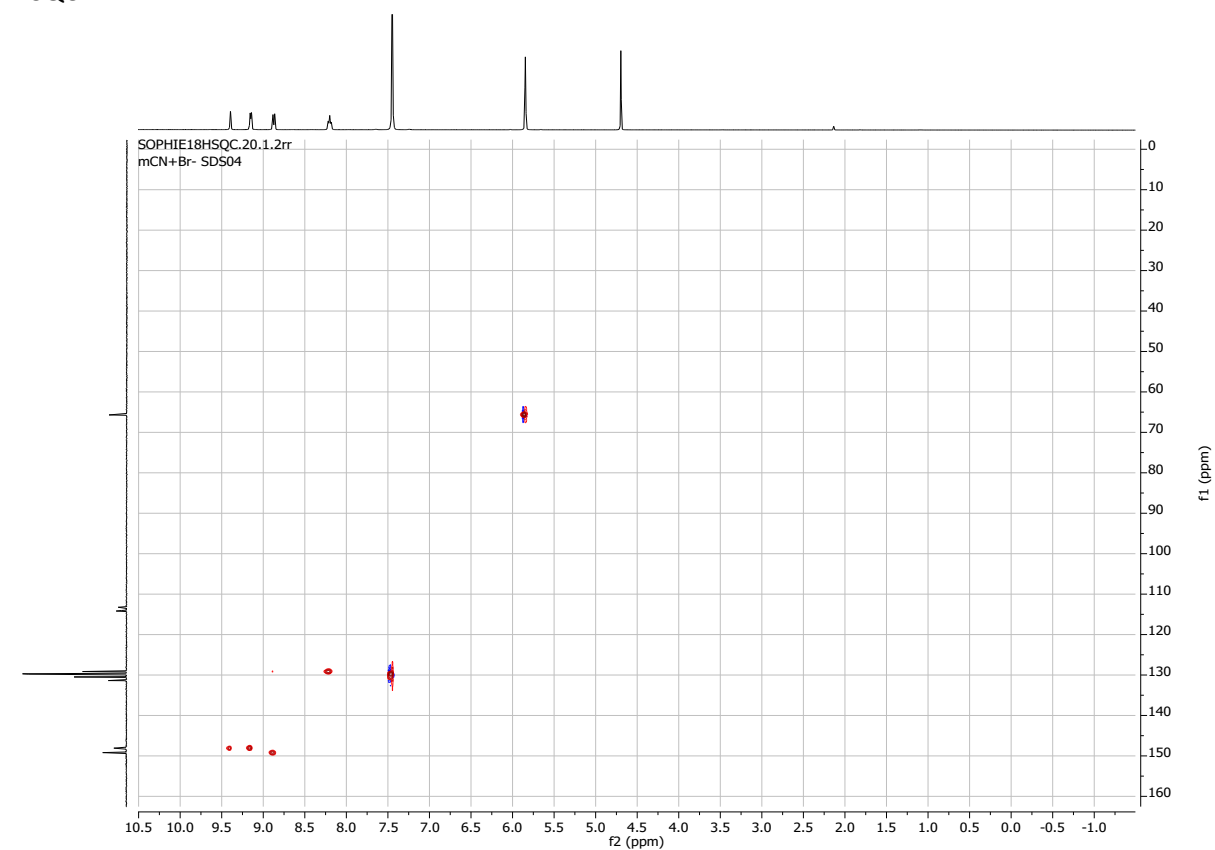
SOPHIE18C.20.fid
mCN+Br- SDS04



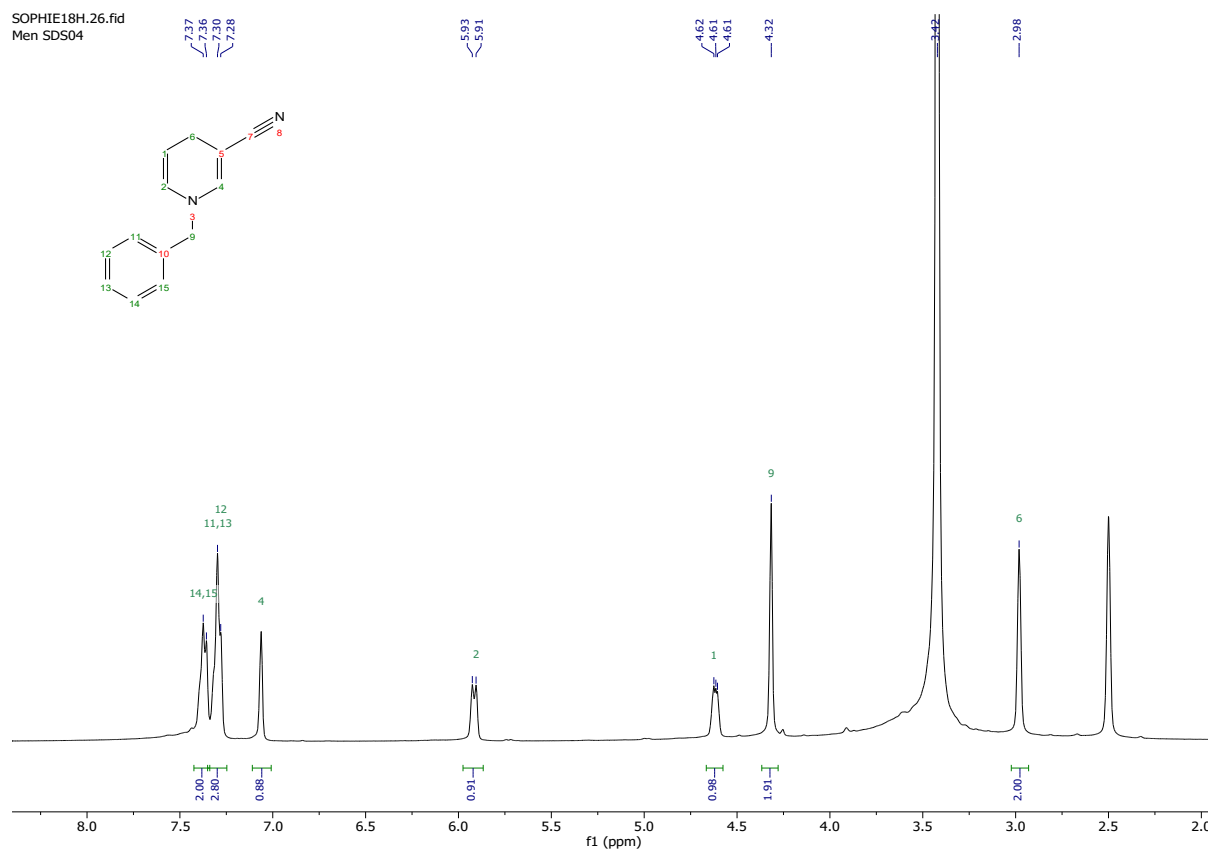
COSY



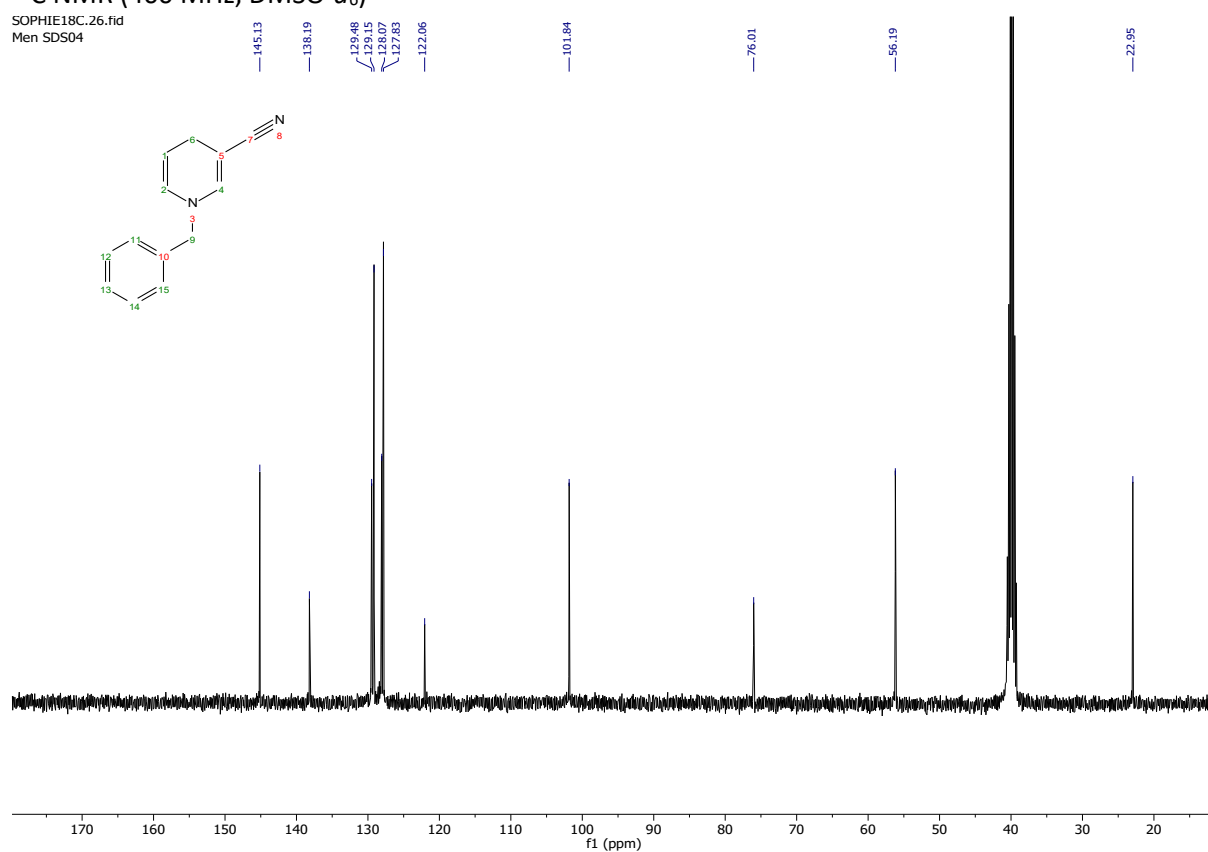
HSQC



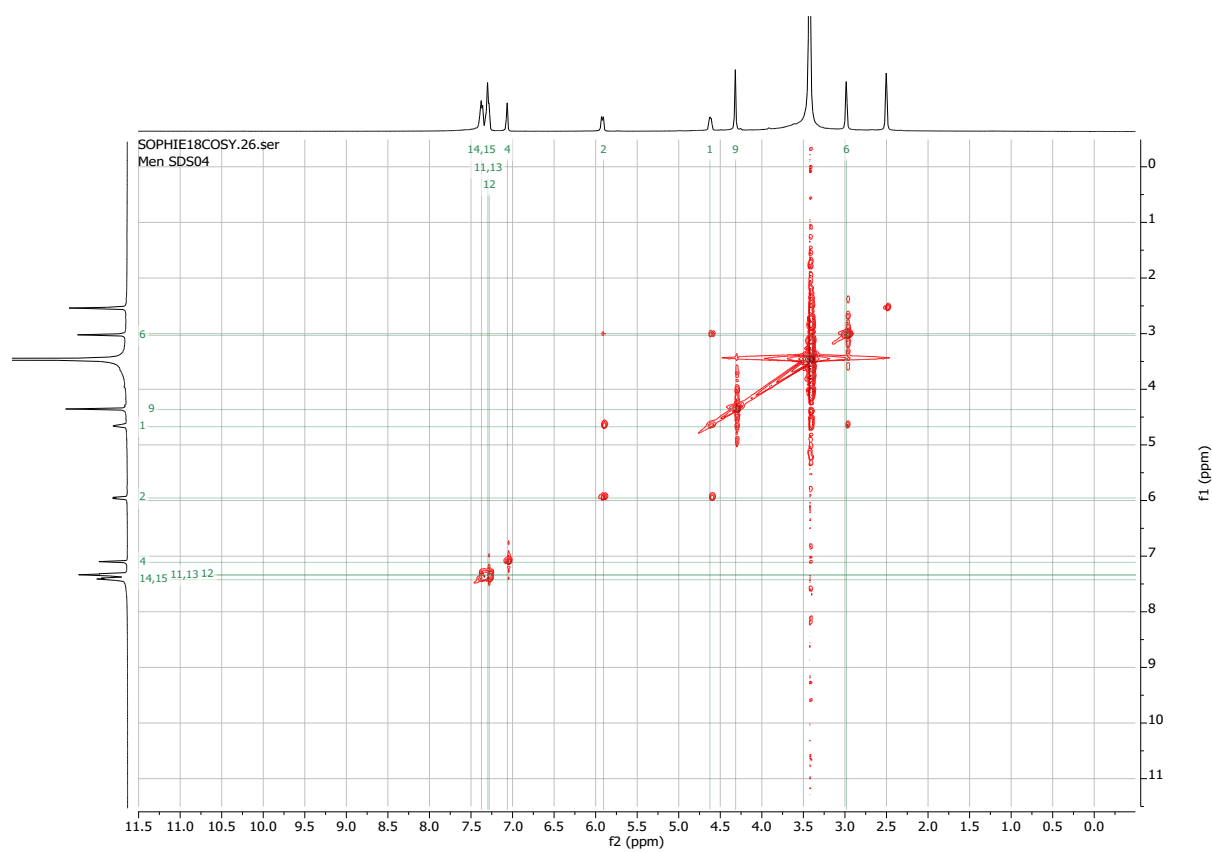
^1H NMR (400 MHz, $\text{DMSO-}d_6$) δ 7.37 (d, $J = 6.9$ Hz, 2H), 7.29 (d, $J = 6.9$ Hz, 3H), 7.07 (d, $J = 3.9$ Hz, 1H), 5.92 (d, $J = 8.1$ Hz, 1H), 4.67 – 4.58 (m, 1H), 4.32 (s, 2H), 2.98 (s, 2H).



^{13}C NMR (400 MHz, $\text{DMSO-}d_6$)



COSY



HSQC

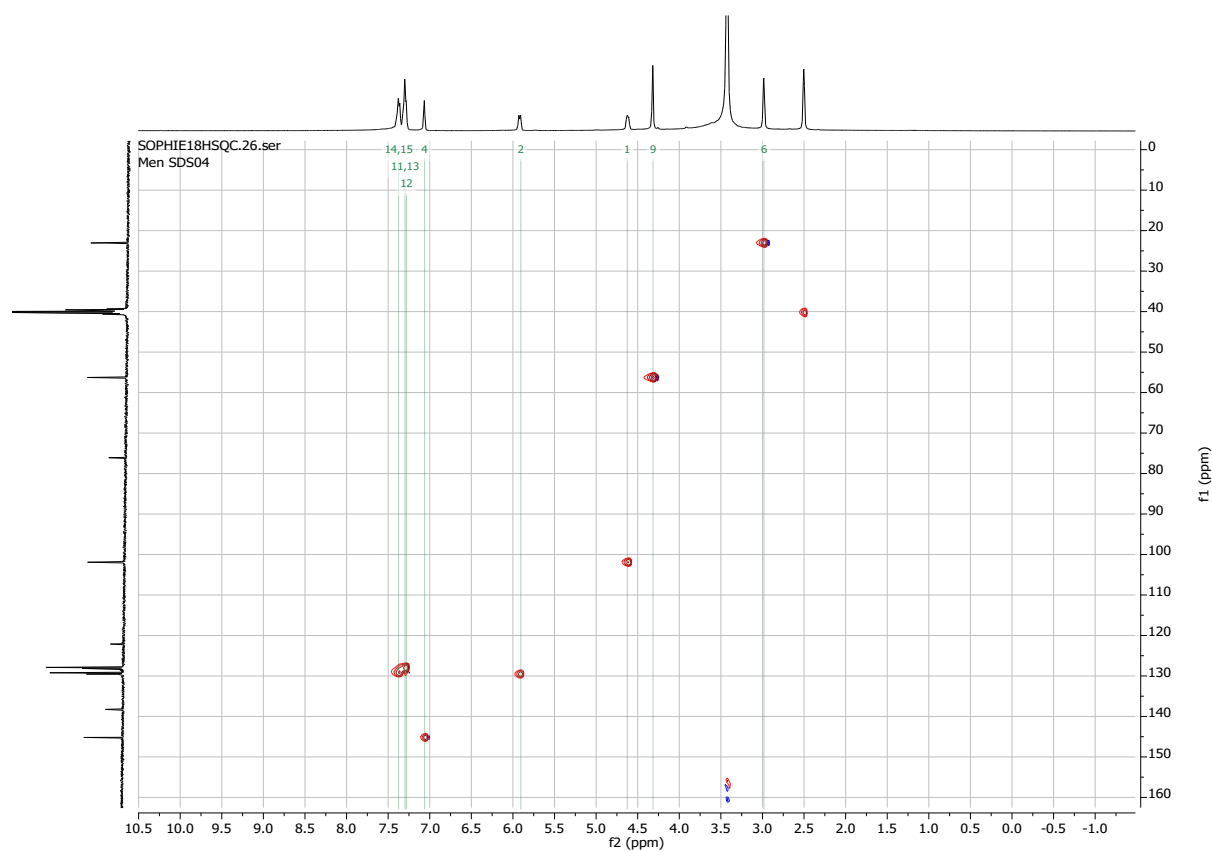
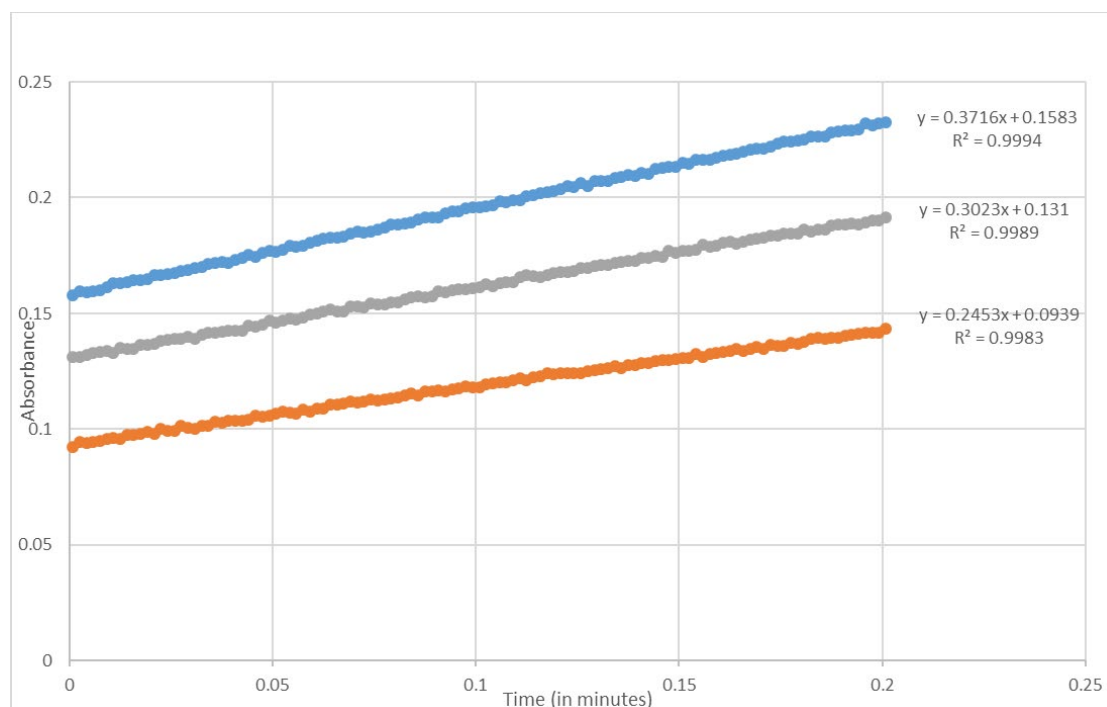


Figure 18: Sequence of the *TADH* gene isolated from *Thermus* sp. ATN1: obtained from GenBank EU681191.113. The *EcoRV* restriction site is highlighted in red.

```
>ENA|ACD50896|ACD50896.1 Thermus sp. ATN1 alcohol dehydrogenase
ATGCGCGCAGTGGTTTTTAAAAACAAAGAGCGCGTCGCCGTC AAGGAGGTCAATGCCCCT
CGCCTACAACATCCCCTAGATGCCCTCGTGC GCGTGACCTGGCCGGCATATGTGGCTCG
GACTTGACCTTTACCACGGCAAATACCTGTTCTCCCCGGAAGTGTACTGGGCCACGAG
TTCGTGGGCCAAGTGGAAGCCGTGGGCGAAGGTATCCAAGATCTTCAGCCAGGGGACTGG
GTTGTTGGACCGTTCCACATCGCCTGTGGCACCTGCCCCTACTGCCGAAGGCACCAAGTAC
AACCTGTGTGAACGGGGAGGCGTCTACGTTATGGCCCCATGTTTGGCAATCTCCAAGGA
GCCCAGGCGGAAATCCTTCGGGTTCCCTTCAGCAACGTCAATCTCCGAAACTGCCTCCA
AACCTAAGCCCAGAACGGGGCCATCTTTGCCGGCGATATCTCTCCACAGCCTATGGAGGA
CTCATCCAGGGCCAGCTCCGGCCCCGGTGATAGCGTGGCTGTCATCGAGCGGGGCCCGTG
GGATTGATGGCCATTGAAGTAGCCAGGTATTGGGTGCGAGCAAATACTTGCCATAGAT
CGCATTCTGAGCGATTGGAACGCGCCGCTTCCTGGGCGCCATCCCCATCAACGCCGAA
CAAGAAAATCCTGTCCGGCGAGTTCGCTCTGAAACCAACGATGAGGGGCCAGATTGTC
CTCGAGGCTGTAGCGGAGCTGCCACCCTCAGCTTGGCCCTGGAGATGGTACGCCCTGGG
GGAAGGGTATCAGCTGTTGGGGTGGATAACGCCCCCTCTTTCCATTCCCTTTAGCATCG
GGCCTGGTCAAGGACCTAACCTTCCGTATAGTTTGGCCAACGTCCACCTCTACATTGAT
GCGGTTCTGGCCCTTTTGCTAGCGGCCGTTTGCAACCGAGCGGATTGTTCCCACTAT
CTCCCCTTGAGGAAGCTCTCGAGGGTATGAGCTTTTGACCGGAAAGAAGCGCTAAAA
GTCCTTTTGGTTGTCAGGGGGTGA
```

Figure 19: Kinetic measurement on the combined, dialysed and concentrated AEX fractions



Calculations of the enzyme concentration:

$$\text{Average slope} = (0.3716 + 0.3023 + 0.2453) / (3) = 0.3064 / \text{min}$$

$$(0.3064 / \text{min}) / (6220 \text{ M/cm}) = 4.9 \times 10^{-5} \text{ M/min}$$

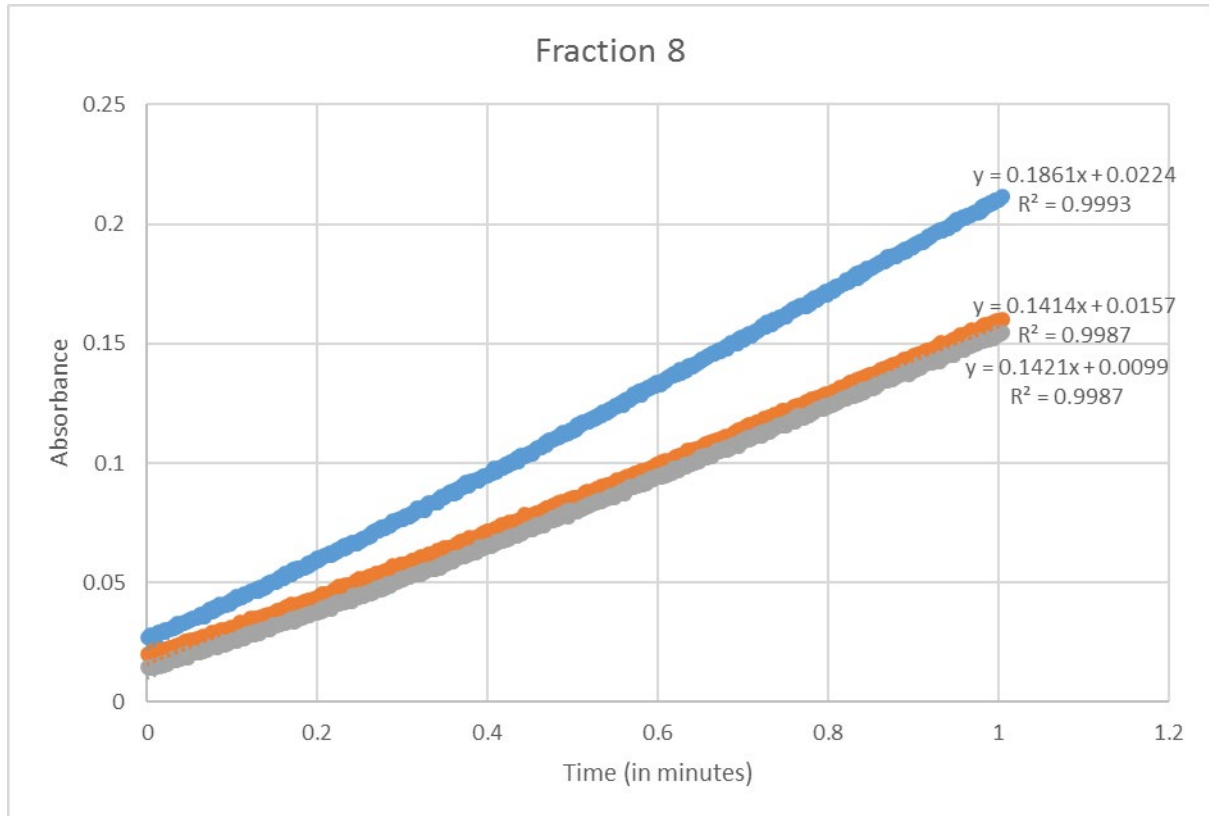
$$= 4.9 \times 10^{-8} \text{ mol/min}$$

$$= 4.9 \cdot 10^{-2} \mu\text{mol}/\text{min}$$

$$(100 \cdot \text{dilution}, 10 \mu\text{L in } 1 \text{ mL}) = 2.52 \text{ U/mL}$$

$$2.52/29.5076 \text{ U/mg} = 0.0853 \text{ mg/mL}$$

Figure 20: Kinetic measurement on SEC fraction 8



$$\text{Average slope} = (0.1861 + 0.1414 + 0.1421) / (3) = 0.15653 / \text{min}$$

$$(0.15653/\text{min}) / (6220 \text{ M/cm}) = 2.52 \cdot 10^{-5} \text{ M/min}$$

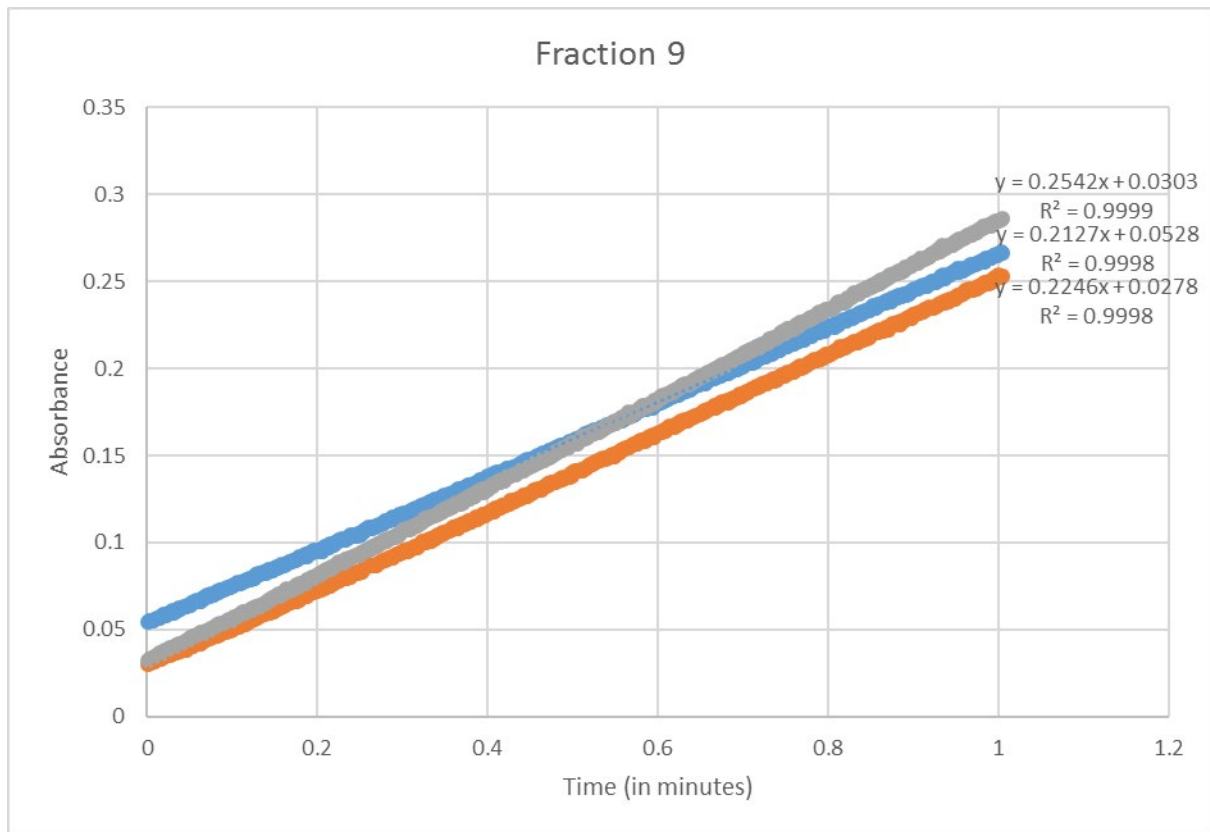
$$= 2.52 \cdot 10^{-8} \text{ M/min}$$

$$= 2.52 \cdot 10^{-2} \mu\text{mol}/\text{min}$$

$$(100 \cdot \text{dilution}, 10 \mu\text{L in } 1 \text{ mL}) = 2.52 \text{ U/mL}$$

$$2.52/29.5076 \text{ U/mg} = 0.0853 \text{ mg/mL}$$

Figure 21: Kinetic measurement on SEC fraction 9



Average slope= $(0.2542+0.2127+0.2246) / (3) = 0.2305 / \text{min}$

$(0.2305/\text{min}) / (6220 \text{ M/cm}) = 3.71 \cdot 10^{-5} \text{ M/min}$

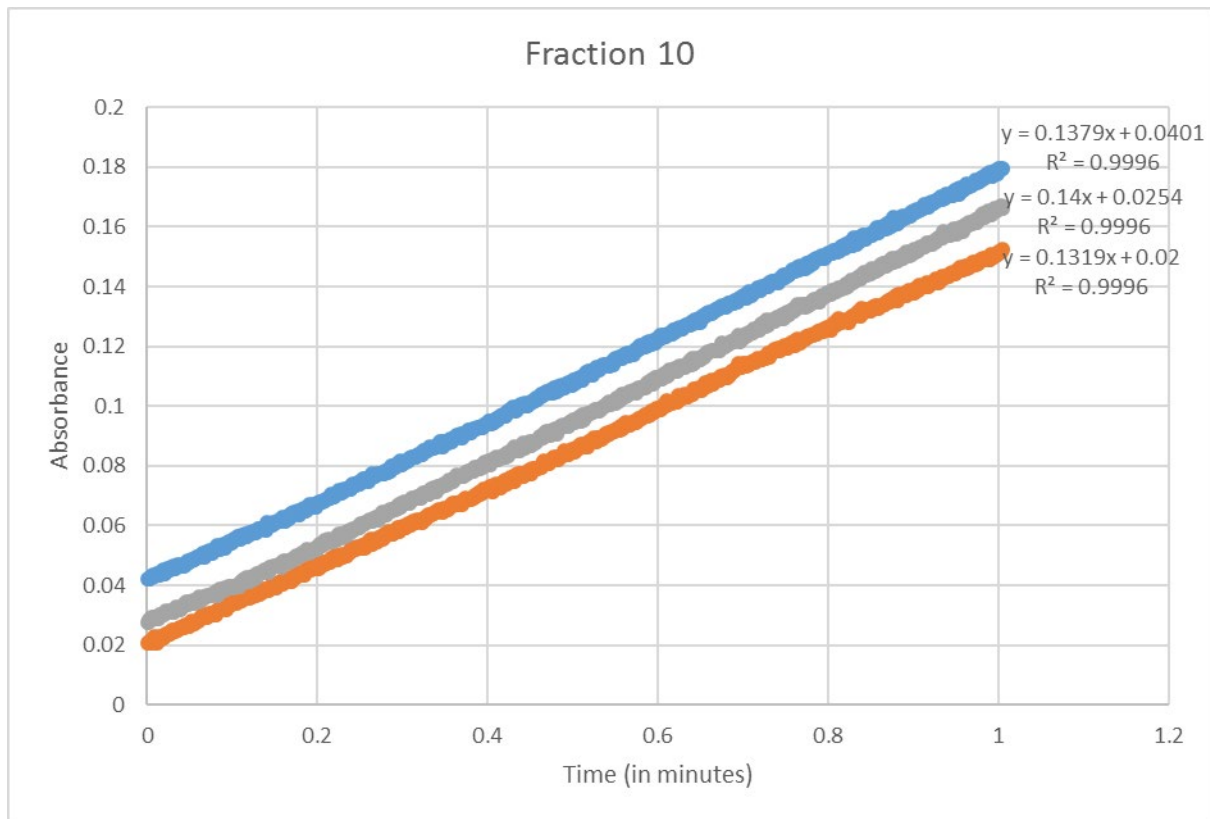
$= 3.71 \cdot 10^{-8} \text{ mol/min}$

$= 3.71 \cdot 10^{-2} \mu\text{mol/min}$

$(100 \cdot \text{dilution}, 10 \mu\text{L in } 1 \text{ mL}) = 3.71 \text{ U/mL}$

$3.71/29.5076 \text{ U/mg} = 0.126 \text{ mg/mL}$

Figure 22: Kinetic measurement on SEC fraction 10



Average slope= $(0.1379+0.14+0.1319) / (3) = 0.1366 / \text{min}$

$(0.1366 / \text{min}) / (6220 \text{ M/cm}) = 2.20 \cdot 10^{-5} \text{ M/min}$

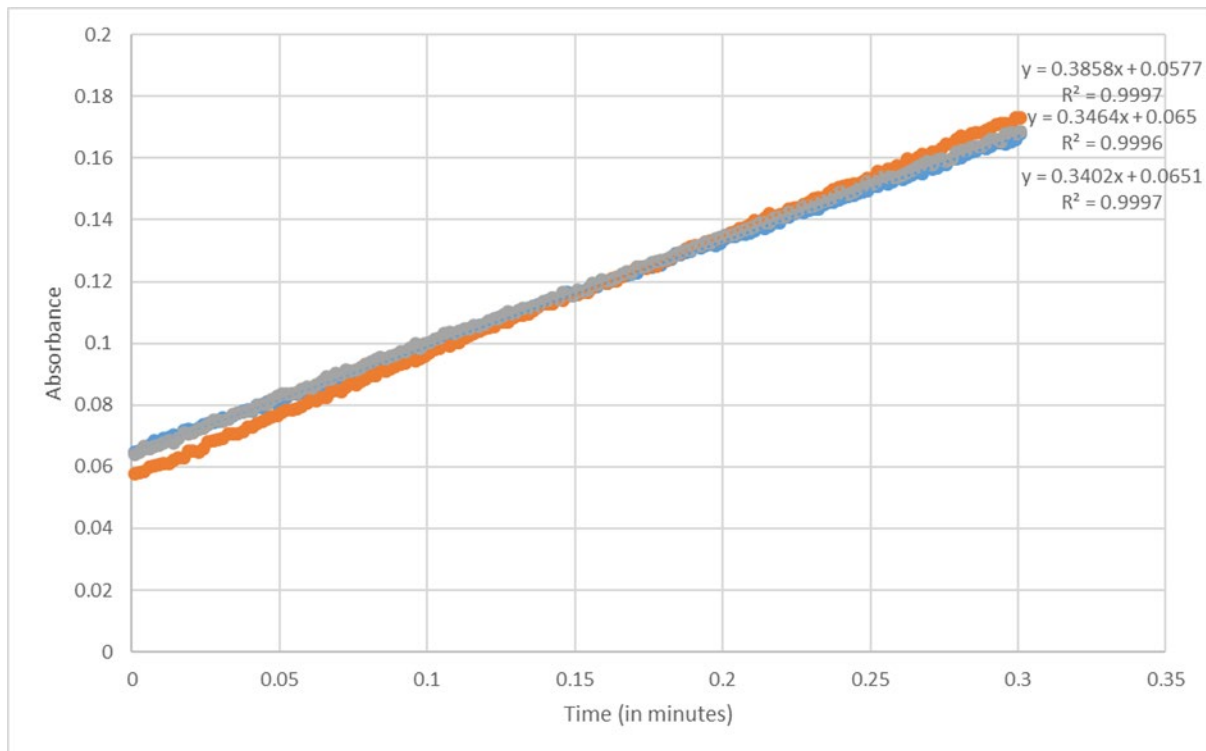
$= 2.20 \cdot 10^{-8} \text{ mol/min}$

$= 2.20 \cdot 10 \cdot 10^{-2} \mu\text{mol/min}$

$(100 \cdot \text{dilution}, 10 \mu\text{L in } 1 \text{ mL}) = 2.20 \text{ U/mL}$

$2.20/29.5076 \text{ U/mg} = 0.0743 \text{ mg/mL}$

Figure 23: Kinetic measurement on the combined, dialysed and concentrated SEC fractions



Average slope= $(0.3858+0.3464+0.3402) / (3) = 0.357/ \text{ min}$

$(0.357/\text{min}) / (6220 \text{ M/cm}) = 5.747 \cdot 10^{-5} \text{ M/min}$

$= 5.747 \cdot 10^{-8} \text{ mol/min}$

$= 5.747 \cdot 10 \cdot 10^{-2} \mu\text{mol/min}$

$(100 \cdot \text{dilution}, 10 \mu\text{L in } 1 \text{ mL}) = 5.747 \text{ U/mL}$

$5.747 / 29.5076 \text{ U/mg} = 0.195 \text{ mg/mL}$

Figure 24: BSA dilution series for BCA total protein determination

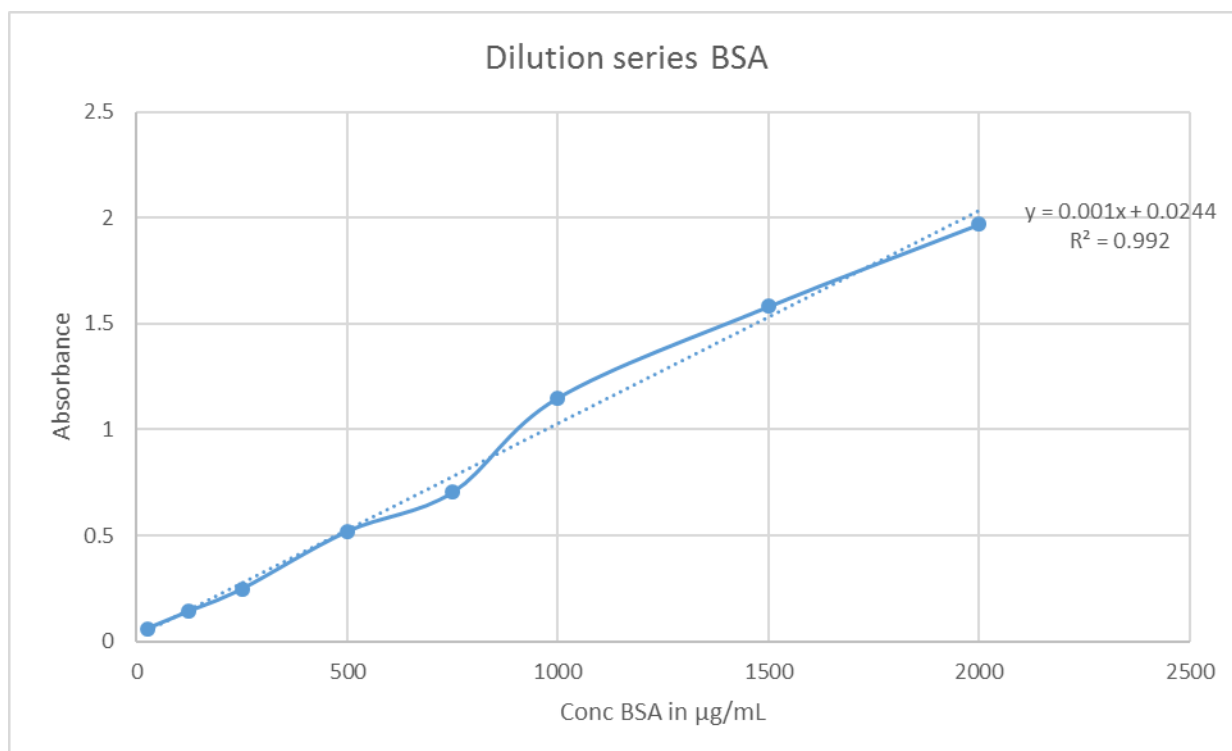


Table 3 Raw data from BSA determination of total protein concentration

TADH sample dilution factor	Un	2x	5x	10x	100x	Blanc
Absorbance (duplicate)	1.982	1.281	0.438	0.248	0.144	0.105
	2.16	1.299	0.437	0.307	0.149	0.107
Average abs after blanc correction	1.965	1.184	0.3315	0.1715	0.0405	x
Average abs/0.001 (equation std dilution)	1965	1184	331.5	171.5	40.5	x
Conc in µg/mL	1965	2368	1657.5	1715	4050	x

The total protein concentration in the TADH sample determined by taking the average of concentrations as measured for the undiluted, 2x 5x 10 x and 100 x diluted samples. The 100 x dilution was not taken into account for the final determination as its absorbance was only slightly higher than the blanc measurement.

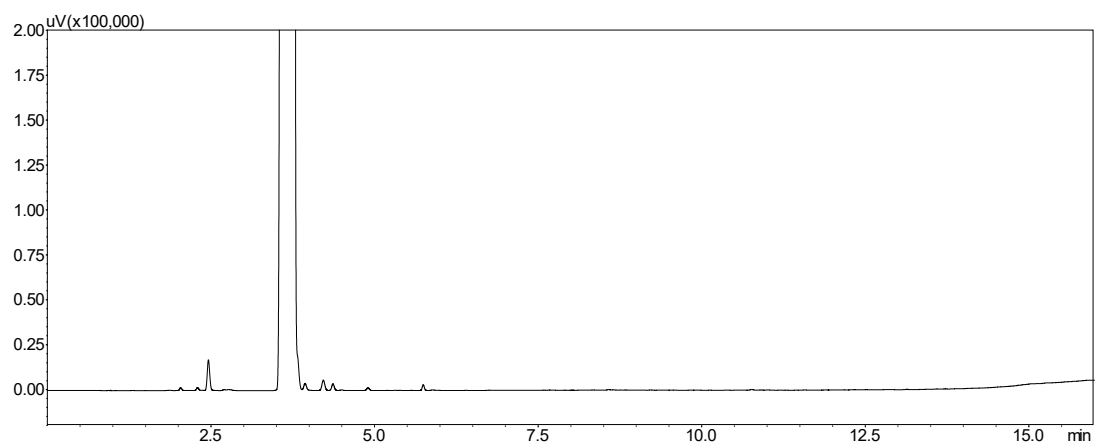
Figure 25: set-up of the reaction for the acceptance study of AmNAH by TADH. In figure A: the two water jacketed beakers, on the left ready for induction with the and Lightningcure® LC8 light source setup, the beaker on the right wrapped with LEDS for white light induction. In figure B a close up of the samples in the water jacketed beaker.



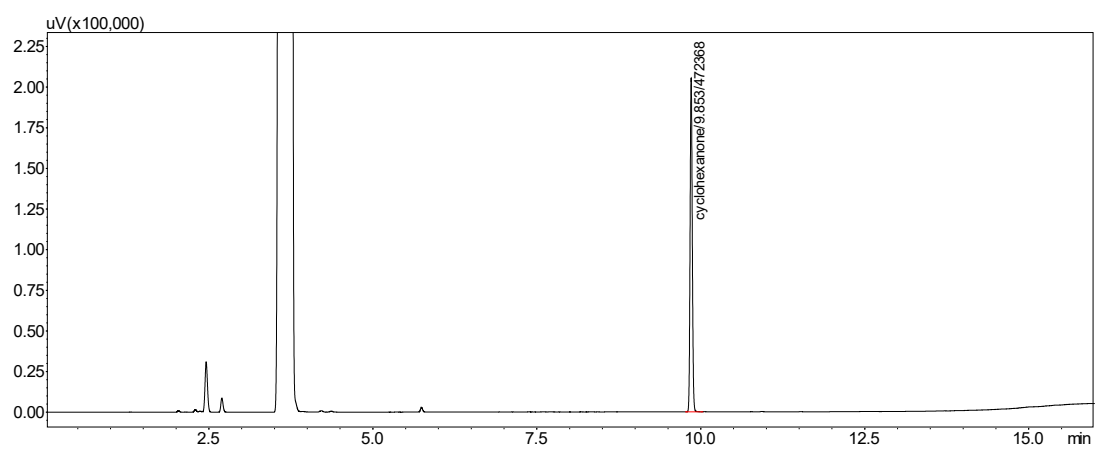
GC chromatograms

Control samples EtOAc, 10 mM cyclohexanone and 10 mM AmNAH

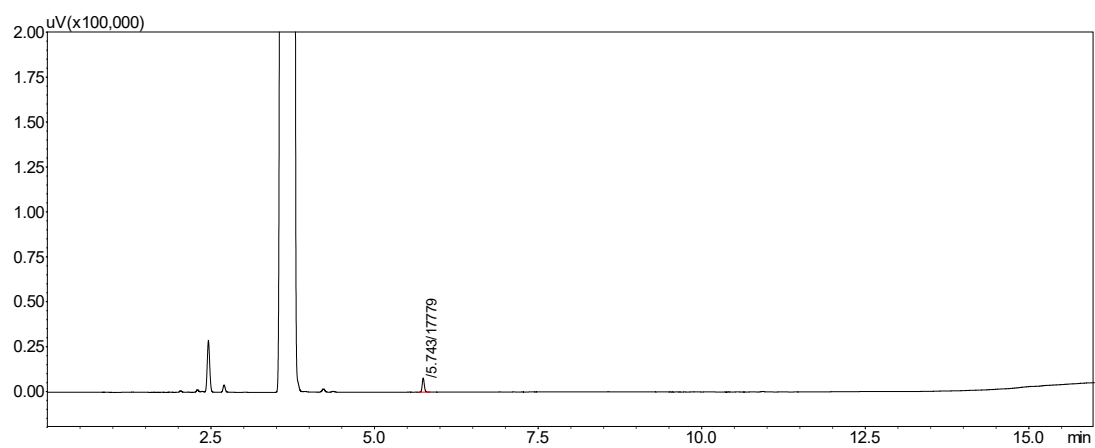
EtOAc



10 mM cyclohexanone

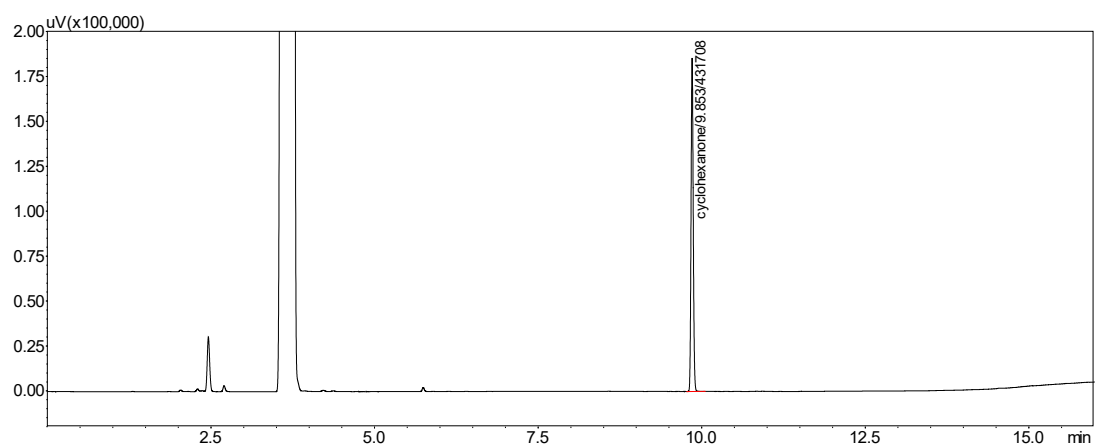


10 mM AmNAH

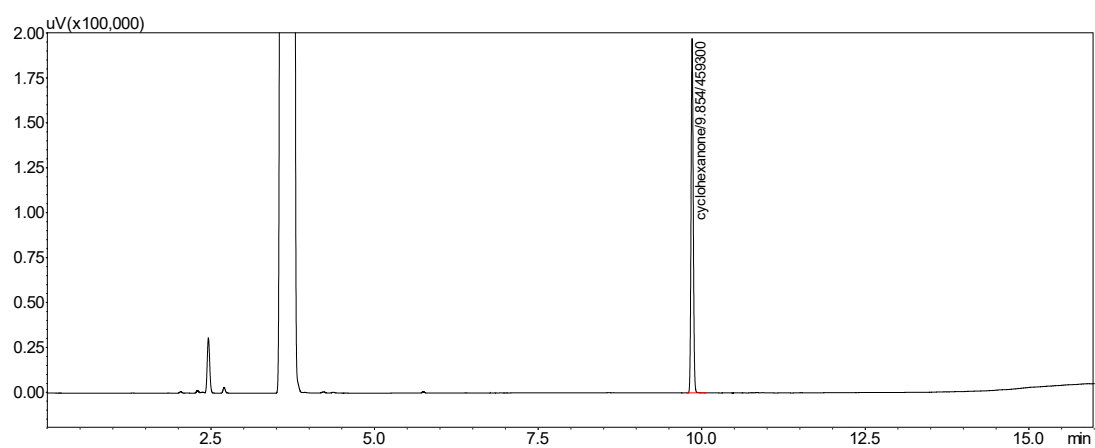


Reaction samples without light induction ("dark" conditions)

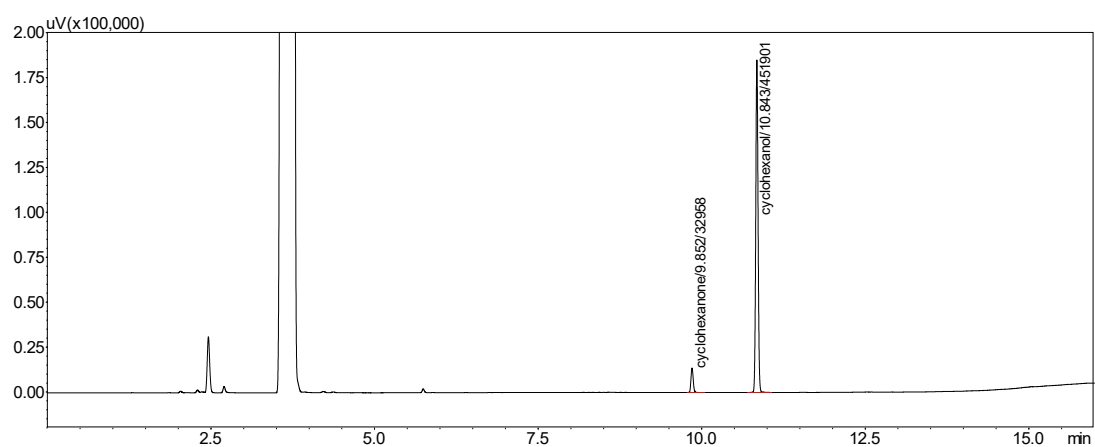
100 µg/mL TADH, 10 mM cyclohexanone no cofactor



100 µg/mL TADH, 10 mM cyclohexanone and 10 mM AmNAH

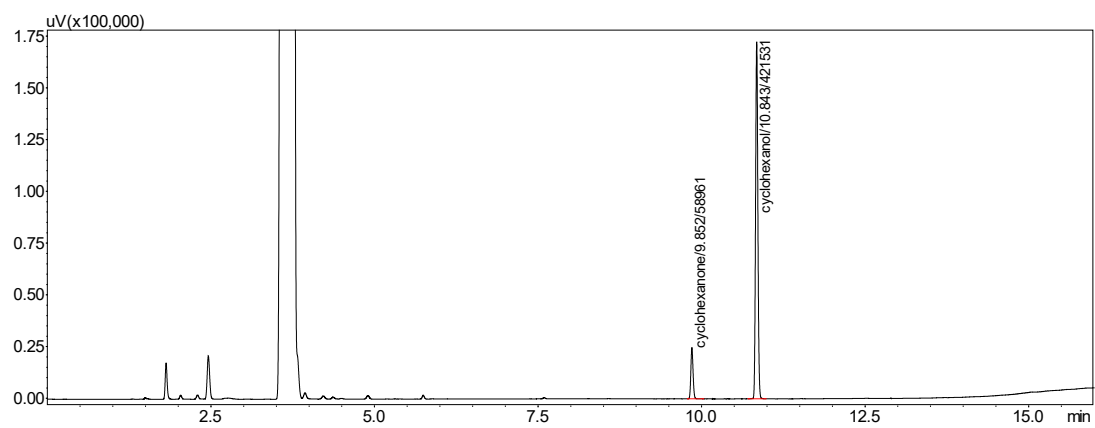


100 µg/mL TADH, 10 mM cyclohexanone and 10 mM AmNAH

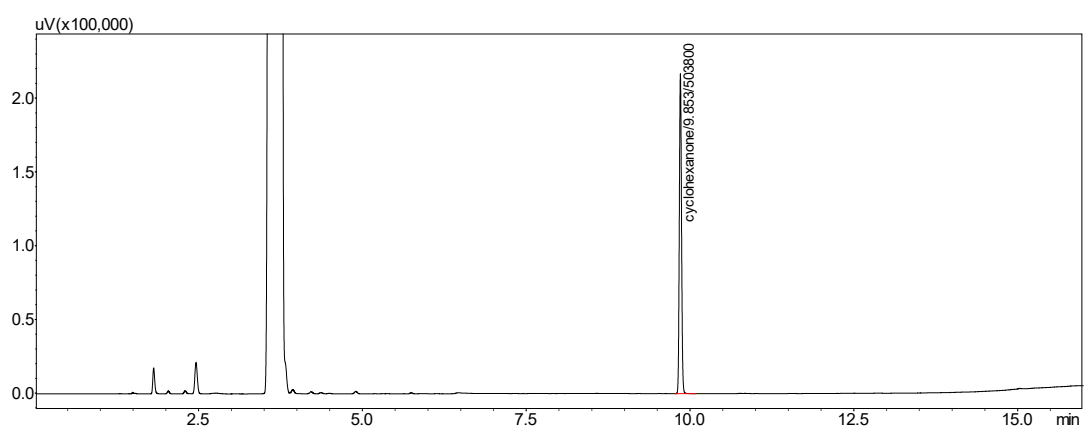


Reactions with LEDs induction (400-700nm)

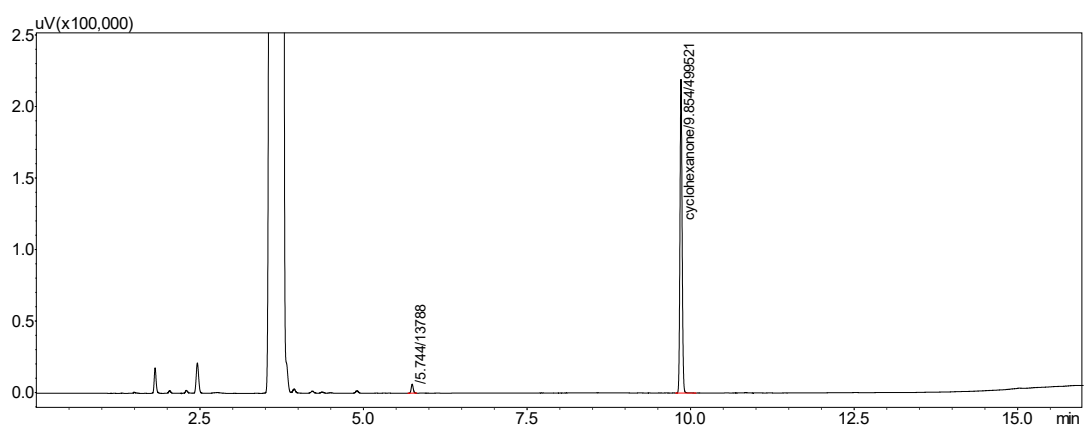
100 µg/mL TADH, 10 mM cyclohexanone and 10 mM NADH



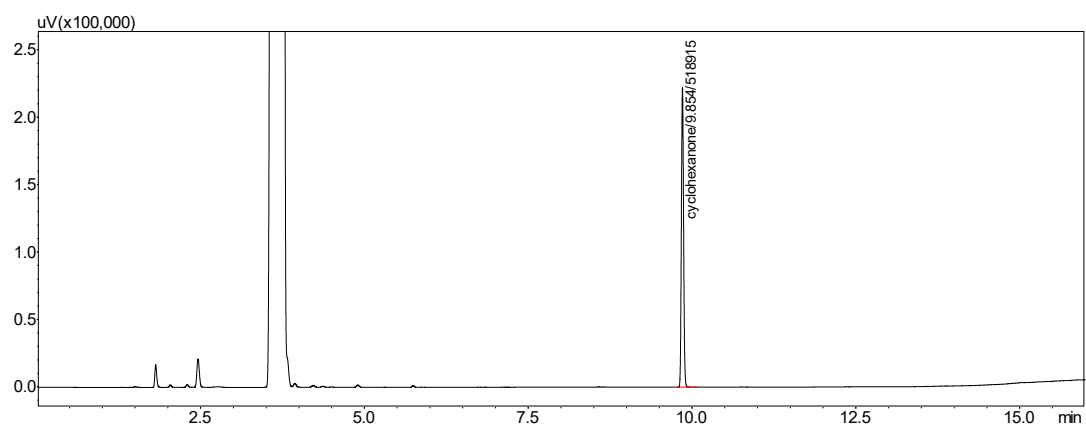
100 $\mu\text{g/mL}$ TADH, 10 mM cyclohexanone and 10 mM BNAH



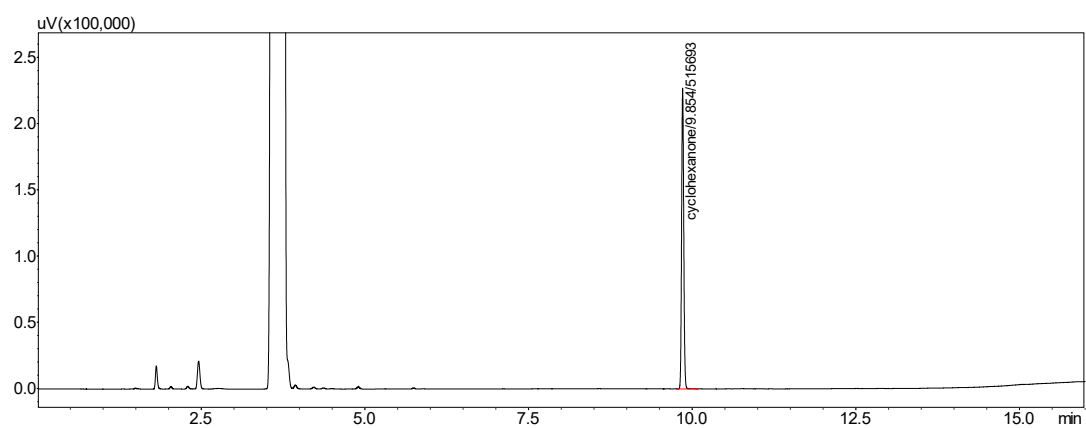
100 $\mu\text{g/mL}$ TADH, 10 mM cyclohexanone and 10 mM AmNAH



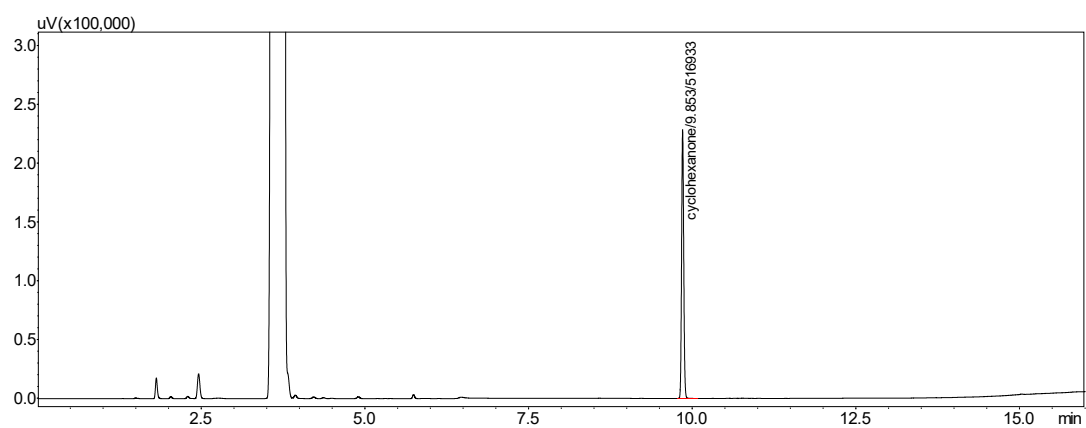
No TADH, 10 mM cyclohexanone and 10 mM NADH



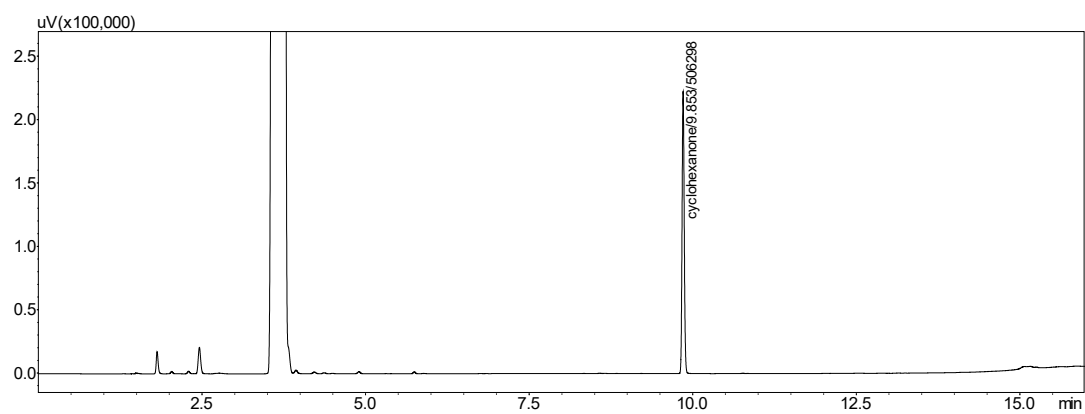
No TADH, 10 mM cyclohexanone and 10 mM AmNAH



No TADH, 10 mM cyclohexanone and 10 mM BNAH

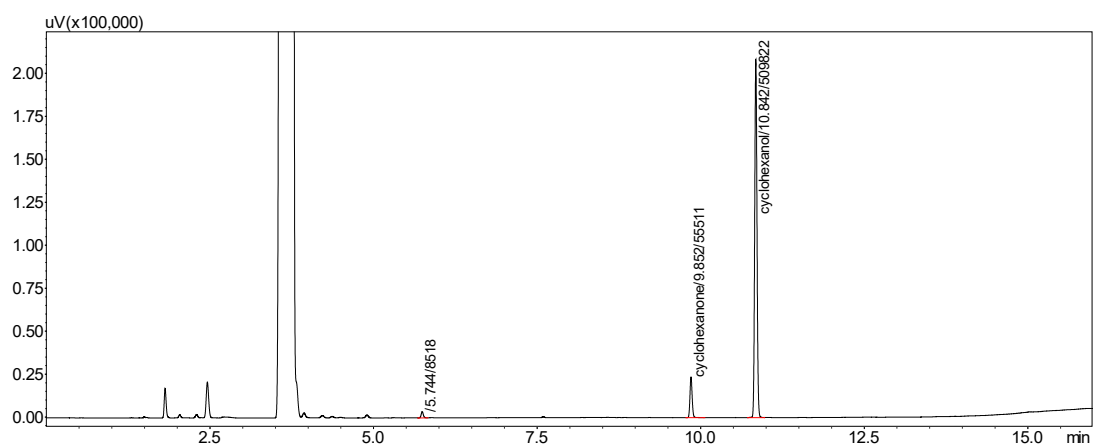


100 µg/mL TADH, 10 mM cyclohexanone

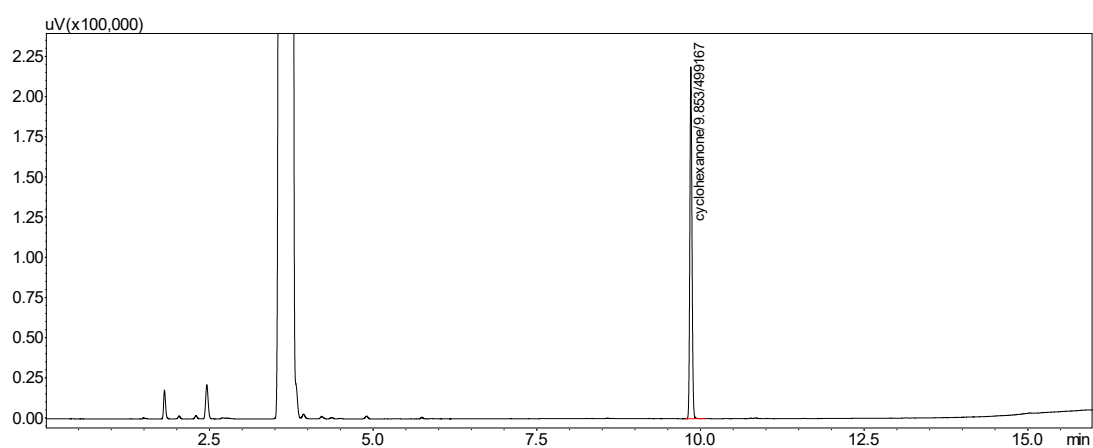


Reaction with UV-Vis induction (400-700nm)

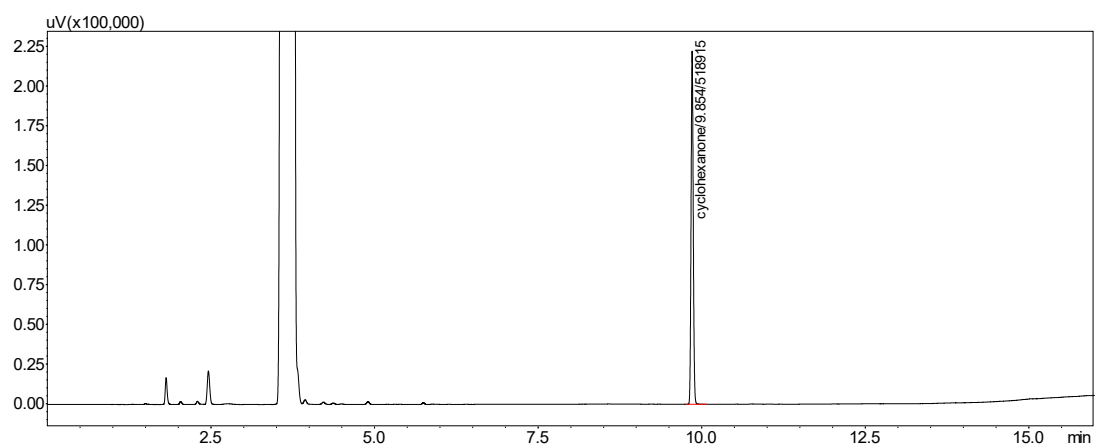
100 µg/mL TADH, 10 mM cyclohexanone and 10 mM NADH



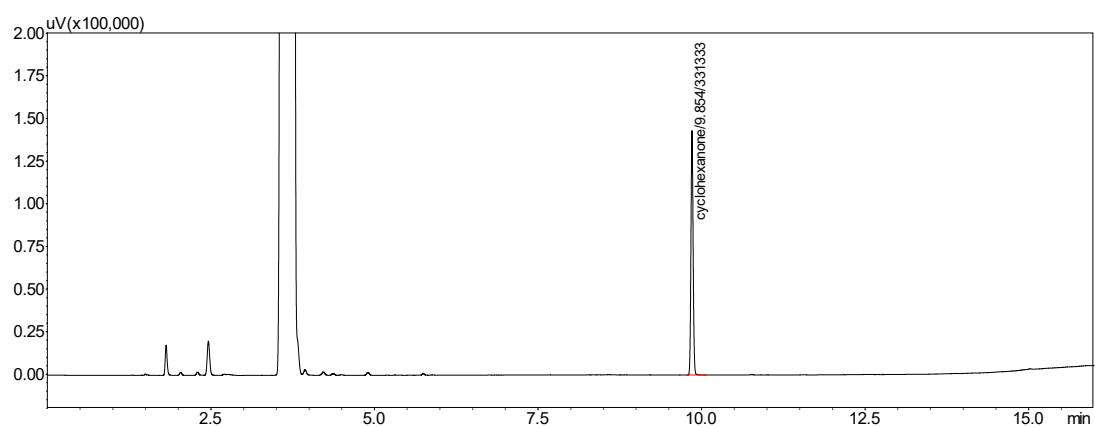
100 µg/mL TADH, 10 mM cyclohexanone and 10 mM BNAH



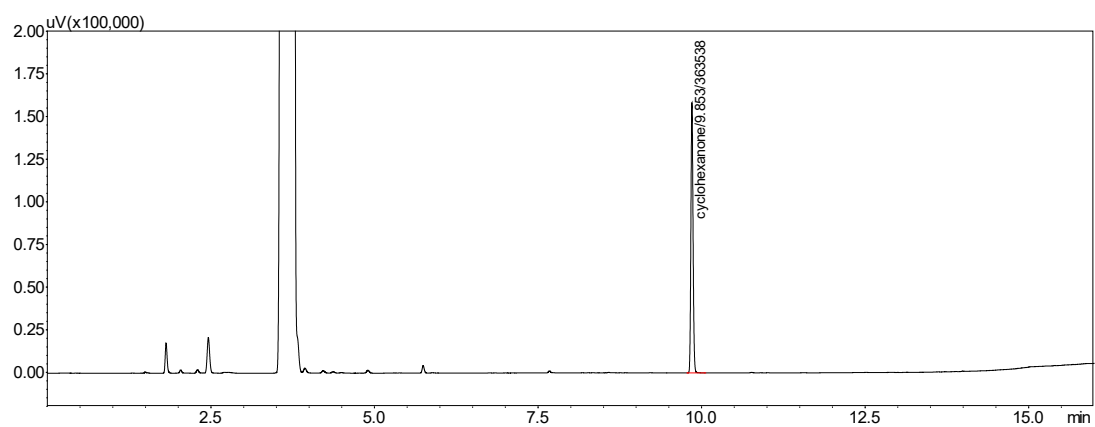
100 µg/mL TADH, 10 mM cyclohexanone and 10 mM AmNAH



No TADH, 10 mM cyclohexanone and 10 mM NADH



No TADH, 10 mM cyclohexanone and 10 mM AmNAH



No TADH, 10 mM cyclohexanone and 10 mM AmNAH

